IntechOpen

HVAC System

Edited by Mohsen Sheikholeslami Kandelousi

HVAC SYSTEM

Edited by **Mohsen Sheikholeslami Kandelousi**

HVAC System
http://dx.doi.org/10.5772/intechopen.73114
Edited by Mohsen Sheikholeslami Kandelousi

Contributors

Steven Hoff, Annunziata D'Orazio, Alessandro Carbonari, Massimo Vaccarini, Emanuela Quaquero, Andrei Melekhin, Anthony Adeyanju, Igor Gritsuk, Vasyl Mateichyk, Vladimir Volkov, Yurii Gutarevych, Valery Aleksandrov, Valeriy Verbovskiy, César Martín Gómez, Lizbeth Salgado-Conrado, María Ibáñez Puy, José Antonio Sacristán Fernández, Anum Tanveer, Carlos Pérez T., Héctor Campbell, Alejandro Suastegui, Marianela Soledad Reinhardt, Shaimaa Seyam

First published in London, United Kingdom, 2018 by IntechOpen
eBook (PDF) Published by IntechOpen, 2019
IntechOpen is the global imprint of INTECHOPEN LIMITED, registered in England and Wales, registration number: 11086078, The Shard, 25th floor, 32 London Bridge Street
London, SE19SG – United Kingdom
Printed in Croatia

British Library Cataloguing-in-Publication Data
A catalogue record for this book is available from the British Library

Additional hard and PDF copies can be obtained from orders@intechopen.com

HVAC System
Edited by Mohsen Sheikholeslami Kandelousi

p. cm.

Print ISBN 978-1-78984-432-0

Online ISBN 978-1-78984-433-7

eBook (PDF) ISBN 978-1-83881-719-0

Meet the editor

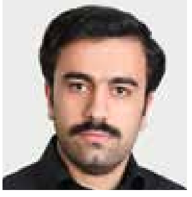

Dr. Mohsen Sheikholeslami Kandelousi works at the Babol Noshirvani University of Technology's Department of Mechanical Engineering in Iran. His research interests are CFD, nanofluid, mesoscopic modeling of fluid, nonlinear science, magnetohydrodynamics, ferrohydrodynamics and electrohydrodynamics. He has written several papers and books in various fields of mechanical engineering. According to the reports of Thomson Reuters and Clarivate Analytics, he was selected as a Web of Science Highly Cited Researcher (Top 0.01%) in 2016 and 2017. He is the editor of various journals and was selected as a distinguished reviewer in various high-impact journals.

Contents

Preface

In this book, various aspects of heating, ventilation, and air-conditioning (HVAC) systems are investigated. HVAC systems are milestones of building mechanical systems that provide thermal comfort for occupants accompanied with indoor air quality. HVAC systems can be classified into central and local systems according to multiple zones, location, and distribution. Primary HVAC equipment includes heating equipment, ventilation equipment, and cooling or air-conditioning equipment. Central HVAC systems are located away from buildings in a central equipment room and deliver the conditioned air by a delivery ductwork system. Central HVAC systems contain all-air, air-water, or all-water systems. These two systems are presented in Chapter 1. In Chapter 2, two methods for sizing the network for the transport of the air, from the air handling unit to the terminal units, are explained. Chapter 3 deals with a methodology of energy management intended to analyze, evaluate, and suggest actions to save and encourage the efficient use of electric energy of HVAC systems during stages of planning, design, construction, or audit existing systems applied to regions with hot and dry climates such as desert or semidesert locations. Chapter 4 focuses on HVAC systems for modern animal housing systems. The advanced simulation tools for transient energy simulation of existing buildings are studied in Chapter 5. The relevance of the topic due to the decision of problems of the economy of resources in heating systems of buildings is presented in Chapter 6. Chapter 7 discusses the use of the vehicular combined thermal development system with phase-transitional thermal accumulators. A techno-economic analysis of a thermoelectric heating unit (THU) prototype is reported on in Chapter 8. This chapter shows a technical description, which includes design, improvements, operating conditions, and mathematical model of THU system. In Chapter 9, authors analyze theoretically the temperature distribution and energy storage ability of a simultaneous charging and discharging concrete bed storage system.

Mohsen Sheikholeslami Kandelousi (M. Sheikholeslami)
Department of Mechanical Engineering
Babol Noshirvani University of Technology
Babol, Islamic Republic of Iran

Chapter 1

HVAC Techniques for Modern Livestock and Poultry Production Systems

Steven J. Hoff

Additional information is available at the end of the chapter

http://dx.doi.org/10.5772/intechopen.78785

Abstract

Thermal modification for housed livestock and poultry production (HLPP) systems has evolved from outside raised or uncontrolled naturally ventilated building systems into sophisticated computer-controlled cloud-analyzed complexes in the quest for producing a safe, reliable, sustainable, and efficient protein supply for our ever-growing population. This chapter discusses a few of the various HLPP systems used in the USA and details the design process in quantifying the needs for our housed livestock and poultry. Specific emphasis is placed on general building characteristics, general ventilation design features, heat stress control, and systems designed to address animal welfare.

Keywords: livestock, poultry, heat stress, animal welfare, ventilation

1. Introduction

Thermal modification for housed livestock and poultry production (HLPP) systems has evolved from outside raised or uncontrolled naturally ventilated building systems into sophisticated computer-controlled cloud-analyzed complexes in the quest for producing a safe, reliable, sustainable, and efficient protein supply for our ever growing population. This chapter discusses a few of the various HLPP systems used in the USA and details the design process in quantifying the needs for our housed livestock and poultry. Specific emphasis is placed on general building characteristics, general ventilation design features, heat stress control, and systems designed to address animal welfare.

2. General thermal modification systems for housed livestock and poultry

In the USA, the raising of food animals in controlled climate facilities has progressed rapidly since the 1980s. It was not uncommon for livestock and poultry producers to rear food animals in outdoor lots or partially contained facilities with minimal modification to the thermal environment. This small-scale production practice has now given way, for the most part, to intensive housing systems where thousands of food production livestock and poultry are raised in tightly controlled climates, with sophisticated thermal modification techniques. The following sections outline some of the systems in use today. For a more complete historical perspective on the development of HLPP systems, see [1].

2.1. Structural design basis for the USA HLPP building system

The majority of HLPP buildings in the USA are composed of wood-frame construction supplemented with concrete stub walls, polyethylene or equivalent curtain sidewall openings, and light-gauge steel roofing and siding (**Figure 1a**, **b**). Waste products are handled in repositories below a slotted flooring system (pigs, beef; **Figure 1b**), within the flooring material (e.g., sawdust) itself (broiler, turkey, hens; **Figure 1c**) or outside below- or above-grade earthen, concrete, or steel containment systems (pigs, beef, dairy, hens; **Figure 1d**). Insulation levels

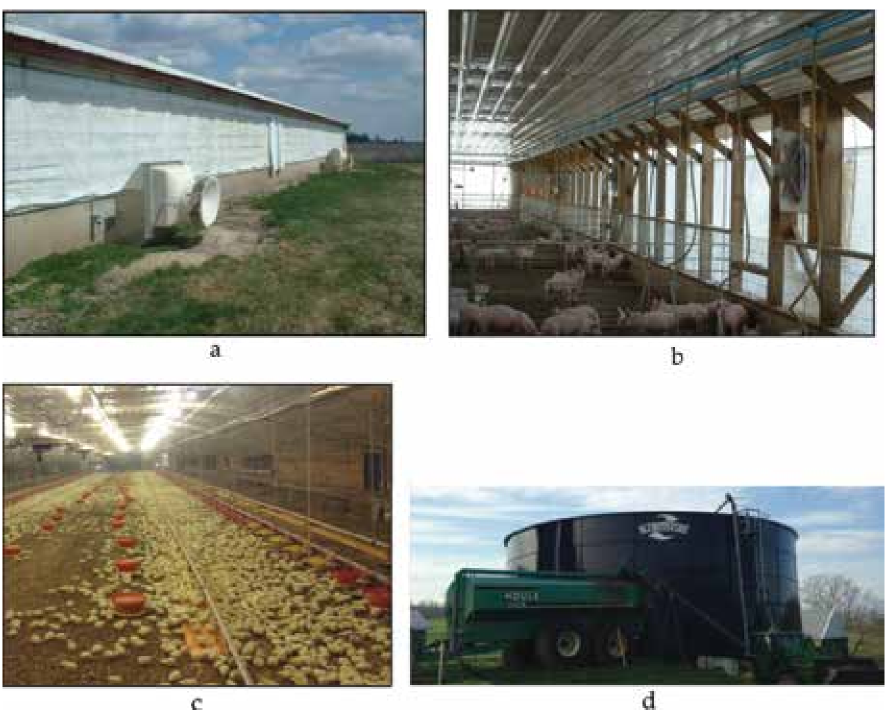

Figure 1. (a) A common Midwestern USA swine finisher with curtain sidewalls and (b) metal flat interior ceiling with concrete slatted flooring, (c) common broiler housing [2], and (d) common above-ground metal manure storage system [3].

http://dx.doi.org/10.5772/intechopen.78785

vary greatly by region of the country. For all intensive purposes, HLPP buildings are considered thermally light, responding quickly to outside weather influences.

2.2. Ventilation design basis for the USA HLPP building system

Ventilation designs for HLPP systems range from complete natural ventilation (NV) to a combined hybrid natural/mechanical ventilation (NMV), to full mechanical ventilation (MV).

2.2.1. The naturally ventilated HLPP system

The NV building design (**Figure 2**) features controlled sidewall curtain and ridge vent openings. The sidewall and ridge vents are either manually or automatically controlled. The NV barn design has traditionally been used in broiler, turkey, beef, pig finishing, and dairy housing.

Orientation of building relative to historical summer winds is critical, as well as the percent calm periods during warm weather. For example, **Figure 3a** outlines the historical August wind rose pattern for Des Moines, Iowa, USA. For this region, the predominant summer winds are from the S-SE and a properly oriented NV building would have the ridge axis E-W or slightly tilted counter-clockwise to expose the sidewall curtains to the predominant summer winds. Deviation from predominant summer winds will significantly affect the potential fresh-air exchange rate in the building. **Figure 3b** outlines the predicted fresh air exchange rate (air changes per hour; ach) for a typical pig finishing facility designed to house 1000 pigs. The design maximum hot weather rate for this type of facility is 100–120 ach. For this example, both sidewall curtains are open 1.2 m. If the building is oriented completely E-W, with a perpendicular southern (180^{o}) or northern (0^{o}, 360^{o}) wind, a 3 m s^{-1} and above wind speed will sufficiently ventilate this building at and above design criteria. An orientation that deviates from the predominant wind direction significantly reduces ventilation potential. In theory, a lateral (along the ridge line) wind direction (90^{o}, 270^{o}) will not ventilate the building at all, although certainly some low-level exchange of fresh air will still take place. The NV building design is still a staple for many animal groups, especially dairy, beef, broilers, turkeys, and swine finishers.


a b

Figure 2. Naturally ventilated (a) pig finishing building with (b) close-up of modern controlled ridge vents.

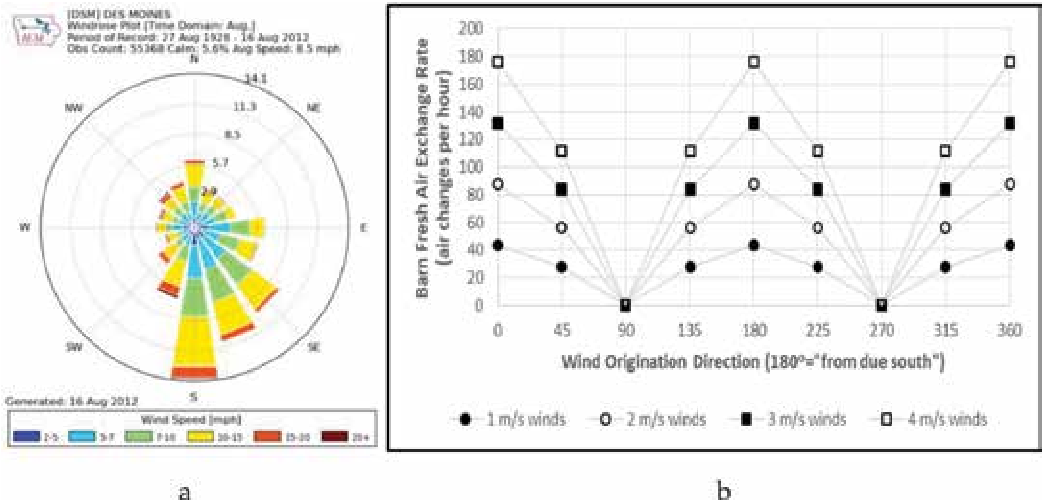

Figure 3. Typical (a) wind rose pattern evaluated when planning for a naturally ventilated building and (b) the influence of improper alignment relative to predominant summer winds.

2.2.2. The hybrid natural/mechanical HLPP system

The NV method of HLPP building ventilation, although once the predominant method of ventilating HLPP systems, has given way in many cases to NMV or MV approaches where tighter control of the thermal environment is desired. The NMV method uses exhaust fan ventilation in cold-to-mild conditions with sidewall curtains and wind potential handling warm weather ventilation (see **Figure 1a**). The NMV method was developed to replace the NV action during cold weather in an attempt to better control the thermal environment. Warm and hot weather ventilation is handled with sidewall curtain opening action and wind, requiring the same basic orientation requirements of an NV building. The NMV method does not require cold weather ridge vents and therefore in the NMV method a flat interior ceiling is often used (see **Figure 1b**) with a heavily insulated attic space.

2.2.3. The mechanically ventilated HLPP system

The vast majority of modern intensive HLPP systems use a negative pressure MV system with exhaust fans connected in parallel and fresh inlet air drawn in through ceiling diffusers (**Figure 4**) in cold-to-mild conditions and sidewall and/or endwall curtains (**Figure 1a**, **b**) in warm-to-hot conditions. In modern HLPP systems, the ceiling diffusers are cable controlled to stage inlet action with fan staging, using static pressure differential as feedback. Typical operating static pressures range from 10 to 30 Pascals ($P_{outside}$-P_{inside}). The MV system will typically incorporate at least one sidewall 'drop' curtain opening for emergency power loss events. The negative pressure MV arrangement has become a popular choice, preventing moisture and gas-laden air from exfiltrating through uncontrolled locations where condensation and building deterioration could be an issue. Specialty-designed positive pressure systems are becoming more popular, which are discussed in a later section.

Figure 4. Example ceiling fresh-air diffuser commonly used in HLPP systems. The cable shown passing through the diffuser is used to automatically control baffle opening in response to ventilation rate changes with static pressure control as the ultimate diffuser opening control objective.

3. Space and zone heating for housed livestock and poultry

Space and/or zone heating are integral components of modern HLPP systems. Space heating has been traditionally accomplished with unvented forced air furnaces. Heated air distribution is handled primarily with a single diffuser attached to the heater outlet, providing minimal distribution and thus uniformity. Ducting of heated air to targeted locations is traditionally not employed in the HLPP systems. Zone heating has traditionally been handled with radiant spot (**Figure 5a**), radiant tube, or heat lamps (**Figure 5b**). In some of the colder regions of the USA (e.g., Minnesota), additional microclimate enclosures with heat lamps are provided for immature animals in the coldest weather (**Figure 5b**). Cold climate ventilation rates are designed to control moisture, gases, and temperature, with moisture control almost always governing the cold weather ventilation rates. Many HLPP ventilation control platforms available today allow the producer to control for building temperature, with relative humidity sensing as a backup for assessing moisture control. Gases such as ammonia, carbon dioxide, hydrogen sulfide, and methane can be an issue in many HLPP systems. In most cold weather situations, and during

Figure 5. (a) Radiant spot heater with shielded radiant sensor for feedback control and (b) microclimate with heat lamps.

normal operating conditions, ventilating for moisture control will also control targeted gases below occupational standards such as those provided by ACGIH or OSHA [4, 5].

4. Space and zone cooling for housed livestock and poultry

Space and/or zone cooling methods have been traditionally limited to evaporative pad cooling systems, high pressure foggers, or direct low pressure water spray systems accompanied most often with elevated airspeed control. Compression-based cooling is not traditionally used, except in specialty cases not covered in this chapter. Heat stress control for housed livestock and poultry is becoming an ever growing concern, fueled mainly by our changing climate, global expansion of HLPP systems in hot and humid climates, and the increased productivity levels of modern food animals where increased internal heat generation must be released to the environment.

4.1. Heat production of modern food animals

Modern genetics has increased the productivity levels of our food animals. This in turn has increased the internal heat produced that must be dissipated to the surrounding thermal environment. For example, one study found that comparing pre-1988 to post-1988 heat production data, the total heat produced by modern pigs increased by 12–35% for 90 kg pigs at 15°C and 5 kg pigs at 35°C, respectively [6]. Similar increases are known in other animal and poultry groups as a natural outcome of increased productivity. Dissipating this heat to prevent heat stress has become challenging.

4.2. Methods to increase animal heat dissipation

The typical HLLP system for heat stress control is a tunnel ventilated (TV) arrangement of fresh air inlets and fans along the long axis of the building (**Figure 6a**) or arranged in cross-flow perpendicular to the long axis (**Figure 6b**). TV systems were first developed in the southeastern quadrant of the USA where the percent calm periods in the summer months can be high. For example, in North Carolina, the hot weather months are associated with up to 18% calm periods, far in excess of desired for proper hot weather NV ventilation performance. The TV HLLP system guarantees a specific average airspeed in the barn when required. The typical design airspeed is 2 m s^{-1}, but some broiler systems are being designed as high as 3 m s^{-1} [7].

Designing the hot weather ventilation rate for airspeed control will in most cases significantly increase the overall building ventilation rate. For example, take the cases depicted in **Figure 6**. If the barn in question houses 1000–600 kg lactating dairy cows, the ventilation rate typically used, designed to keep internal temperature rise less than about 2°C, is roughly 1.90 m^3 $hr.^{-1}$ kg^{-1}. This equates to a maximum building ventilation rate of about 1.14×10^6 m^3 $hr.^{-1}$. A typical dairy barn housing 1000 lactating cows would be about 75 m

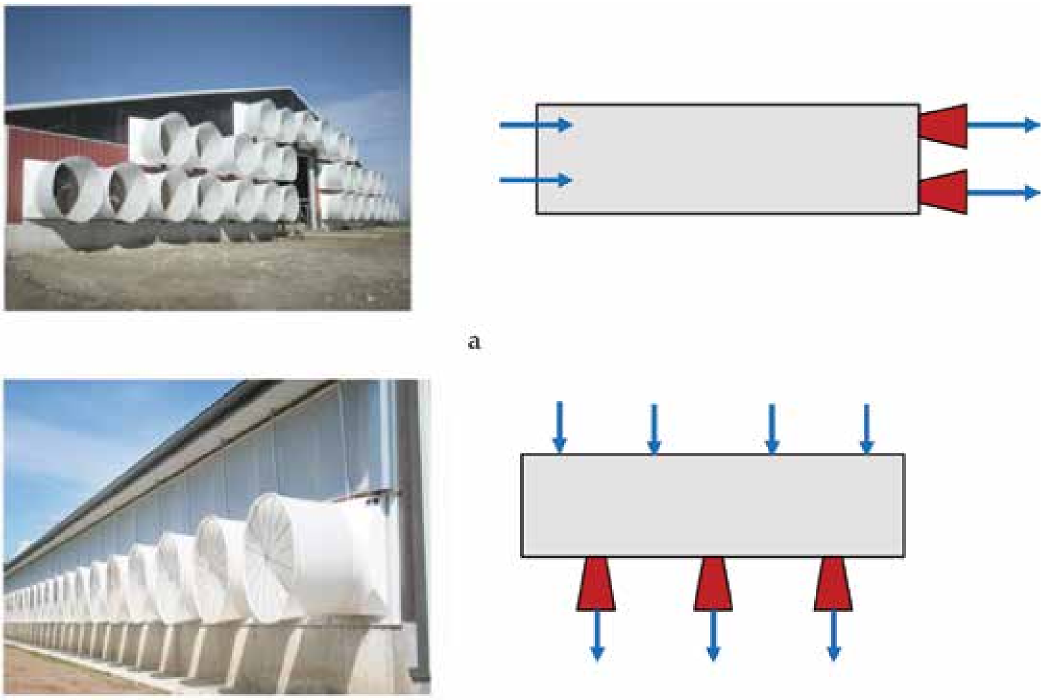

a

b

Figure 6. (a) True tunnel ventilated fan/inlet and (b) cross-flow tunnel ventilated fan/inlet arrangements for airspeed control.

wide, 140 m long, with 4.25 m high sidewalls. If this building was ventilated for a 2 m s^{-1} airspeed in true tunnel ventilation mode (**Figure 6a**), the maximum ventilation rate would be 2.30×10^6 m^3 $hr.^{-1}$; a 200% increase from typical. If designed in cross-flow tunnel, a more common dairy housing arrangement, the maximum ventilation rate would be $4.28 \times 106\ m^3\ h^{-1}$; a 375% increase from typical and a 186% increase from true tunnel. In some cases, dairy buildings would be fitted with drop panels over the cow resting area, to accelerate cross-flow ventilation over the cows, allowing the overall maximum cross-flow tunnel ventilation rate to be reduced (see **Figure 7b**).

In many cases, the elevated airspeed with TV systems is supplemented with evaporative pad cooling at the fresh-air intake and/or low pressure water sprinkling, especially in pig and dairy systems. Strategies are being developed to actively select the most effective cooling strategy in a suite of options based on the climate's ability to dissipate the sensible and latent heat generated by the animals [8, 9]. For example, in some situations, evaporative pad cooling might raise the humidity ratio to a point detrimental for latent heat release from the animals, instead, warranting the use of low pressure water sprinkling. Heat production and heat/mass transfer models continue to be developed to assist heat stress mitigation decisions [8, 9].

a b

Figure 7. (a) Dairy housing sidewall inlet with or without evaporative cooling pads and in some cases (b) drop curtains/walls to force cross-flow ventilation over rows of cows, enhancing airspeed maintenance.

5. HVAC design for virus control

Disease transmission from herd-to-herd via aerosol transport is a concern, driving significant HLLP system changes to accommodate new and innovative ventilation designs. Many HLLP systems are being designed today to capture viruses before entry into a building. This movement has been especially prevalent in pig housing systems where the porcine reproductive and respiratory syndrome virus (PRRSv) has caused significant economic hardship. Building ventilation systems have been retrofitted to incorporate high efficiency filters at fresh-air intakes as a physical capture of the virus.

Two basic ventilation retrofit strategies have been implemented, one that maintains traditional negative pressure MV and a second option that utilizes a positive pressure MV system in a 'push-only' or 'push-pull' fan configuration. In a negative pressure filtration arrangement, primary (MERV 8) and secondary (MERV 16) filters are attached in the attic space to the existing fresh-air ceiling intakes as depicted in **Figure 8a** for an inlet depicted in **Figure 4**. This method suffers tremendously from the high infiltration rates common in many HLLP systems [10]. In negative pressure filtration systems, significant sealing of the building is required to limit unfiltered air from entering the animal zone through air leakage points, and this can be an annual challenge after each seasonal freeze/thaw cycle.

In a positive pressure filtered barn, industrial blowers (**Figure 8b**), or equivalent are used to push air through primary and secondary filter banks (**Figure 8c**), maintaining the building operating pressure slightly above ambient, bypassing the infiltration issues common with negative pressure systems. The major drawback with positive pressure filtered systems is the tendency for moisture laden air to exfiltrate, potentially condensing in the building cavity. In positive pressure systems, care must be taken as well to control exfiltration for this reason.

http://dx.doi.org/10.5772/intechopen.78785

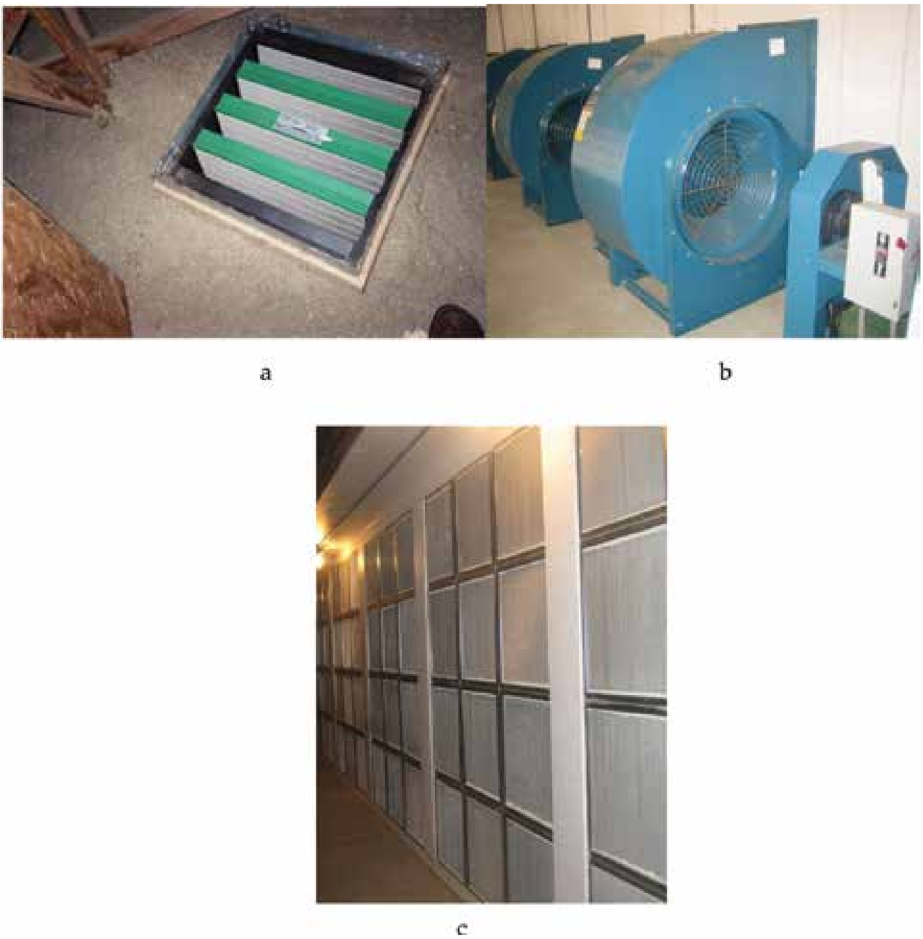

Figure 8. Virus filtration with (a) filters attached directly to ceiling fresh-air intakes in a negative pressure system, or (b) using blowers and (c) filtration banks in a positive pressure filtration system.

6. HLLP design for livestock and poultry welfare

Producers of food animals place animal welfare at the forefront of their operation. Several building design changes have evolved as a result of public pressure stemming from concerns related to animal welfare. The most prominent changes have been made in pig gestation and egg-laying facilities. Traditional gestation housing uses individual stalls (**Figure 9a**) from which precise nutritional needs can be maintained and monitored. Due to public pressure, the traditional stall gestation has given way, in some cases, to group housing gestation facilities, with, in many cases, electronic feed dispensing and pig monitoring (**Figure 9b**).

Figure 9. (a) Sow gestation housing using stalls [10], and (b) the alternative group housing with electronic feeding and monitoring systems [11].

Unquestionably, the biggest change in HLPP systems has occurred in the egg-laying sector. Many large fast-food chains have demanded bird space allocation changes and overall free-roaming requirements that have significantly changed the hen housing system. The conventional caged-layer system is rapidly being replaced by enriched colony or aviary systems where birds are allowed extensive movement and ample opportunity for perching and nesting behavior. An excellent overview of the various hen housing systems can be found in [12].

7. Conclusions

Thermal modification for housed livestock and poultry production (HLPP) systems has evolved from outside raised or uncontrolled naturally ventilated building systems into sophisticated computer-controlled cloud-analyzed complexes in the quest for producing a safe, reliable, sustainable, and efficient protein supply for our ever growing population. This chapter summarized a few of the various HLPP systems used in the USA. Specific emphasis was placed on general building characteristics, general ventilation design features, heat stress control, and systems designed to address animal welfare. Significant advances have been made in HLPP systems in response to global food demand and as a matter of efficiency. Advances will continue as we strive to ensure a safe, environmentally sustainable, and efficient food supply.

Author details

Steven J. Hoff

Address all correspondence to: hoffer@iastate.edu

Department of Agricultural and Biosystems Engineering, Air Dispersion Laboratory,
Iowa State University, Ames, Iowa, USA

References

[1] Koenig W. Techniques for analyzing mechanically ventilated livestock facilities [thesis]. Ames: Iowa State University; 1994

[2] Available from: http://www.roysfarm.com/broiler-poultry-housing/. [Accessed: 2018-04-02]

[3] Available from: https://www.cstindustries.com/manure-slurry-storage-tanks-manufacturer/. [Accessed: 05-01-2018]

[4] American Conference of Governmental Industrial Hygienists. https://www.acgih.org/

[5] Occupational Safety and Health Administration. https://www.osha.gov/

[6] Brown-Brandl T, Nienaber J, Xin H, Gates R. A literature review of swine heat production. Transactions of the ASABE. 2004;**47**(1):259-270. DOI: 10.13031/2013.15867

[7] Luck B, Davis J, Purswell J, Kiess A, Hoff S. Assessing air velocity distribution in three sizes of commercial broiler houses during tunnel ventilation. Transactions of the ASABE. 2017;**60**(4):1313-1323. DOI: 10.13031/trans. 12107

[8] DeVoe K. Climate dependent heat stress mitigation modeling for dairy cattle housing [thesis]. Ames: Iowa State University; 2017

[9] Ramirez B. A novel approach to measure, understand, and assess the thermal environment in grow-finish swine facilities [thesis]. Ames: Iowa State University; 2017

[10] Available from: https://www.minnpost.com/minnesota-blog-cabin/2015/02/why-we-use-individual-gestation-pens-our-sows. [Accessed: 2018-04-24]

[11] Available from: https://www.wattagnet.com/articles/31258-how-to-minimize-sow-stress-aggression-in-group-housing?v=preview. [Accessed: 2018-04-24]

[12] Available from: https://uepcertified.com/choices-in-hen-housing/. [Accessed: 2018-04-24]

Chapter 2

Methodology of Energy Management in Housing and Buildings of Regions with Hot and Dry Climates

Carlos Pérez-Tello, Héctor Campbell-Ramírez,
José Alejandro Suástegui-Macías and
Marianela Soledad Reinhardt

Additional information is available at the end of the chapter

http://dx.doi.org/10.5772/intechopen.78341

Abstract

In this chapter, power consumption and electrical demand in buildings or housing due to the utilization of HVAC systems are shown to be intimately linked to construction materials. This work proposes a methodology of energy management intended to analyze and evaluate actions aimed at saving and efficient use of electric energy of HVAC systems applied to regions with hot and dry climates. The methodology consists of: (1) characterization of local climatology using the concept of degree-hours (DH). (2) Utilization of a Fourier-type mathematical model to calculate hourly temperature using only daily maximum and minimum temperatures as well as an empirical model to compute energy efficiency (EER) of air-cooled air conditioning units. (3) Thermal simulation applying a software developed by the authors based on ASHRAE's Transfer Functions methodology to calculate hourly cooling loads, the adequate sizing of air conditioning equipment and the rate of heat extraction. (4) System analysis, identification of improvement actions, evaluation of viable alternatives of saving and efficient use of energy. The advantage of this proposal is its flexibility because it can be applied to any climatology and easily adaptable to the conditions of energy usage anywhere in the world.

Keywords: energy management, HVAC systems, degree-hours

1. Introduction

In regions of extreme climates, whether warm, cold or both, the use of HVAC systems is important to maintain comfort and adequate conditions for its occupants. However, the amount of electricity consumed depends on several factors such as the cooled/heated area, construction materials, climate of the region, fenestration, user's energy management, thermal insulation, lighting or internal heat loads, among the most important ones. However, social-economic and cultural issues also play a significant role [1].

One of the main problems encountered in HVAC systems is oversizing. This leads to an unnecessary increase of electrical demand on the power supply system and its consequent environmental impact [2]. For example, in the northwest region of Mexico which is characterized by a dry hot climate in summer, maximum outdoor temperatures of 45–47°C and even higher are usually encountered in July and August. For these conditions, retailers and HVAC technicians normally size the capacity of air conditioning using a rule of thumb that has been deeply rooted for years: "1 ton capacity for 20 square meters of cooled area." This criterion is generally applied without any valid technical or scientific basis.

This heuristic approach does not take into account if the building is well insulated or if there are elements for energy saving. As a consequence, the air conditioner is generally oversized by a factor which varies from 1.5 to 2. On the other hand, since 1990, in Mexicali, Baja California, Mexico, a city with more than one million inhabitants, the federal government initiated a sponsored program through Comisión Federal de Electricidad (CFE), the state electric power company, intended to support energy saving strategies and specific actions oriented to the residential sector. These actions started by financing insulation of ceilings and the replacement of incandescent lamps with fluorescent ones. Subsequently, in 1997 began the replacement of old low-efficiency air conditioning units with high-efficiency equipment. In this program, the package, split, mini-split and window type units were considered and by 2003 the actions to replace old low-efficiency refrigerators were launched. This program called Program for Integral Systematic Saving [(ASI) by its acronym in Spanish] still continues to operate and has even expanded to other cities with hot climate in the country [3].

Energy efficiency of residential housing and buildings is of concern not only in Mexico but around the world because of its impact on future energy requirements, due to the accelerated growth of our modern cities during the next decades. Thus, several studies oriented to analyze and improve efficiency of this sector using regional passive elements (attics, ventilation, gardening, wall materials, roof ponds, and insulation) or feasible strategies of energy saving have been carried out [4–7].

On the other hand, recent studies are being developed to investigate the utilization of nanoparticles as energy carriers or thermal storage materials for applications in heat transfer systems. The effect of these materials on the effectiveness of heat transfer in heat exchangers of different geometries has been simulated by taking advantage of latent heat of melting-solidification change of phase. The use of nanoparticles added to reflective paints as an additional energy saving option has also been proposed. However, even more research is still needed in this field to consider these materials as a truly effective, technical, safe and economic option [8–12].

Nevertheless, there is still no standardized criterion for the correct sizing of cooling or heating units applicable in Mexico, so oversizing becomes a serious problem for the energy supplier and makes the user pay unjustifiably for additional and unnecessary capacity. For this reason, the UABC's Institute of Engineering has been working on several projects oriented toward the efficient use and energy saving which at the same time let us obtain a reliable methodology to determine and characterize the energy performance of the residential sector as well as public and private buildings in order to standardize the energy calculation and provide solid technical elements to analyze, implement and evaluate effective actions of saving and efficient use of electric energy.

2. Energy management methodology

2.1. Climatology: degree-days and degree-hours

For understanding the energy behavior of a building or a household, it is imperative to know very well the climate of the region where it is located since its climate determines whether heating, cooling or both are required for any period of the year. This is also essential for calculation of heat gain or heat losses. It does not matter if the building is in the design stage or it has already been built; any energy analysis is intimately related to local climate. As previously mentioned, degree-days have been the main variable used to correlate energy and climate. Before having the advantages provided today by the availability of current online weather databases, the cooling or heating degree-days were computed just considering a simple arithmetic addition or subtraction between the outdoor temperature and an estimated base temperature.

As an example, at any given day, the maximum temperature reached 35°C and the minimum temperature was 22°C, the average temperature is $T_{av} = (35 + 22)/2 = 28.5$°C. The most used base temperature in the USA is 18.3°C (65°F). Since T_{av} is greater than 18.3°C, the degree-days are then (28.5−18.3) = 10.2 cooling degree-days. The same base temperature is also utilized for estimating heating degree-days [13].

However, there are other criteria for calculating degree-days as indicated by Bromley [14] who takes into account not only a variable base temperature but also the duration of the temperature above or below such reference temperature. This information can be obtained online when a weather station in the city or location of interest is available, but what happens if information is not reliable or does not exist at all? In such a case, data from the nearest station or from a region with a similar climate would be useful. Once the degree-day values are obtained for a particular location, then they could be correlated seeking for some relationship between, for example, power consumption or demand to establish patterns of energy behavior in buildings or even to estimate the impact of global warming on the climatology of a particular location [15–17].

In developed countries, a large amount of climatological information is available; however, in nondeveloped countries such as Mexico or in Latin America, there is a lack of data for many locations excepting maybe for the most important cities. Therefore, we have been working on collecting and processing information provided by the National Meteorological Service of 40

Mexican cities with a population of at least 100,000 inhabitants. Instead of working with the degree-day approach, hourly averages were obtained and analyzed on this basis. These are called degree-hours (DH). DH take into account not only the degrees of the outdoor temperature above or below the reference temperature but also the duration of these variations over a day. This procedure can be done for every single day of the year. In **Figure 1**, the concept of degree-hours is shown graphically. This figure also shows the mathematical definition once a function for hourly outdoor temperature is provided.

Two temperatures were set as baselines for summer and winter: 29.5°C (85°F) for cooling DH and 15.5°C (60°F) for heating DH. These values were selected based upon the weather conditions of the northwest of Mexico where the most severe climate in the country is said to be, especially in summertime. As an example, the maximum recorded temperature in Mexicali occurred on July 28, 1995—51.8°C (124°F). In addition, the inhabitants of this region have developed a special acclimatization for these severe conditions not existing in other cities with less aggressive climates. These conditions lead us to consider that the comfort zone is slightly different for the population living in our region from that commonly reported by The American Society of Heating, Refrigerating and Air-Conditioning Engineers (ASHRAE) [18].

As an example of the application of the DH in the climatological analysis, the results for two cities of northwestern Mexico, Mexicali and Hermosillo, during the summer season are shown in **Figure 2**. Mexicali, the capital of Baja California, is located just on the border with the State of California, USA, while Hermosillo, the capital of Sonora, is 700 km apart to the south. The average monthly temperature in July and August for both locations is very similar, 33°C and 32.2°C, respectively. Statistically there is no difference between them. For each day of a given

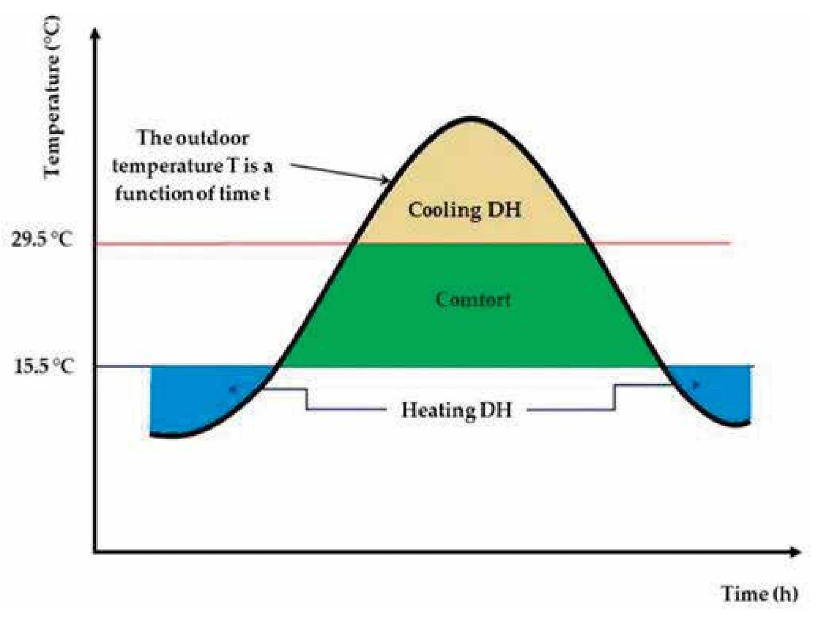

Figure 1. Degree-hours definition.

month, the daily average temperature is calculated as $T_{daily} = (T_{max} + T_{min})/2$ and the monthly average temperature is obtained by averaging the corresponding daily average temperatures. On the other hand, the electricity tariffs in Mexico are based on the average monthly summer temperature. However, even if the monthly average temperature of two or more places is quite similar, this does not mean that the degree-hours are to be the same too. This can be clearly observed in **Figure 2** where the totalized degree-hours during summertime of these two Mexican cities located at the Northwest of the country are compared. The period analyzed was from May to October, and the data were recorded from 1993 to 2001. The statistical difference between DH for both locations is 15%. Thus, as indicated by several authors, the difference, (in percentage) of DH should be similar to the difference (in percentage) of the consumed power by two buildings with the same characteristics situated one in each city, when their energy consumption is compared to each other. In fact, a recent work performed by a graduate student at the Institute of Engineering analyzed the energy consumption of a sample of just over one hundred homes of residential users in these two cities. For the results to be valid, the factors that could introduce variability such as cooled area, constructive system, orientation, occupancy, fenestration or air conditioners efficiency were carefully revised and controlled when analyzed statistically. The results effectively point out that Mexicali users spent, on average, 15% more energy in the summer than Hermosillo's [19]. This figure confirms that electricity consumption and DH are proportional.

The averaged monthly DH for a period of 9 years (1993–2001) for the same two cities are shown in **Figure 3**. As it is seen, there are appreciable variations between one region and another. Mexicali's DH are greater for the period of May to September except in June where both cities behave in a very similar way. October is still a summer month in Hermosillo but not in Mexicali. Otherwise, for the nonsummer months, Mexicali's DH have large negative values while Hermosillo's DH are practically zero. This indicates that Mexicali is significantly colder than the capital of Sonora, an example of an extreme climate. Nevertheless, it should be noted

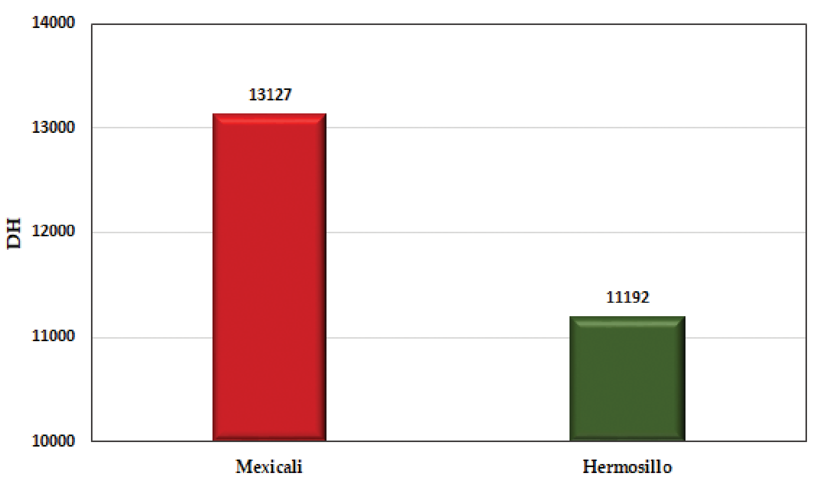

Figure 2. Average summertime cooling degree-hours for two Mexican cities with similar climate.

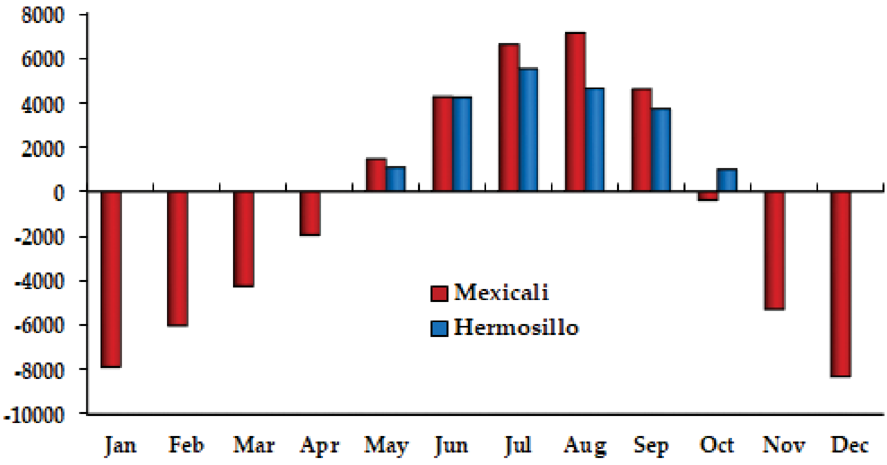

Figure 3. Average monthly DH for two Mexican cities (1993–2001). T_{ref} = 29.5°C (summer), 15.5°C (winter).

that carrying out this type of analysis requires having reliable climatological information. On this depends greatly the success of our work.

2.2. Outdoor temperature model

In order to facilitate the calculation of either DH analysis or thermal simulation of a building the authors developed a simple Fourier-type model for estimating hourly outdoor temperature from data recorded by meteorological stations. When working with climate data for the first time, there is a huge amount of information to process and organize and it is a common practice to work with extensive databases. The aim of using a mathematical model is to reduce the complexity of calculation when performing thermal simulation in buildings. This led us to simplify the energy analysis and assessment of a particular system. Besides, the use of a model let us working with only a few set of correlation coefficients instead of an enormous quantity of data, thus releasing disk and memory space. When analyzing the outdoor temperature of a particular region, no significant changes have been observed in its seasonal patterns along a period of several years. This means that the monthly average temperature remains almost the same year after year over a period of time and the natural variation encountered from a year to another is compensated when more years are taken into account. Although this premise is valid for monthly temperature, Mexicali's DH have increased consistently since 2007 [20].

Since the outdoor temperature is given on an hourly arrangement, the model was intended to be on the same basis. So, the model for estimating the hourly temperature is stated as

$$\Theta(t) = \langle \mu \rangle + A\cos\left(\frac{2\pi t}{24}\right) + B\sin\left(\frac{2\pi t}{24}\right) \tag{1}$$

where $\Theta(t)$ represents the dimensionless hourly outdoor temperature for a particular day defined in Eq. (2), T_{max} and T_{min} are the recorded maximum and minimum temperature and $T(t)$ the calculated value of temperature for time t.

http://dx.doi.org/10.5772/intechopen.78341

$$\Theta(t) = \frac{T_{max} - T(t)}{T_{max} - T_{min}} \tag{2}$$

$\langle \mu \rangle$, A and B are the mean value and the two coefficients of correlation given by:

$$\langle \mu \rangle = \frac{1}{24} \sum_{t=1}^{24} \mu(t) \tag{3}$$

$$\mu(t) = \frac{1}{N} \sum_{n=1}^{N} \Theta_n(t), n = 1, 2, \dots Ndays \tag{4}$$

$$A = \frac{2}{24} \sum_{t=1}^{24} [\mu(t) - \langle \mu \rangle] \cos\left(\frac{2\pi t}{24}\right) \tag{5}$$

$$B = \frac{2}{24} \sum_{t=1}^{24} [\mu(t) - \langle \mu \rangle] \sin\left(\frac{2\pi t}{24}\right) \tag{6}$$

The model was tested using hourly data for various locations in Mexico and Cuba as well as for different years. The statistical deviation from experimental and calculated values did not exceed 5%. For purposes of thermal analysis calculation and buildings simulation, this figure is more than acceptable. Furthermore, the model was integrated as a linked module into the simulator which was developed by the authors to compute the hourly outdoor temperature for a selected location provided the maximum and minimum temperature of any given day. On the other hand, the simulator is based on the ASHRAE's Transfer Function method [21] which, instead of using a large climate database, it used the Fourier model which was incorporated to generating daily hourly temperatures by using only T_{max} and T_{min}. The main reason for doing this is that for certain locations only maximum and minimum temperatures are recorded or available. In **Figure 4**, the experimental and the calculated values using Eq. (1) are shown for the day August 21.

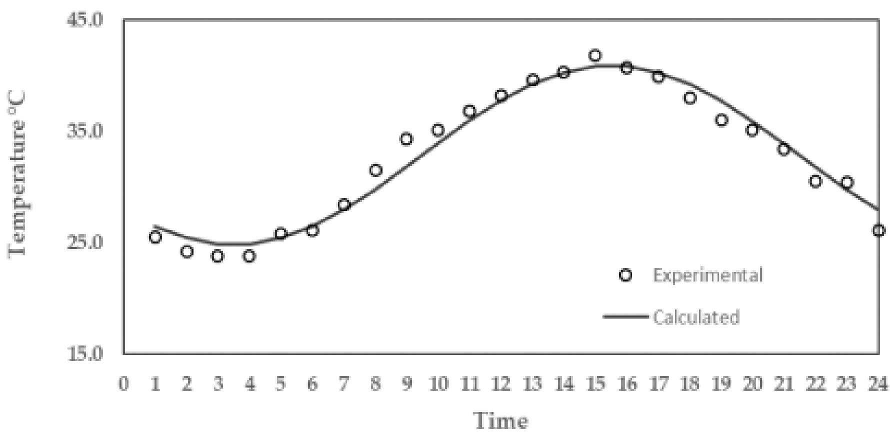

Figure 4. Outdoor temperature using the Fourier-type model. Mexicali, August 21.

Another advantage of using the Fourier-type model is that DH calculation becomes quite simple, so it is not necessary to integrate numerically a large quantity of data every time it is needed, but only performing the integration once by using the model already obtained and substituting the appropriate values of $\langle \mu \rangle$, A and B for the location of interest. In this manner, the cooling DH are defined as

$$DH_{cooling} = \int_{T_0}^{T} \int_{0}^{24} T(t) dt dT \tag{7}$$

After substitution of Eq. (1) and Eq. (2) onto Eq. (7) and integrating, we obtain

$$DH_{cooling} = 24\left[(T_{max} - T_0) - \langle \mu \rangle (T_{max} - T_{min})\right] \tag{8}$$

where T_0 is the reference temperature. The same procedure applies for heating DH.

2.3. Thermal simulation

The computational program has been one of the most useful tools for energy analysis. The software is built in modular form, and each module performs a specific type of calculation; moreover, because of its versatility, it is programmed on Excel spreadsheets. The general structure of the program is shown in **Figure 5**. In the module of data entry, all the required information about location, building dimensions, orientation, materials, occupancy, fenestration, internal loads, lighting, actual or estimated HVAC efficiency, and so on, is entered. The module is linked to an internal database where other information such as latitude, longitude, maximum and minimum temperatures, solar parameters, ASHRAE coefficients and thermal resistances is stored.

The next stage is calculating the hourly outdoor temperature, the sol-air temperature and the amount of direct and diffuse radiation over the surfaces of the building. The ASHRAE Transfer Function method is then used for estimating hourly heat gains, cooling load and heat extraction rate. As mentioned earlier, instead of using a large climatological database for each location, the program was configured to work with only a representative sample of data. We have observed that correlation between degree-hours (DH) and the rate of heat gain, cooling load and heat extraction is excellent for regions of dry, hot climates. It is common to encounter a correlation coefficient over 97% with these three factors. However, the DH correlate very well not only with cooling load or heat gain but also with monthly electricity consumption or demand as well as with air conditioning consumption.

2.3.1. ASHRAE transfer functions method

The simulator used in this work is based on the Transfer Functions method (TFM), as reported by the ASHRAE [22]. The authors developed an earlier version of the simulator in 1996 adapting this methodology from the version published in 1992. However, the program has been updated and improved constantly ever since. TFM consists basically in providing a model to consider the dynamic response of a building to heat transfer. As it is known, heat is introduced into a space by mean of three basic mechanisms, namely, radiation, convection and

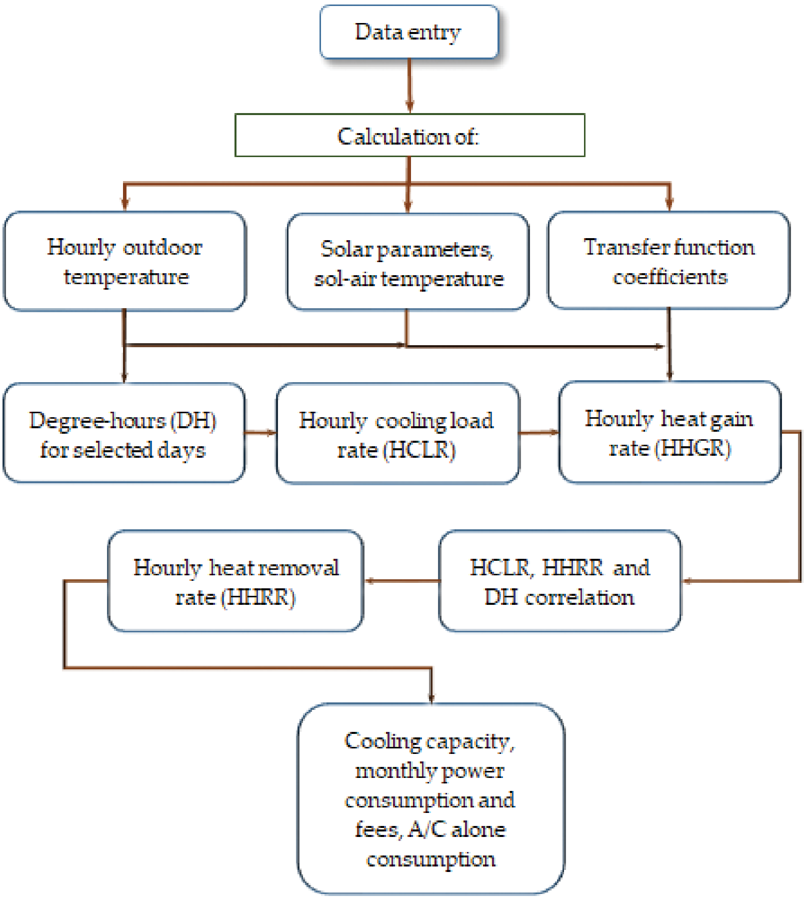

Figure 5. General structure of the thermal simulator.

conduction. TFM converts radiation heat gains on walls as a function of the named sol-air temperature defined as

$$t_e = t_0 + \frac{\alpha I_t}{h_0} - \varepsilon\delta R \tag{9}$$

The heat flow can be calculated from a heat balance as

$$\frac{q}{A} = \alpha I_t + h_0(t_0 - t_s) - \varepsilon\delta R \tag{10}$$

where

t_e = Sol-air temperature

t_0 = Outdoor temperature

t_s = External surface temperature

$\frac{q}{A}$ = Heat flow per unit area

α = Surface absorptivity

I_t= Total solar incident radiation on the surface

h_0 = Convection heat transfer on the external surface

δR = Difference between long-wave radiation from surroundings and the radiation emitted by a black body at the same temperature as outdoor temperature

ε = Surface emittance

Also, TFM requires generating a series of Transfer Function coefficients which are used to estimate U-values for each wall or roof into the equation of energy balance. The first step is calculating hourly heat gains by means of the equation

$$q_{e,\theta} = A\left[\sum_{n=0} b_n(t_{e,\theta-n\delta}) - \sum_{n=1} d_n\left\{\frac{\left(q_{e,\theta-n\delta}\right)}{A}\right\} - t_{rc}\sum_{n=0} c_n\right] \tag{11}$$

where

$q_{e,\theta}$ = Wall or roof heat gain for time θ

$q_{e,\theta-n\delta}$ = Wall or roof heat gain for the time $\theta - n\delta$

A = Surface area

θ = time

δ = Time interval

$t_{e,\theta-n\delta}$ = Sol-air temperature at time $\theta - n\delta$

t_{rc} = Constant interior temperature

b_n, c_n, d_n = Conduction transfer coefficients

Once hourly heat gains have been computed, they can be transformed into hourly cooling loads with the expression

$$Q_\theta = v_0 q_\theta + v_1 q_{\theta-\delta} + v_2 q_{\theta-2\delta} - w_1 Q_{\theta-\delta} - w_2 Q_{\theta-2\delta} \tag{12}$$

where

Q_θ = Cooling load for time θ

q_θ = Conduction heat gain for time θ

v_0, v_1, v_2, w_1, w_2 = Space weight coefficients

Eq. (12) takes into account the dynamic response of the building from a semi-steady state approach once the other variables such as fenestration, occupancy or lighting coefficients are

http://dx.doi.org/10.5772/intechopen.78341

provided. ASHRAE publications enlist a large amount of data for materials mostly used in nonresidential and residential buildings. Nevertheless, some materials and construction designs commonly encountered in Latin America do not match as the ones reported by ASHRAE exactly. Therefore, for these cases, the corresponding data and coefficients had to be estimated and incorporated to the simulator. For a more detailed discussion of TFM, see [18, 23–25].

2.3.2. Simulation improvement by using DH correlations

When performing a thermal simulation of a building using the Transfer Functions method, calculated heat gains, cooling loads and heat extraction rates are delivered by the program on an hourly basis for a given day. This characteristic allows sizing the capacity of HVAC system and determines when the highest peak demand will occur or what the most important elements responsible for gaining/releasing heat or consuming/demanding power are. Then the results are totalized for that particular day. This procedure must be repeated every single day over a year or for a certain period of time as needed.

In order to improve the calculation performance of the simulator without decreasing accuracy and reliability of the results, the authors decided to carry out a simpler procedure by correlating the degree-hours with daily heat gain, cooling load and heat extraction rates for a few representative days of a year. The reason for doing this is the hypothesis that if the degree-hours are a realistic way of correlating the climate, then they would be capable of explaining or, at least, correlating the energy behavior of a building with reasonable feasibility. According to this premise, the DH for several arrangements were tested and finally it was concluded that 20 summer days are quite enough to reach the same quality and accuracy of results than if a 365-day calculation was made.

In **Figures 6** and **7**, the plot of DH versus daily heat gain, cooling load and extraction rates is shown for Mexicali, México and Cienfuegos and Cuba, respectively. It can be observed that the

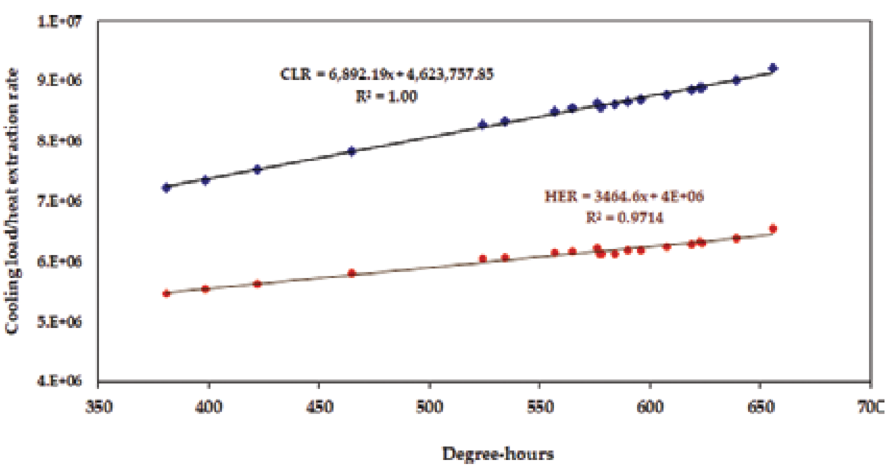

Figure 6. DH correlation with cooling load and heat extraction rates. Mexicali, México.

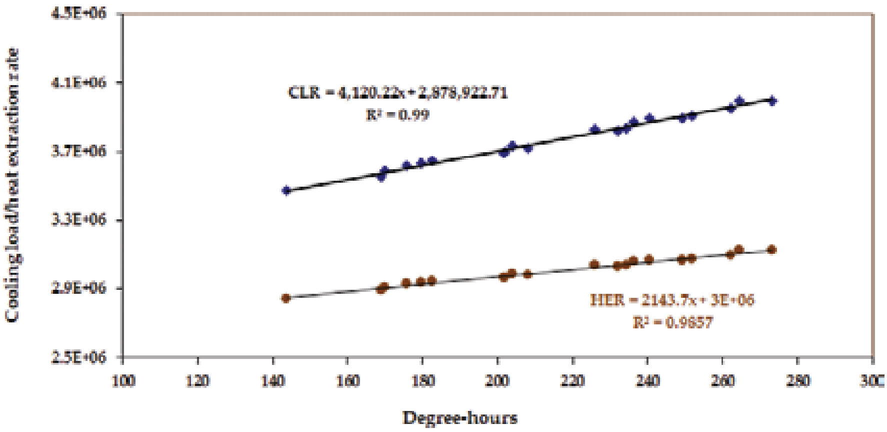

Figure 7. DH correlation with cooling load and head extraction rates. Cienfuegos, Cuba.

correlation coefficients R^2 are excellent for both cities. It must be noted that meteorological data for Cienfuegos are available only on a 3-h basis. In spite of this poor quantity of data, the results are still quite satisfactory. Correlation equations are readily obtained from DH and the three variables mentioned earlier, although DH versus cooling load rate (CLR) and DH versus heat extraction rate (HER) are most useful for our purposes.

Thermostat temperature is the reference baseline to calculate DH for the rest of the days of the year. Once the equation is available for CLR, its daily values are generated for the entire year and linked to the next module where daily heat extraction rates are estimated in the same manner as done for cooling load. When the TFM calculation is complete, the results of daily heat extraction rates are then correlated with DH for estimating the power consumption of the building while also including the variation of the air conditioning efficiency. The model that describes how the energy efficiency ratio (EER) varies as the outdoor temperature does is given below. At this stage, the EER values can now be applied together with HER correlation equation for computing the power consumed by HVAC system over the analyzed period of time.

2.3.3. *Efficiency of HVAC systems of air-cooled condensing units*

It is well known that the energy efficiency of air-conditioning systems varies strongly with the outdoor temperature, and in turn, temperature varies throughout the day. This is especially true for HVAC systems whose condensing units are cooled by outdoor air. Air is not a good conductor of heat and special care must be taken to maintain the proper operating conditions of the equipment. For this reason, a model considering this hourly variation has been incorporated into the simulator for calculating the rate of heat extraction. This allows better accuracy of the results. The model is quite simple and takes the form [26].

$$EER = e^{(a-bT)} \tag{13}$$

where EER is the Energy Efficiency Ratio (W/W, kBtu/kWh), a and b are correlation coefficients depending on the unit model and system (package or split) and T is the outdoor temperature (°F). It should be noted that Eq. (13) fits EER for new units within less than a ± 1% difference between calculated and measured values reported by manufacturers [26]. For older or used equipment, a less than unity correction factor must be used. This factor depends on several issues such as type of unit, age, model or dirt on heat transfer surfaces and should be found experimentally. Of course, such an investigative task is not feasible for most situations. In regions where humidity is small and if the HVAC unit receives appropriate maintenance, the factor value is 1 for all practical purposes. Besides, according to manufacturers, if any significant reduction of EER occurs during the first 5 years of use, it will be attributable to different causes such as refrigerant leakage or major damage to the equipment, among others.

An example of the EER variation for a given day is presented in **Figure 8**. For that day, the minimum and maximum temperatures are 43.3 and 27.5°C, respectively. EER is plotted as a function of time and its corresponding value can be read on the left axis while the outdoor temperature is allocated on the right axis. From this graph, it can be seen that as the temperature rises, the efficiency decreases proportionally.

2.3.4. Integrating results

Once the calculations described in previous sections have been completed, the program generates a set of daily and monthly values of DH, cooling load and power consumption. Likewise, the values and percentage of the most important variables contributing to cooling/heating loads are internally stored and displayed for a better understanding. The most important results are presented in a separate spreadsheet where power consumption, maximum peak demand and billing are displayed on a monthly basis. Also, the contribution to cooling load of roof, walls, fenestration, occupancy, lighting, internal loads and infiltration/ventilation is displayed in a graph to show the user in an easy way how the heat loads are distributed all over the building and which of them are the most relevant over the total load.

Finally, beside the monthly consumption table of results, the billing is added. In this manner, not only the energy balance is in sight but also the economic aspects can be visualized at the same time which as a whole allow the user to make better decisions.

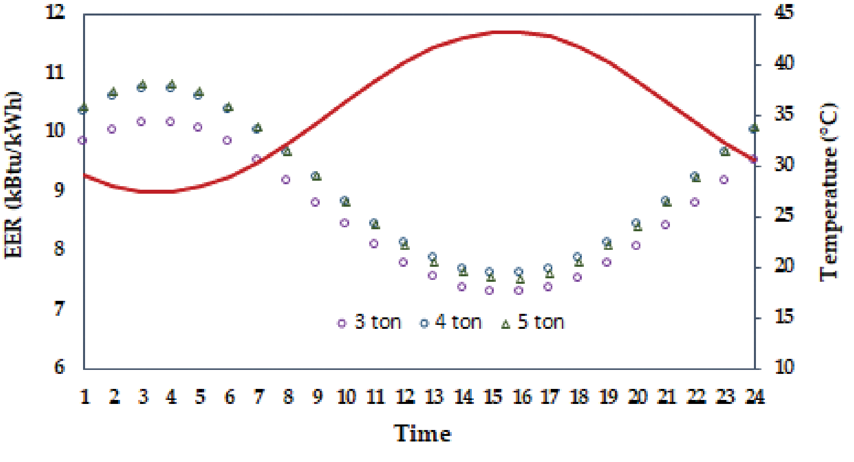

Figure 8. EER variation as a function of outdoor temperature (split units).

2.4. Successful application of the management approach

In 1990, the Mexican federal government started a local program intended to save energy in residential households in the city of Mexicali. The first stage of the program consisted of roof insulation and by 1997, the replacement of old low-efficiency air conditioning systems with new high-efficiency units was initiated. The replacement of refrigerators with more than 10 years of use began in 2003. This program for energy saving is called Program for Integral Systematic Saving ((ASI) by its acronym in Spanish) and remains in progress currently.

The application of the methodology outlined earlier allowed to sustain the energy saving strategies and actions of the ASI program, first in the city of Mexicali then in the rest of the country. Thermal simulation and DH methodology have proven to be a powerful tool for over more than 20 years in which a large number of projects have been developed with the residential, public, governmental and industrial sectors. One of them provided the technical support for the creation of the ASI program. [27]. An evaluation of the impact on consumption habits of inhabitants due to the actions and strategies carried out by the ASI program was made recently [28].

3. Conclusions

The methodology described earlier has proven to be a useful tool for the analysis and evaluation of projects related to saving and efficient use of energy. The use of DH as a primary variable has shown to be an excellent option for the characterization of the climate of a region, especially in hot-dry environments. However, its application is not restricted only to these climates, but it can also be extended to any climate without reducing reliability. Likewise, the utilization of DH greatly simplifies and speeds up the calculation when performing thermal simulation due to its excellent degree of correlation with heat gain, cooling load and heat extraction rates. At the same time, applying the DH criterion also allows to estimate the electrical consumption and demand of HVAC systems in a reliable way. A representative example of the usefulness of this methodology has been its application to the development and assessment of those projects sustaining the energy saving programs of the Mexican federal government, which are currently grouped as the ASI program.

The ASI program started its application as a local energy-saving program in 1990 in the city of Mexicali, with a current population of over 1 million inhabitants, and because of the success and positive impacts achieved in reducing peak demand and energy saving, it has been extended to warm-climate regions all over the country.

Acknowledgements

The authors wish to thank to PFCE program 2018 for funding publishing fees to Universidad Autónoma de Baja California, Instituto de Ingeniería.

Author details

Carlos Pérez-Tello*, Héctor Campbell-Ramírez, José Alejandro Suástegui-Macías and Marianela Soledad Reinhardt

*Address all correspondence to: carlosperez@uabc.edu.mx

Instituto de Ingeniería, Universidad Autónoma de Baja California, Mexicali, México

References

[1] Yang L, Yan H, Lam J. Thermal comfort and building energy consumption implications—A review. Applied Energy. 2014;**115**:164-173. DOI: 10.1016/j.apenergy.2013.10.062

[2] Djunaedy E, van den Wymelenberg K, Acker B, Thimmana H. Oversizing of HVAC system: Signatures and penalties. Energy and Buildings. 2011;**43**:468-475. DOI: 10.1016/j.enbuild.2010.10.011

[3] Program for Integral Systematic Saving. 2016. Available from: http://programaasibc.com.mx/nosotros.php. [Accessed: May 03, 2018]

[4] Dabaieha M, Wanas O, Amer Hegazyc M, Johanssona E. Reducing cooling demands in a hot dry climate: A simulation study for non-insulated passive cool roof thermal performance in residential buildings. Energy and Buildings. 2015;**89**:142-152. DOI: 10.1016/j.enbuild.2014.12.034

[5] Goudarzia H, Mostafaeipour A. Energy saving evaluation of passive systems for residential buildings in hot and dry regions. Renewable and Sustainable Energy Reviews. 2017;**68**:432-446. DOI: 10.1016/j.rser.2016.10.002

[6] Chwieduk D. Impact of solar energy on the energy balance of attic rooms in high latitude countries. Applied Thermal Engineering. 2018;**136**:548-559. DOI: 10.1016/j.applthermaleng.2018.03.011

[7] Raut A, Gomez C. Assessment of thermal and energy performance of thermally efficient sustainable wall system for Malaysian low cost housing. Applied Thermal Engineering. 2018;**136**:309-318. DOI: 10.1016/j.applthermaleng.2018.03.017

[8] Kaiser J, Diener L, Wick P. Nanoparticles in paints: A new strategy to protect façades and surfaces. Journal of Physics. 2013;**429**. conference 1. DOI: 10.1088/1742-6596/429/1/012036

[9] Aranzabe E, Villasante P, March R, Arriortua M, Vadillo J, Larranaga A, Aranzabe A. Preparation and characterization of high NIR reflective pigments based in ultramarine blue. Energy and Buildings. 2016;**126**:170-176. DOI: 10.1016/j.enbuild.2016.05.011

[10] Sheikholeslami M. Numerical simulation for solidification in a LHTESS by means of nano-enhanced PCM. Journal of the Taiwan Institute of Chemical Engineers. 2018;**86**:25-41. DOI: 10.1016/j.jtice.2018.03.013

[11] Sheikholeslami M. Numerical modeling of nano enhanced PCM solidification in an enclosure with metallic fin. Journal of Molecular Liquids. 2018;**259**:424-438. DOI: 10.1016/j.molliq.2018.03.006

[12] Sheikholeslami M, Ghasemi A. Solidification heat transfer of nanofluid in existence of thermal radiation by means of FEM. International Journal of Heat and Mass Transfer. 2018;**123**:418-431. DOI: 10.1016/j.ijheatmasstransfer.2018.02.095

[13] National Weather Service. National Oceanic and Atmospheric Administration. 2012. Available from: https://www.weather.gov/key/climate_heat_cool [Accessed: April 10, 2018]

[14] Degree Days: Understanding heating and cooling degree days. Available from: http://www.degreedays.net/introduction. [Accessed: April 06, 2018]

[15] Christenson M, Manz H, Gyalistras D. Climate warming impact on degree-days and building energy demand in Switzerland. Energy Conversion and Management. 2006; **47**(6):671-686. DOI: 10.1016/j.enconman.2005.06.009

[16] De Rosa M, Bianco V, Scarpa F, Tagliafico L. Heating and cooling building energy demand evaluation; a simplified model and a modified degree days approach. Applied Energy. 2014;**128**:217-229. DOI: 10.1016/j.apenergy.2014.04.067

[17] Büyükalaca O, Bulut H, Yilmaz T. Analysis of variable-base heating and cooling degree-days for Turkey. Applied Energy. 2001;**69**(4):269-283. DOI: 10.1016/S0306-2619(01)00017-4

[18] American Society of Heating Refrigeration and Air Conditioning Engineers, editor. ASHRAE Handbook—Fundamentals. 9th ed. Atlanta: American Society of Heating, Refrigerating and Air-Conditioning Engineers, Inc.; 2009. pp. 9-12

[19] Reyes Rodríguez C. Analysis of the electric consumption of residential housing in two cities of Mexico [thesis]. Mexicali: Autonomous University of Baja California; 2017

[20] Pérez Tello C, Magaña Almaguer H, Suástegui Macías A, Reyes Rodríguez C. Degree-hour methodology for determining energy behavior of residential housing in Mexico. Congreso Universidad. 2016;**5**. ISSN-e: 2306-918 X, RNPS-e: 2318. Available from: http://www.congresouniversidad.cu/revista/index.php/congresouniversidad/index

[21] McQuinston F, Spitler J. American Society of Heating, Refrigerating and Air-Conditioning Engineers. Cooling and Heating Load Calculation Manual. 2nd ed. Atlanta: American Society of Heating, Refrigerating and Air-Conditioning Engineers, Inc.; 1992

[22] American Society of Heating Refrigeration and Air Conditioning Engineers, editors. ASHRAE Handbook—Fundamentals. Section IV. Load Energy Calculations. Atlanta: American Society of Heating, Refrigerating and Air-Conditioning Engineers, Inc.; 1985. Section IV. Load Energy Calculations

[23] McQuiston FC, Parker JD, Spitler JD. Heating, Ventilating, and Air Conditioning: Analysis and Design. 6th ed. Hoboken: John Wiley & Sons Inc.; 2005

[24] Carrier (TFM). Available from: http://dms.hvacpartners.com/docs/1004/public/01/hap_ehelp_004.pdf [Accessed: January 10, 2018]

[25] Al-Rabghi O, Al-Johani K. Utilizing transfer function method for hourly cooling load calculations. Energy Conversion and Management. 1997;**38**(4):319-332. DOI: 10.1016/S0196-8904(96)00051-9

[26] Núñez-Cerezo M. Thermodynamic behavior of air-conditioning systems in Mexicali residential sector [thesis]. Mexicali: Autonomous University of Baja California; 1999

[27] Pérez Tello C, Galindo Duarte M, Villa Carrillo J, Ramírez Galán M. Evaluation of air-conditioning systems, motors and refrigerators for the residential sector of Mexicali, B.C. Technical Report. Mexicali: Autonomous University of Baja California, Electric Federal Commision, Government of the State of Baja California; 1996

[28] Suástegui Macías J, Pérez Tello C, Acuña Ramírez A, Lambert Arista A, Magaña Almaguer H, Rosales Escobedo P, Ruelas Puente A. Assessment of electrical saving from energy efficiency programs in the residential sector in Mexicali, Mexico. Sustainable Cities and Society. 2018;**38**:795-805. DOI: 10.1016/j.scs.2018.01.031

Chapter 3

Air Conditioning Systems with Dual Ducts: Innovative Approaches for the Design of the Transport Network of the Air

Annunziata D'Orazio

Additional information is available at the end of the chapter

http://dx.doi.org/10.5772/intechopen.80093

Abstract

We present two methods for sizing the network for the transport of the air, from the air handling unit to the terminal units, for a dual duct system, where air flows in the "cold" duct at a temperature less than the ambient temperature, while air flows in the "hot" duct at a temperature higher than the ambient temperature. The methods, compared to the traditional design criteria, lead to a reduction of channel size and, therefore, of overall network size and cost as well. The first method requires the "cold" channel to transport air at a temperature value slightly lower (1 ÷ 2°C) than the minimum inlet temperature (variable with time) required by the zones. The second requires the "hot" channel to transport air at a temperature value slightly higher (1 ÷ 2°C) than the maximum inlet temperature (variable with time) required by the zones. The methods have been applied to some reference networks. The saving of side surface of the networks varies between 14 and 27% with respect to the traditional approach; the constraint on the maximum speed of the air through the ducts is always respected, while this does not always occur with traditional criteria.

Keywords: dual duct, ductwork design, healthcare facilities, network size, cost saving

1. Introduction

The control of the thermo-hygrometric conditions and indoor air quality (IAQ) in rooms generally requires extensive networks for the transport of heat transfer fluids, most commonly water and air. A network of air distribution, due to the low density of the air, is considerably bulky. In general in healthcare facilities, and in any case in many critical environments contained therein, the indoor air quality (IAQ) plays a significant role. For the health of patients, particularly immunosuppressed patients, it is necessary to maintain at the lowest possible levels the concentration of particulate matter, which may also be a support for the formation of colonies of microorganisms, and the concentration of chemical pollutants. This is achieved with a significant dilution of the contaminants, by means of the introduction into the environment of considerable airflows. Italian law [1–3] establishes that the air is drawn exclusively from outside (therefore recirculation is forbidden) and subjected to various filtration stages.

In these cases (particularly in operating rooms, intensive care units, or departments for immunosuppressed patients), the air conditioning systems generally used are all-air systems with (outdoor) constant flow (CAV), since the high number of air changes per hour (ACH) must be guaranteed (sometimes values up to 50 are achieved). The leading value of the flow rate is that related to ventilation, rather than to summer or winter loads, and all-air systems with variable airflow (VAV) have to be excluded.

The constraint on the airflow rate is very strict in all those cases in which the protection of persons from the propagation of pathogens and/or the action of chemical pollutants must be guaranteed, even outside strictly health-related environments. In fact, new problems always emerge relative to air quality: the resurgence of diseases originally eradicated, not least tuberculosis (TB); the onset of respiratory syndromes of acute type, some resistant to drugs and therefore potentially pandemics, as SARS [4–8]; and the threats of chemical and biological terrorism.

If it is necessary to remain in the context of the constant flow rate systems, one of the options is that of the dual duct system. It ensures a local control of temperature conditions, up to the individual environments (rooms), even if some require "hot" while others require "cold", and an excellent level of air quality.

On the other hand, this type of system implies expensive and bulky air distribution networks, requiring spaces for the installation of the duct systems not easily available in the building sector, and high energy consumption [9–14], conceivably due to the remarkable availability of cheap energy at the time when this type of system has been developed (1940s–1960s of the last century).

As it is known, two parallel branched networks transport the air from the air handling unit (AHU) to the terminal units. Air flows through the so-called hot duct at higher temperature, compared to the required temperature in the room [15–17], whereas it flows at lower temperature (than the room temperature) through the so-called cold duct. A mixing box, thermostatically controlled, draws air from the hot and cold ducts and supplies each zone with the required flow rate, at the appropriate supply air conditions.

By virtue of these supply air conditions, more specifically the supply air temperature, widely variable during daytime and along the course of the year, the conditions of comfort into the room can be ensured, for which the mean radiant temperature is not taken into account.

The mixing box limits the noise levels as well. Indeed, in order to avoid huge overall dimensions of ducts that may become excessive with respect to the spaces normally available for their installation, high values, depending on the flow rate, are set for velocities through the ducts. At values between 12.5 and 30 m/s, the arising aerodynamic noise may be greatly disturbing, and this noise problem is only partially solved by properly designing the channel configuration [18]. Nevertheless, the overall dimensions of the dual-channel networks still remain high.

The choice of constant temperature values for the cold duct and for the hot duct, respectively, lower and higher than the room temperature, implies that the hot and the cold flow rates, arising from the calculations, have high values, significantly close to the total flow rate that must be carried by the trunks. In fact, while the supply air temperature varies over time, tending to t_c in summer and to t_h in winter, the air temperatures of cold and hot ducts are generally kept almost constant. When the zones require cold (presumably in summer), almost entire flow rates of the zones come from the cold duct; if the zones require heat, presumably in winter, the most part of the total airflow rates comes from the hot duct. Then, both the cold and the hot duct should each be able to carry more than 80—90% of the flow rate of the zone.

In this chapter, an innovative approach is presented for the dimensioning of the channels, based on the choice of not constant values for the temperatures of hot and cold duct. The cold channel carries air at a temperature equal or slightly lower than the minimum supply air temperature, among those required by the different zones, variable with time. The hot duct delivers air at a constant temperature, higher than the absolute maximum value of the zone supply temperature [19]. As alternative, the hot channel transports air at a temperature value slightly higher ($1 \div 2°C$) than the maximum inlet temperature (variable with time) required by the zones, while the cold duct delivers air at a constant temperature, lower than the absolute minimum value of the zone supply temperature.

The method has been applied to some reference buildings, a day center for dialysis located in the Italian city of Lecce and a private hospital located in the Italian city of Rome. A comparison is produced with the results obtained from the design criteria traditionally used.

2. Dimensioning criteria for the channel network

The network of channels has a tree structure with the root representing the AHU and the leaves the terminal units of each zone.

The different supply air conditions determine the different thermal zones. The calculation proceeds by considering the sensible thermal load $\Phi_i(\tau)$ (of the ith environment), variable over time, and evaluating the constant flow rate G_i able to compensate these loads in each room. The calculation is also based on the usual constraint related to the temperature difference between air supply and room and takes into account the flow rate required for ventilation. The mixing box serving the zone, where the ith room is included, will supply the computed airflow rate required by the zone; into the mixing box will enter hot and cold airflow rates coming from the terminal trunks of the dual duct system.

For the first trunk departing from AHU, one can write the conservation of mass and energy as

$$G = \sum_i G_i = G_c(\tau) + G_h(\tau) \tag{1}$$

$$\sum_i \Phi_i(\tau) + c_p G_h(\tau)[t_h(\tau) - t_r(\tau)] + c_p G_c(\tau)[t_c(\tau) - t_r(\tau)] = 0 \tag{2}$$

where G is the total mass flow rate carried by the trunk; $G_c(\tau)$ and $G_h(\tau)$ are the flow rates carried by the cold and hot trunks at the temperatures $t_c(\tau)$ and $t_h(\tau)$, respectively; $t_r(\tau)$ is the room temperature; c_p is the specific heat at constant pressure of moist air; and $\Phi_i(\tau)$ is the thermal load, varying over time, in each environment. The subscripts "c" and "h" refer to the cold and hot channels, respectively. These relationships, in conditions of maximum sensible load in summer $\Phi_{s,\,sum}$ and in winter $\Phi_{s,\,win}$ (subscripts "sum" and "win" refer to these conditions, respectively) become

$$G = G_{c,\,sum} + G_{h,\,sum} \tag{3}$$

$$\Phi_{s,\,sum} + c_p G_{h,\,sum}(t_{h,\,sum} - t_{r,\,sum}) = c_p G_{c,\,sum}(t_{r,\,sum} - t_{c,\,sum}) \tag{4}$$

$$G = G_{c,\,win} + G_{h,\,win} \tag{5}$$

$$\Phi_{s,\,win} + c_p G_{c,\,win}(t_{r,\,win} - t_{c,\,win}) = c_p G_{h,\,win}(t_{h,\,win} - t_{r,\,win}) \tag{6}$$

We can write similar equations for any trunk.

For the channels of the first trunk, departing from AHU, the airflow rates $G_{c,\,sum}$, $G_{c,\,win}$, $G_{h,\,sum}$, and $G_{h,\,win}$ can be calculated from the equations above, once the temperature values $t_{c,\,sum}$, $t_{c,\,win}$, $t_{h,\,sum}$, and $t_{h,\,win}$ are properly set; similar equations allow one to calculate the airflow rates for the other trunks, for cold and hot air, and winter and summer conditions, at all levels of the network.

With regard to the control of the relative humidity in the environment, it should be recalled that by normal practice, it is performed centrally, while the temperature control is assigned to the mixing boxes. Usually the air treated by the AHU exits with a moisture content corresponding to the thermodynamic state characterized by the temperature of the environment ($t_{r,\,sum}$ or $t_{r,\,win}$) and 45% of relative humidity.

Once the layout of the network is given, the sizing of the channels can be derived if the air speeds in the various trunks k are properly set; a usual criterion to choose the air speeds, starting from the range of values of the airflow rates Q_{hk}, Q_{ck} carried by the trunks, is reported as example in **Table 1** [20, 21].

In practical cases, as it is well known, a conventional sizing criterion is used. The criterion is based on the assumption that for each trunk, and therefore for each level of the network, it is possible to establish a priori the distribution between heat demand and cold demand, satisfied by hot duct and cold duct, respectively, once this distribution is known for the main trunk departing from the AHU (and therefore for the system as a whole). The method proceeds as follows:

a. The total airflow rates at each level of the network, that related to system (departing from the AHU) and those related to the various trunks, are determined from the supply airflow

Airflow rate through the trunks Q_{hk}, Q_{ck}, m^3/h	v_{max}, m/s
10^5–7×10^4	30
7×10^4–4.5×10^4	25
4.5×10^4–2.5×10^4	22.5
2.5×10^4–1.7×10^4	20
1.7×10^4–10^4	17.5
10^4–5×10^3	15
5×10^3–2×10^3	12.5

Table 1. Maximum air speed in the ducts.

A	**B**	**C**
$G_{c,sum}/G$	$G_{c,k}/G_k$	$G_{h,k}/G_{c,k}$
1.0–0.90	1	0.7
0.89–0.85	0.95	0.7
0.84–0.80	0.9	0.75
0.79–0.75	0.85	0.75
≤0.74	0.8	0.8

Table 2. Conventional ratios for the sizing of hot and cold ducts, in the absence of perimeter heating.

rates required by individual environments and served by the trunk, as it has been previously described.

b. Similarly, the airflow rates of hot and cold channels in the first trunk departing from the AHU are evaluated, once that the temperatures $t_{c,sum}$, $t_{c,win}$, $t_{h,sum}$, and $t_{h,win}$ have been set.

c. By considering the summer case, the ratio is calculated between the total flow rate in the cold channel, $G_{c,sum}$, and the total airflow rate of the plant G.

d. Once this ratio, representing the request of cold, is known, the corresponding values for the kth trunk of the same ratio $G_{c,k}/G_k$ are chosen, for example, according to the values of column B of **Table 2** [21]. In **Table 2**, one can set the range of values in column A, related to the first trunk departing from the AHU, and then obtain, from column B and C, the values of the ratio to assign to the trunks, for cold and hot duct, respectively, at each level of the network. This procedure avoids to solve the equations for each trunk, which require the thermal loads be known for each level of the network.

e. From the total flow rate G_k of the trunk, one can obtain the airflow rate of the cold channel $G_{c,k}$ of the trunk from the ratio of column B.

f. For each trunk, one can calculate the airflow of the hot duct $G_{h,k}$ as a percentage of the flow rate of the relative cold duct, with reference to the column C of **Table 2**.

In order to evaluate the order of magnitude of the airflow rate, let us consider the mass balance:

$$G_n = \left[\sum G_i\right]_n = G_{c,n}(\tau) + G_{h,n}(\tau) \tag{7}$$

with reference to the generic zone n of the plant, and the energy balance

$$\left[\sum_i \Phi_i(\tau)\right]_{n,sum} + c_p G_{h,sum,n}(\tau)[t_{h,sum}(\tau) - t_{r,sum}] = c_p G_{c,sum,n}(\tau)[t_{r,sum} - t_{c,sum}(\tau)] \tag{8}$$

in summer and

$$\left[\sum_i \Phi_i(\tau)\right]_{n,win} + c_p G_{c,win,n}(\tau)[t_{r,win} - t_{c,win}(\tau)] = c_p G_{h,win,n}(\tau)[t_{h,win}(\tau) - t_{r,win}] \tag{9}$$

in winter. On the other hand, we also have in summer:

$$\left[\sum_i \Phi_i(\tau)\right]_{n,sum} = c_p G_n[t_{r,sum} - t_{in,sum}(\tau)] = [G_{c,n}(\tau) + G_{h,n}(\tau)][t_{r,sum} - t_{in,sum}(\tau)] \tag{10}$$

and in winter:

$$\left[\sum_i \Phi_i(\tau)\right]_{n,win} = c_p G_n[t_{in,win}(\tau) - t_{r,win}] = [G_{c,n}(\tau) + G_{h,n}(\tau)][t_{in,win}(\tau) - t_{r,win}] \tag{11}$$

where the subscript "in" refers to the variable for inlet conditions (supply air conditions). By substitution, one obtains for both summer and winter:

$$G_{h,n}(\tau)[t_h(\tau) - t_{in}(\tau)] = G_{c,n}(\tau)[t_{in}(\tau) - t_c(\tau)] \tag{12}$$

$$\frac{G_{c,n}}{G_{h,n}} = \frac{[t_h(\tau) - t_{in}(\tau)]}{[t_{in}(\tau) - t_c(\tau)]} = \frac{\Delta t_{h,in}}{\Delta t_{c,in}} \tag{13}$$

Generally, temperatures of the cold and hot channel are kept almost constant, while the zone supply temperature varies over time, tending to t_c in summer and to t_h in winter. It implies that the computed airflow rates, for the hot and the cold duct, are significant fractions of the total airflow rate in the trunks. The air supplied to each zone, in summer, comes largely from the cold duct and in winter flows largely in the hot one. Then, both the cold and the hot ducts should each be able to carry more than 80–90% of the flow rate of the zone.

The trunk, which consists of the pair of hot and cold ducts, is coherently dimensioned to carry 1.7–1.8 times the supply airflow rate of the zone, once that one sets the values of the airspeed, and this occurs at all the levels of the network, with consequently considerable overall dimensions and high costs.

3. The new method for network dimensioning

As alternative method for network dimensioning, an innovative approach is presented here, based on the choice of not constant values for the temperatures of hot and cold duct, where either one of the hot and cold networks always carries the most part of the flow rate of the trunks k.

In the first case (method 1), the cold channel carries air at a temperature equal to or slightly lower (1 or 2°C) than the minimum supply air temperature, among those required by the different zones (which varies in time). The hot duct delivers air at a constant temperature t_h, higher than the absolute maximum value of the zone supply temperature [19]. The value of the minimum supply air temperature $t_{in,\,\mathrm{min}j}$ can be over time either lower or higher than the room temperature t_r (this occurs generally in summer time and in winter time, respectively); as a consequence, the value t_c of the cold network temperature can be either lower or higher than t_r. As alternative (method 2), the hot channel transports air at a temperature value slightly higher (1 ÷ 2°C) than the maximum inlet temperature (variable with time) required by the zones, while the cold duct delivers air at a constant temperature, lower than the absolute minimum value of the zone supply temperature.

The new approach implies reduced overall dimensions (reduced space requirements) and lower installation costs of the networks and therefore represents an improvement with regard to the two critical aspects of the dual duct systems currently designed.

For the generic zone n, once that the values of

$$t_c(\tau) = t_{in,\,min}(\tau) - \delta, \qquad \delta = 1 - 2^{\circ}C \tag{14}$$

are fixed and the mass balance is written as

$$G_n = \left[\sum G_i\right]_n = G_{c,\,n}(\tau) + G_{h,\,n}(\tau) \tag{15}$$

the energy balance becomes

$$\Phi_{s,\,sum} + c_p G_{h,\,sum}(t_{h,\,sum} - t_{r,\,sum}) = c_p G_{c,\,sum}\left(t_{r,\,sum} - t^*_{c,\,sum}\right) \tag{16}$$

$$\Phi_{s,\,sum} = c_p G_{n,\,sum}[t_{r,\,sum} - t_{in}(\tau)] \tag{17}$$

for summer conditions and

$$\Phi_{s,\,win} + c_p G_{c,\,win}\left(t_{r,\,win} - t^*_{c,\,win}\right) = c_p G_{h,\,win}(t_{h,\,win} - t_{r,\,win}) \tag{18}$$

$$\Phi_{s,\,win} = c_p G_{n,\,win}[t_{in}(\tau) - t_{r,\,win}] \tag{19}$$

for the winter ones.

By substitution we obtain for both summer and winter:

$$G_{c,\,n}(\tau)\left[t_{in}(\tau) - t^*_c(\tau)\right] = G_{h,\,n}(\tau)[t_h - t_{in}(\tau)] \tag{20}$$

$$\frac{G_{c,\,n}}{G_{h,\,n}} = \frac{[t_h(\tau) - t_{in}(\tau)]}{\left[t_{in}(\tau) - t^*_c(\tau)\right]} \tag{21}$$

Eq. (21) says that, both in winter and summer, the cold airflow rates $G_{c,n}$ flowing through the cold trunks and supplying the mixing boxes represent higher fractions of the total flow rates of the zones if the differences, between the constant hot duct temperature and the supply temperatures, are high and if the differences between those and the minimum supply air temperature are small.

For each zone, sensible thermal loads can be calculated as a function of time, and the same can be done for the supply air temperature values in the environments of the zone:

$$t_{in}(\tau) = t_r - \frac{\Phi_{s,n}(\tau)}{c_p G_n} \tag{22}$$

The minimum value of the supply air temperature $t_{in,min}(\tau)$ reduced by δ, hour by hour, represents the temperature of the cold channel $t_c^*(\tau)$. For each trunk k of the network, for each time interval j, one can write the energy and mass balances, in winter and in summer, as

$$G_k = G_{c,kj} + G_{h,kj} \tag{23}$$

$$\Phi_{s,sum,kj} + c_p G_{h,sum,kj}[t_{h,sum} - t_{r,sum}] = c_p G_{c,sum,kj}\left[t_{r,sum} - t_{cj}^*\right] \tag{24}$$

$$\Phi_{s,win,kj} + c_p G_{c,win,kj}\left[t_{r,win} - t_{cj}^*\right] = c_p G_{h,win,kj}[t_{h,win} - t_{r,win}] \tag{25}$$

Once that the air velocity values in all different trunks are fixed, referring to **Table 1**, for example, and from the maximum values of the cold and hot airflow rates in the trunks, the diameters of the hot and cold ducts of each trunk can be evaluated. Once the lengths of the various trunks of the network are known, one can calculate the surfaces of the ducts and so the weight of the network.

With a similar approach, we can write

$$t_h(\tau) = t_{in,max}(\tau) + \delta, \qquad \delta = 1 - 2^{\circ}C \tag{14'}$$

and fix the temperature $t_c(\tau)$, for example, equal to the dew point value. With the same consideration of the previous case, we obtain Eq. (20′) and Eq. (21′) as

$$G_{c,n}(\tau)[t_{in}(\tau) - t_c] = G_{h,n}(\tau)\left[t_h^*(\tau) - t_{in}(\tau)\right] \tag{20'}$$

$$\frac{G_{c,n}}{G_{h,n}} = \frac{\left[t_h^*(\tau) - t_{in}(\tau)\right]}{[t_{in}(\tau) - t_c]} \tag{21'}$$

4. Application example of the proposed method

The proposed method is applied here to calculate the dual duct networks of two reference buildings. The first (building A) is a day center for dialysis located in the city of Lecce (Southern Italy); the second is a private hospital located in the city of Rome (Central Italy).

The room temperature in summer is equal to 26°C for both the buildings; the room temperature in winter is equal to 22 and 20°C, respectively, for building A and building B.

For a day type for each month of the year and a daily period of 12 h (from 6:00 AM to 6:00 PM), the thermal loads of the different zones have been obtained as a function of time. Therefore, it has been possible to define the thermal zones and to evaluate the airflow rates required for each environment, to cope with the maximum sensible load in summer, the maximum sensible load in winter, and the ventilation needs. The AHU processes a total flow rate of air that obviously is the sum of the greatest of the three previous values, extended to all the zones.

In order to limit a priori the network extension, two AHUs have been used for building A, one serving 12 zones and 20 trunks as one serving 11 zones and 18 trunks. For building B, three AHUs have been used, each one serving 6 zones and 11 trunks.

Data for each network, namely, the lengths, airflow rates and maximum speeds in the trunks, are given in **Tables 3** and **4** for building A and building B, respectively.

Network AA				**Network AB**		
k	$l_k[m]$	$v_{max}[m/s]$	$Q_k[m^3/h]$	$l_k[m]$	$v_{max}[m/s]$	$Q_k[m^3/h]$
1	2.00	22.50	35980.30	2.00	22.50	32022.85
2	3.00	15.00	7582.58	3.00	15.00	7877.03
3	1.00	12.50	2641.67	1.00	12.50	2708.71
4	2.00	12.50	1993.48	2.00	12.50	2708.71
5	3.00	12.50	2947.43	3.00	12.50	2459.61
6	7.00	22.50	28397.72	7.00	20.50	24145.83
7	4.50	20.00	19172.40	4.50	17.50	15317.31
8	1.00	15.00	8705.97	1.00	20.00	9131.37
9	1.00	12.50	2697.94	1.00	12.50	2247.55
10	3.00	12.50	2033.26	3.00	12.50	2708.71
11	2.00	12.50	3974.76	2.00	12.50	4175.11
12	4.00	15.00	10466.43	4.00	15.00	6185.94
13	10.00	12.50	3919.05	10.00	12.50	3203.69
14	1.00	15.00	28397.72	1.00	15.00	24145.83
15	1.00	12.50	2861.81	1.00	12.50	2950.86
16	3.00	12.50	3517.49	3.00	12.50	2944.17
17	1.00	12.50	2846.02	1.00	12.50	2933.49
18	2.00	15.00	10466.43	2.00	12.50	6185.94
19	2.00	12.50	3562.29			
20	2.00	12.50	2985.09			

Table 3. Data of the networks AA and AB of building A.

Network BA				Network BB			Network BC		
k	$l_k[m]$	$v_{max}[m/s]$	$Q_k[m^3/h]$	$l_k[m]$	$v_{max}[m/s]$	$Q_k[m^3/h]$	$l_k[m]$	$v_{max}[m/s]$	$Q_k[m^3/h]$
1	3.00	17.50	12551.76	3.00	17.50	14691.15	3.00	17.50	13593.78
2	2.50	12.50	1774.82	2.50	12.50	2143.52	2.50	12.50	2089.40
3	5.00	17.50	10776.94	5.00	17.50	12547.63	5.00	17.50	11504.38
4	3.00	17.50	8573.20	3.00	17.50	10790.94	3.00	17.50	9563.88
5	2.50	12.50	2562.82	2.50	12.50	2586.83	2.50	12.50	2043.60
6	8.00	15.00	6010.38	8.00	15.00	8204.11	8.00	15.00	7520.28
7	3.00	15.00	4166.51	3.00	15.00	5965.41	3.00	15.00	5385.96
8	2.50	12.50	1982.66	2.50	12.50	3402.44	2.50	12.50	3463.73
9	6.00	12.50	2183.85	6.00	12.50	2562.98	6.00	12.50	1922.23
10	2.50	12.50	1843.87	2.50	12.50	2238.69	2.50	12.50	2134.32
11	2.50	12.50	2203.74	2.50	12.50	1756.69	2.50	12.50	1940.50

Table 4. Data of the networks BA, BB, and BC of building B.

The diameters of the hot and cold channels are representative of the size of the whole network; the peripheral surface of the ducts stands as indicative parameter for the weight of the network and therefore of its cost. As an index of the overall dimension of the single trunk $\boldsymbol{k}$, the covering factor $\boldsymbol{F_k}$ was also introduced, according to [16, 19]:

$$\boldsymbol{F_k} = \frac{\boldsymbol{G_{k,\,max}}}{\boldsymbol{G_k}} \tag{26}$$

It is defined as the ratio between the airflow rate $\boldsymbol{G_k}$ that flows through the $\boldsymbol{k}$th trunk and $\boldsymbol{G_{k,\,max}}$

$$\boldsymbol{G_{k,\,max}} = \frac{\pi}{4} v_k \left[\boldsymbol{D_{hk}^2} + \boldsymbol{D_{ck}^2}\right] \tag{27}$$

which represents the flow rate that the trunk, already dimensioned, could carry if the air flowed at the maximum set speed.

The $\boldsymbol{F_k}$ factor takes values between 1 and 2; it approaches 1 when only one of the two ducts actually carries the entire flow rate of the trunk, while the other duct carries only a small correction. The factor tends instead to 2 when the both hot and cold ducts can both carry the entire flow rate of the trunk. With regard to the whole network, the $\boldsymbol{F_{net}}$ factor can be defined as the weighted average of $\boldsymbol{F_k}$, where the weights are the products between the lengths and the flow rates of the trunks:

$$\boldsymbol{F_{net}} = \frac{\sum_k \boldsymbol{F_k G_k l_k}}{\sum_k \boldsymbol{G_k l_k}} \tag{28}$$

http://dx.doi.org/10.5772/intechopen.80093

5. Analysis of results

The results of the dimensioning of the networks with the first approach (method 1) refer to the networks AA, AB and BA, BB, and BC in the case of air temperature t_c in the cold duct taken equal to the minimum required (minus 1°C) and of the air temperature t_h in the hot duct taken as equal to 40°C. Results obtained with the second approach (method 2) refer to the same networks, in the case of air temperature t_h in the hot duct taken equal to the maximum required (plus 1°C) and of air temperature t_c in the cold duct taken as equal to the dew point value (for building A, 13°C in summer and 10°C in winter, for building B, 13°C in summer and 7°C in winter).

In order to make a comparison between the results obtained with the traditional sizing method, the savings are briefly presented in **Tables 5** and **6**, respectively, for building A and building B, as they are obtained for the five networks, in terms of the peripheral surface of the channels and of the evaluated values of the network factor F_{net}.

In **Table 7** we report the savings of side surface and the network factor by considering the whole building A and the whole building B.

For the building A, the maximum value obtained for F_{net} is 1.33, and it occurs for the network AA when the hot duct temperature t_h varies (method 2); it decreases to 1.15, for the networks AB when we use the method 1. For the building B, the maximum is obtained for the network BC when method 2 is used; the minimum occurs for the network BA with method 2 again. The achieved values of F_{net} with the proposed methods are always smaller than those obtained by using the traditional design criteria.

	Method 1	**Method 2**	**Traditional method**
	Saved surface (%)-F_{net}		F_{net}
Network AA	31–1.26	14–1.33	1.76
Network AB	22–1.15	13–1.21	1.60

For method 1: $t_h = 40^\circ$C. For method 2: $t_{c,sum} = 13^\circ$C, $t_{c,win} = 10^\circ$C.

Table 5. Savings' percentage of the total side surface and network factors for building A.

	Method 1	**Method 2**	**Traditional method**
	Saved surface (%)-F_{net}		F_{net}
Network BA	18–1.41	14–1.283	1.65
Network BB	25–1.34	18–1.36	1.70
Network BC	19–1.43	15–1.47	1.80

For method 1: $t_h = 40^\circ$C. For method 2: $t_{c,sum} = 13^\circ$C, $t_{c,win} = 7^\circ$C.

Table 6. Savings' percentage of the total side surface and network factors for building B.

	Method 1	Method 2	Traditional method
	Saved surface (%)-F_{net}		F_{net}
Building A	27–1.21	14–1.28	1.7
Building B	21–1.35	17–1.37	1.72

Table 7. Savings' percentage of the total side surface and network factors for buildings A and B.

The results prove that the new methods allow a substantial reduction in the overall dimensions. This reduction is largely shared by the whole network. For all trunks, and with regard to method 1, a substantial equivalence, or a weak increase of the diameters of the cold duct (compared to those obtained with the traditional methods), is counteracted by a significant reduction of the diameters of the hot duct. Vice versa, with regard to method 2, a weak increase of diameters of the hot duct is counteracted by a substantial reduction of diameter of the cold duct. The effect on the overall dimensions can be represented in terms of sum of the diameters of cold and hot ducts. The comparison between the methods is reported in **Figure 1** for each trunk of a network. **Figure 1** refers to the case of the building A (network AA). Similar behaviors occur for the other networks; in terms of reduction of overall dimensions, method 1 seems to be more efficient.

The surface fraction, saved by using both the new methods compared to the traditional one, presents not negligible values. With reference to the traditional method, the savings range

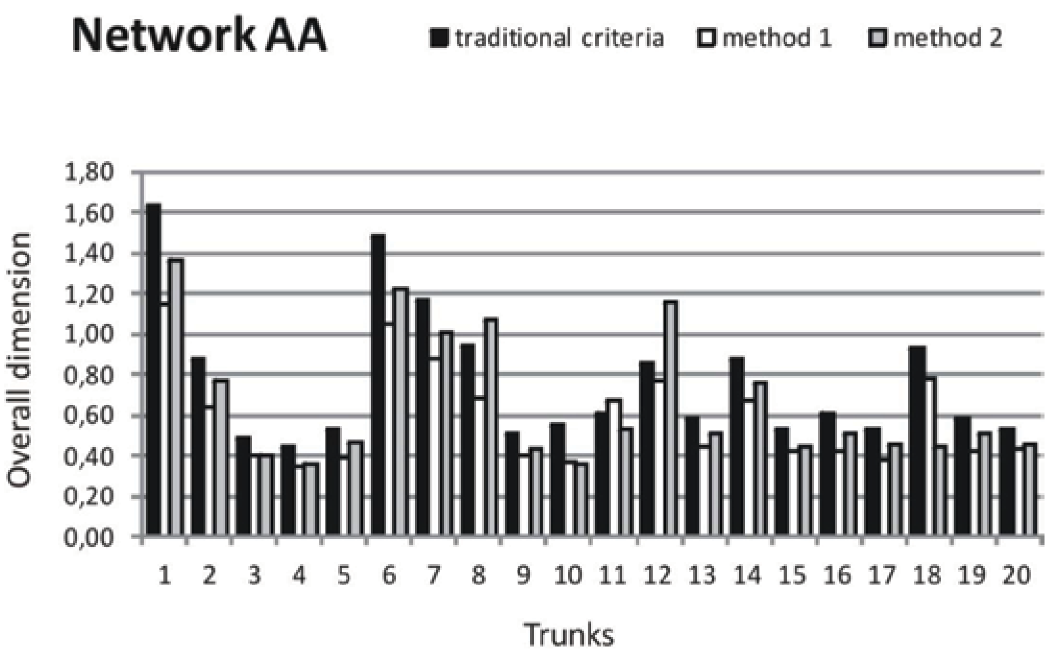

Figure 1. Overall dimensions for each trunk of the network: sum of diameters of cold and hot ducts.

between 14 and 27% for the building A (located in Lecce), when methods 2 and 1 are used, respectively, and between 17 and 21% for the building B.

Therefore, both methods imply a reduction of side surface (and cost). For the building B (located in Rome), for which the room temperature in winter is lower, the savings obtained in terms of surface, by using the two methods, differ only for 4%. For the building A (in Lecce), for which the room temperature in winter is higher, the savings obtained with method 2 is almost half of that obtained with method 1. Method 2 works better for the building B, where room temperature is higher.

Both methods imply lower network factors, with respect to the traditional method, but it is preferable to use one method rather than another according to the summer and winter design temperatures. In our study, a lower winter design temperature implies an increase in savings by using method 2.

If we consider the absolute maximum and minimum values of the supply temperature (for all hours, all year round, and regardless of the zone), we can see that the network factors tend to increase with the difference between these maximum and minimum values, for both methods 1 and 2. In general, method 1 allows to obtain lower network factors.

6. Conclusions

In general in healthcare facilities, and in any case in many critical environments contained therein, the indoor air quality (IAQ) plays a significant role. For the health of patients, particularly immunosuppressed patients, it is necessary to maintain at the lowest possible levels the concentration of particulate matter, which may also be a support for the formation of colonies of microorganisms, and the concentration of chemical pollutants.

In these cases (particularly in operating rooms, intensive care units, or departments for immunosuppressed patients), the air conditioning systems generally used are all-air systems with (outdoor) constant flow (CAV), since the high number of air changes per hour (ACH) must be guaranteed (sometimes values up to 50 are achieved). The leading value of the flow rate is that related to ventilation, rather than to summer or winter loads, and all-air systems with variable airflow (VAV) are to be excluded.

The dual duct system ensures excellent IAQ and good control of the thermo-hygrometric conditions and allows temperature adjustment in each zone, up to individual environments (rooms).

In this chapter, an innovative approach is presented for the channel dimensioning, based on the choice of not constant values for the temperatures of hot and cold duct. More specifically, two approaches are described.

For the first approach, the cold duct carries air at a not constant temperature, equal to or slightly lower than the minimum supply air temperature, among those required hour by hour by the different zones; the hot duct carries air at a constant temperature, higher than the absolute maximum value of the zone supply temperature. For the second one, the hot duct transports air at a temperature value slightly higher than the maximum inlet temperature (variable with time) required by the zones, while the cold duct delivers air at a constant temperature, lower than the absolute minimum value of the zone supply temperature.

The new approach implies reduced overall dimensions and cost of the channel network.

The method has been applied to some networks of channels, and results were compared with those obtained, on the same networks, using the traditional sizing criteria.

The comparison was carried out in terms of diameters, network factors, and total side surfaces of the network. It shows that the overall dimensions of the networks decrease compared to the traditional sizing methods; the factor $\boldsymbol{F_{net}}$ varies between 1.21 and 1.37, while in traditional sizing, it assumes values around 1.7. As it has been seen in previous works [19], the decrease of network factor (and of side surfaces) is more significant for higher temperature of the hot duct (method 1) and lower temperature of cold duct (method 2). The constraint on the maximum speed of the air in the various trunks of the network is always respected, while it does not always occur with traditional criteria. The saving in terms of side surface varies between 27 and 21% with reference to the traditional approach for method 1 and between 14 and 17% for method 2. Both methods imply lower network factors, with respect to the traditional method, but it is preferable to use one method rather than another according to the summer and winter design temperatures. In our study, a lower winter design temperature implies an increase in savings by using method 2.

These new methods of sizing a dual duct network allow for a lighter network, with obvious economic advantages, and are easier to place. The network is able to guarantee the thermo-hygrometric comfort conditions for all conditions of thermal load, even in the medium periods; in addition, it allows a control of the air speed, always remaining below the maximum allowed values (this does not always happen with the traditional method).

It must be remembered that, unlike the traditional method that plans fixed temperature values for the hot and cold ducts, the proposed methods require a more complex control system that, starting from the value of the minimum or maximum supply temperatures of the different zones (which vary over time), can vary the temperature of the cold or hot duct.

For method 1, which guarantees better results compared to method 2, a further postheating battery dedicated to the cold duct must be provided.

Conflict of interest

The author declares that she has no conflict of interest.

Nomenclature

Acronyms

ACH air changes per hour

AHU air handling unit

http://dx.doi.org/10.5772/intechopen.80093

IAQ	indoor air quality
SARS	severe acute respiratory syndrome
TB	tuberculosis

Symbols

c_p	specific heat at constant pressure of moist air (J/kg °C)
D	diameter of the duct (m)
$\Delta t_{h,\boldsymbol{in}} = t_h(\tau) - t_{\boldsymbol{in}}(\tau)$	temperature difference between hot duct and inlet air conditions (°C)
$\Delta t_{c,\boldsymbol{in}} = t_{\boldsymbol{in}}(\tau) - t_c(\tau)$	temperature difference between inlet conditions and cold duct (°C)
F_k	covering factor of the kth trunk
F_{net}	covering factor of the whole network
G	air mass flow rate (kg/h)
$G_{k,\max}$	mass flow rate that the k-trunk could carry if the air flowed at the maximum set speed (kg/h)
$\mathrm{l_k}$	length of the kth trunk (m)
Q	volume airflow rate (m^3/h)
t	temperature (°C)
$t_{in,\min j}$	minimum inlet temperature at the time j (°C)
v_{max}	maximum air speed in the ducts (m/s)
$\Phi(\tau)$	sensible thermal loads (J/h)

Subscripts

r	refers the variables to the room conditions
h	refers the variables to the hot duct
i	refers the variables to the ith environment
in	refers the variables to the supply (inlet) conditions
j	refers the variables to the jth time interval
k	refers the variables to the kth trunk
n	refers the variables to the nth zone
sum	refers the variables to the summer conditions
win	refers the variables to the winter conditions

Author details

Annunziata D'Orazio

Address all correspondence to: annunziata.dorazio@uniroma1.it

Dipartimento di Ingegneria Astronautica, Elettrica ed Energetica, Sapienza University of Rome, Rome, Italy

References

[1] Ministero dei Lavori Pubblici. Circolare n. 13011 Requisiti fisico-tecnici per le costruzioni edilizie ospedaliere. Proprietà termiche, igrometriche, di ventilazione e di illuminazione. [Physical and Technical Requirements for Hospital Buildings. Thermal Properties, Humidity, Ventilation and Lighting] (in Italian). Italy: Italian Government; 1974

[2] Ente italiano di normazione UNI. UNI 10339:1995 Impianti aeraulici a fini di benessere. Generalità, classificazione e requisiti. Regole per la richiesta d'offerta, l'offerta, l'ordine e la fornitura. [Aeraulic Systems for Comfort. General Part, Classification and Requirements. Rules for Request for Quotation, the Offer, the Order and Supply] (in Italian). Milano: UNI; 1995

[3] Presidente della Repubblica. Decreto 14 gennaio 1997 (1). Approvazione dell'atto di indirizzo e coordinamento alle regioni e alle province autonome di Trento e di Bolzano, in materia di requisiti strutturali, tecnologici ed organizzativi minimi per l'esercizio delle attività sanitarie da parte delle strutture pubbliche e private. [Approval of the Act of Guiding and Coordinating to the Regions and the Autonomous Provinces of Trento and Bolzano, in Relation to Structural, Technological and Organizational Minimum Requirements for the Exercise of Health Activities by Public and Private Structures] (in Italian). Italy: President of the Italian Republic; 1997

[4] Shah NS, Wright A, Bai GH, Barrera L, Boulahbal F, Martín-Casabona N, Drobniewski F, Gilpin C, Havelkova M, Lepe R, Lumb R, Metchock B, Portaels F, Rodrigue MF, Rusch-Gerdes S, Van Deun A, Vincent V, Laserson K, Wells C, Cegielski JP. Worldwide emergence of extensively drug-resistant tuberculosis. Emerging Infectious Diseases. 2007:380-387. DOI: 10.3201/eid1303.061400

[5] World Health Organization. The 40th Session of Subcommittee on Planning and Programming of the Executive Committee; 20–22 March 2006; Washington, D.C., USA; 2006

[6] Morawska L. Droplet fate in indoor environments, or can we prevent the spread of infection? Indoor Air Supplement. 2005;**16**(5):335-347. DOI: 10.1111/j.1600-0668.2006.00432.x

[7] Fiegel J, Clarke R, Edwards D. Airborne infectious disease and the suppression of pulmonary bioaerosols. Drug Discovery Today. 2006;**11**(1):51-57. DOI: 10.1016/S1359-6446(05)03687-1

[8] Tellier R. Review of aerosol transmission of influenza A virus. Emerging Infectious Diseases. 2006;**12**(11):1657-1662. DOI: 10.3201/eid1211.060426

[9] Traver D. Air Conditioning System US Patent No. 3,867,980. Washington, DC: U.S. Patent and Trademark Office; 1975

[10] Joo IS, Liu M. Performance analysis of dual-fan, dual-duct constant volume air-handling units. ASHRAE Transactions. 2002;**108**(2):39-46

[11] Petterson B. Double duct Changeover HVAC System. US Patent no. 6,725,914 B2. Washington, DC: U.S. Patent and Trademark Office; 2004

[12] Lu L, Cai W, Xie L, Li S, Soh YC. HVAC system optimization-in building section. Energy and Buildings. 2005;**37**(1):11-22

[13] Liu G, Mingsheng L. Procedure and application for determining the cold deck and hot deck airflow in a dual-duct system. HVAC Technologies for Energy Efficiency. 2006;**IV-11-1**:1-9

[14] Joo IS, Liu M, Song L, Carico M. Demand-based optimal control to save energy: a case-study in a medical center. In: Proceedings of the 16th Symposium on Improving Building Systems in Hot and Humid Climates of Texas A&M University; 15–17 December 2008; Plano, USA ESL-HH-08-12-16:1–8; 2008

[15] Coogan JJ. Air Flow Control System and Method for a Dual Duct System. US Patent no. 5,350,113. Washington, DC: U.S. Patent and Trademark Office; 1994

[16] De Lieto Vollaro R, D'Orazio A, Fontana L. Impianti di condizionamento a doppio canale: Nuovo metodo di dimensionamento della rete di distribuzione. (Air conditioning systems with dual ducts: An innovative approach for the design of the transport network of the air). In: Proceedings of the 66th National Congress of Termotechnics Italian Association ATI; 5–9 September 2011; Rende (Cosenza), Italy. (in Italian)

[17] American Society of Heating, Refrigerating, and Air-Conditioning Engineers. ASHRAE Handbook–Systems and Equipment. Atlanta: ASHRAE; 2012

[18] American Society of Heating, Refrigerating, and Air-Conditioning Engineers. ASHRAE Handbook–HVAC Applications. Atlanta: ASHRAE; 2015

[19] D'Orazio A, Agostini C. Air-conditioning systems with dual ducts: An innovative approach to the design of the transport network of air. Science and Technology for the Built Environment. 2016;**22**:281-289. DOI: 10.1080/23744731.2016.1130515

[20] Ed H, Colombo N. Impianti Termici negli Edifici. Milano: Hoepli. (Heating and Cooling Systems in Buildings, in Italian); 2009

[21] The Chartered Institution of Building Services Engineers. CIBSE Concise Handbook. Norwich: CIBSE; 2008

Chapter 4

Types of HVAC Systems

Shaimaa Seyam

Additional information is available at the end of the chapter

http://dx.doi.org/10.5772/intechopen.78942

Abstract

HVAC systems are milestones of building mechanical systems that provide thermal comfort for occupants accompanied with indoor air quality. HVAC systems can be classified into central and local systems according to multiple zones, location, and distribution. Primary HVAC equipment includes heating equipment, ventilation equipment, and cooling or air-conditioning equipment. Central HVAC systems locate away from buildings in a central equipment room and deliver the conditioned air by a delivery ductwork system. Central HVAC systems contain all-air, air-water, all-water systems. Two systems should be considered as central such as heating and cooling panels and water-source heat pumps. Local HVAC systems can be located inside a conditioned zone or adjacent to it and no requirement for ductwork. Local systems include local heating, local air-conditioning, local ventilation, and split systems.

Keywords: HVAC systems, central HVAC systems, local HVAC systems, heating systems, air-conditioning systems

1. Introduction

Heating, ventilation, and air conditioning (HVAC) system is designed to achieve the environmental requirements of the comfort of occupants and a process.

HVAC systems are more used in different types of buildings such as industrial, commercial, residential and institutional buildings. The main mission of HVAC system is to satisfy the thermal comfort of occupants by adjusting and changing the outdoor air conditions to the desired conditions of occupied buildings [1]. Depending on outdoor conditions, the outdoor air is drawn into the buildings and heated or cooled before it is distributed into the occupied spaces, then it is exhausted to the ambient air or reused in the system. The selection of HVAC systems in a given building will depend on the climate, the age of the building, the individual preferences of the owner of the building and a designer of a project, the project budget, the architectural design of the buildings [1].

HVAC systems can be classified according to necessary processes and distribution process [2]. The required processes include the heating process, the cooling process, and ventilation process. Other processes can be added such as humidification and dehumidification process. These process can be achieved by using suitable HVAC equipment such as heating systems, air-conditioning systems, ventilation fans, and dehumidifiers. The HVAC systems need the distribution system to deliver the required amount of air with the desired environmental condition. The distribution system mainly varies according to the refrigerant type and the delivering method such as air handling equipment, fan coils, air ducts, and water pipes.

2. HVAC system selection

System selection depends on three main factors including the building configuration, the climate conditions, and the owner desire [2]. The design engineer is responsible for considering various systems and recommending more than one system to meet the goal and satisfy the owner of a building. Some criteria can be considered such as climate change (e.g., temperature, humidity, and space pressure), building capacity, spatial requirements, cost such as capital cost, operating cost, and maintenance cost, life cycle analysis, and reliability and flexibility.

However, the selection of a system has some constraints that must be determined. These constraints include the available capacity according to standards, building configuration, available space, construction budget, the available utility source, heating and cooling building loads.

3. Basic components of an HVAC system

The basic components or equipment of an HVAC system that delivers conditioned air to satisfy thermal comfort of space and occupants and the achieve the indoor air quality are listed below [3]:

a. Mixed-air plenum and outdoor air control

b. Air filter

c. Supply fan

d. Exhaust or relief fans and an air outlet

e. Outdoor air intake

f. Ducts

g. Terminal devices

h. Return air system

http://dx.doi.org/10.5772/intechopen.78942

i. Heating and cooling coils

j. Self-contained heating or cooling unit

k. Cooling tower

l. Boiler

m. Control

n. Water chiller

o. Humidification and dehumidification equipment

4. Classification of HVAC systems

The major classification of HVAC systems is central system and decentralized or local system. Types of a system depend on addressing the primary equipment location to be centralized as conditioning entire building as a whole unit or decentralized as separately conditioning a specific zone as part of a building. Therefore, the air and water distribution system should be designed based on system classification and the location of primary equipment. The criteria as mentioned above should also be applied in selecting between two systems. **Table 1** shows the comparison of central and local systems according to the selection criteria [3, 4].

Criteria	Central system	Decentralized system
Temperature, humidity, and space pressure requirements	Fulfilling any or all of the design parameters	Fulfilling any or all of the design parameters
Capacity requirements	• Considering HVAC diversity factors to reduce the installed equipment capacity • Significant first cost and operating cost	• Maximum capacity is required for each equipment • Equipment sizing diversity is limited
Redundancy	Standby equipment is accommodated for troubleshooting and maintenance	No backup or standby equipment
Special requirements	• An equipment room is located outside the conditioned area, or adjacent to or remote from the building • Installing secondary equipment for the air and water distribution which requires additional cost	• Possible of no equipment room is needed • Equipment may be located on the roof and the ground adjacent to the building
First cost	• High capital cost • Considering longer equipment services life to compensate the high capital cost	• Affordable capital cost
Operating cost	• More significant energy efficient primary equipment • A proposed operating system which saves operating cost	• Less energy efficient primary equipment • Various energy peaks due to occupants' preference • Higher operating cost

Criteria	Central system	Decentralized system
Maintenance cost	Accessible to the equipment room for maintenance and saving equipment in excellent condition, which saves maintenance cost	Accessible to equipment to be located in the basement or the living space. However, it is difficult for roof location due to bad weather
Reliability	Central system equipment can be an attractive benefit when considering its long service life	Reliable equipment, although the estimated equipment service life may be less
Flexibility	Selecting standby equipment to provide an alternative source of HVAC or backup	Placed in numerous locations to be more flexible

Table 1. Comparison of central and local HVAC systems.

5. HVAC system requirements

Four requirements are the bases for any HVAC systems [4]. They need primary equipment, space requirement, air distribution, and piping, as shown in **Figure 1**.

Primary equipment includes heating equipment such as steam boilers and hot water boilers to heat buildings or spaces, air delivery equipment as packaged equipment to deliver conditioned ventilation air by using centrifugal fans, axial fans, and plug or plenum fans, and refrigeration equipment that delivers cooled or conditioned air into space. It includes cooling coils based on water from water chillers or refrigerants from a refrigeration process.

Space requirement is essential in shaping an HVAC system to be central or local. It requires five facilities as the following:

a. Equipment rooms: since the total mechanical and electrical space requirements range between 4 and 9% of the gross building area. It is preferable to be centrally located in the building to reduce the long duct, pipe, and conduit runs and sizes, to simplify shaft layouts, and centralized maintenance and operation.

b. HVAC facilities: heating equipment and refrigeration equipment require many facilities to perform their primary tasks of heating and cooling the building. The heating equipment requires boiler units, pumps, heat exchangers, pressure-reducing equipment, control air compressors, and miscellaneous equipment, while the refrigeration equipment requires water chillers or cooling water towers for large buildings, condenser water pumps, heat exchangers, air-conditioning equipment, control air compressors, and miscellaneous equipment. The design of equipment rooms to host both pieces of equipment should consider the size and the weight of equipment, the installation and maintenance of equipment, and the applicable regulations to combustion air and ventilation air criteria.

c. Fan rooms contain the HVAC fan equipment and other miscellaneous equipment. The rooms should consider the size of the installation and removal of fan shafts and coils, the replacement, and maintenance. The size of fans depends on the required air flow rate to condition the building, and it can be centralized or localized based on the availability, location, and cost. It is preferable to have easy access to outdoor air.

d. Vertical shaft: provide space for air distribution and water and steam pipe distribution. The air distribution contains HVAC supply air, exhaust air, and return air ductwork. Pipe distribution includes hot water, chilled water, condenser water, and steam supply, and condenser return. The vertical shaft includes other mechanical and electrical distribution to serve the entire building including plumbing pipes, fire protection pipes, and electric conduits/closets.

e. Equipment access: the equipment room must allow the movement of large, heavy equipment during the installation, replacement, and maintenance.

Air distribution considers ductwork that delivers the conditioned air to the desired area in a direct, quiet, and economical way as possible. Air distribution includes air terminal units such as grilles and diffusers to deliver supply air into a space at low velocity; fan-powered terminal units, which uses an integral fan to ensure the supply air to the space; variable air volume terminal units, which deliver variable amount of air into the space; all-air induction terminal units, which controls the primary air, induces return air, and distributes the mixed air into a space; and air-water induction terminal units, which contains a coil in the induction air stream. All the ductwork and piping should be insulated to prevent heat loss and save building energy. It is also recommended that buildings should have enough ceiling spaces to host ductwork in the suspended ceiling and floor slab, and can be used as a return air plenum to reduce the return ductwork.

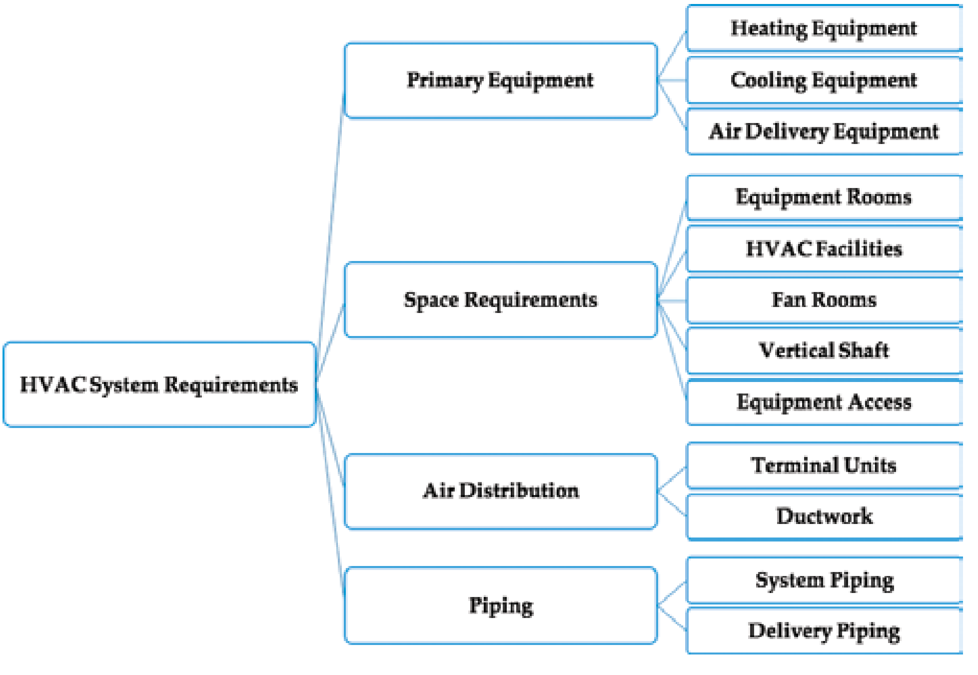

Figure 1. Horizontal hierarchy representation of HVAC system requirements.

The piping system is used to deliver refrigerant, hot water, cooled water, steam, gas, and condensate to and from HVAC equipment in a direct, quiet and affordable way. Piping systems can be divided into two parts: the piping in the central plant equipment room and the delivery piping. HVAC piping may or may not be insulated based on existing code criteria.

6. Central HVAC systems

A central HVAC system may serve one or more thermal zones, and its major equipment is located outside of the served zone(s) in a suitable central location whether inside, on top, or adjacent to the building [4, 5]. Central systems must condition zones with their equivalent thermal load. Central HVAC systems will have as several control points such as thermostats for each zone. The medium used in the control system to provide the thermal energy sub-classifies the central HVAC system, as shown in **Figure 2**.

The thermal energy transfer medium can be air or water or both, which represent as all-air systems, air-water systems, all-water systems. Also, central systems include water-source heat pumps and heating and cooling panels. All of these subsystems are discussed below. Central HVAC system has combined devices in an air handling unit, as shown in **Figure 3**, which contains supply and return air fans, humidifier, reheat coil, cooling coil, preheat coil, mixing box, filter, and outdoor air.

6.1. All-air systems

The thermal energy transfer medium through the building delivery systems is air. All-air systems can be sub-classified based on the zone as single zone and multizone, airflow rate for each zone as constant air volume and variable air volume, terminal reheat, and dual duct [5].

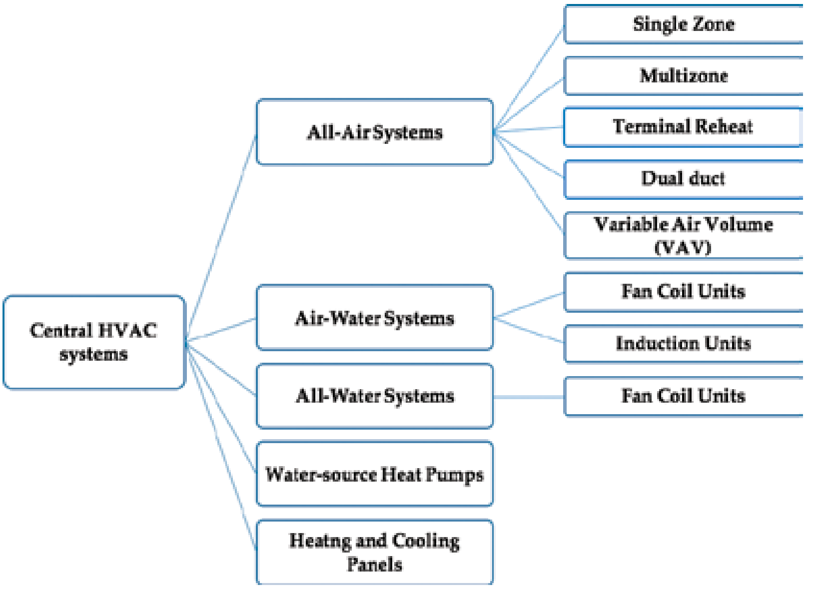

Figure 2. Horizontal hierarchy representation of the main types of central HVAC systems.

http://dx.doi.org/10.5772/intechopen.78942

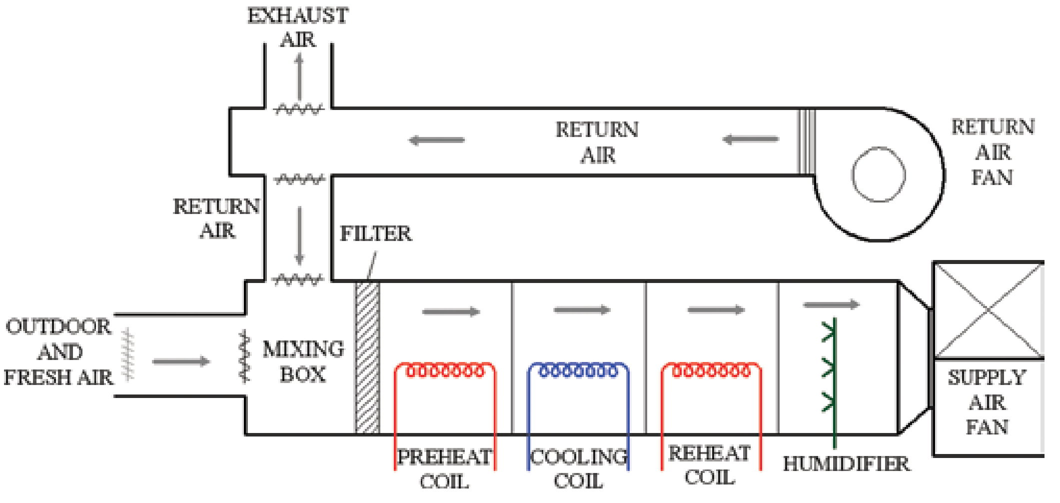

Figure 3. Equipment arrangement for central HVAC system.

6.1.1. Single zone

A single zone system consists of an air handling unit, a heat source and cooling source, distribution ductwork, and appropriate delivery devices. The air handling units can be wholly integrated where heat and cooling sources are available or separate where heat and cooling source are detached. The integrated package is most-commonly a rooftop unit and connected to ductwork to deliver the conditioned air into several spaces with the same thermal zone. The main advantage of single zone systems is simplicity in design and maintenance and low first cost compared to other systems. However, its main disadvantage is serving a single thermal zone when improperly applied.

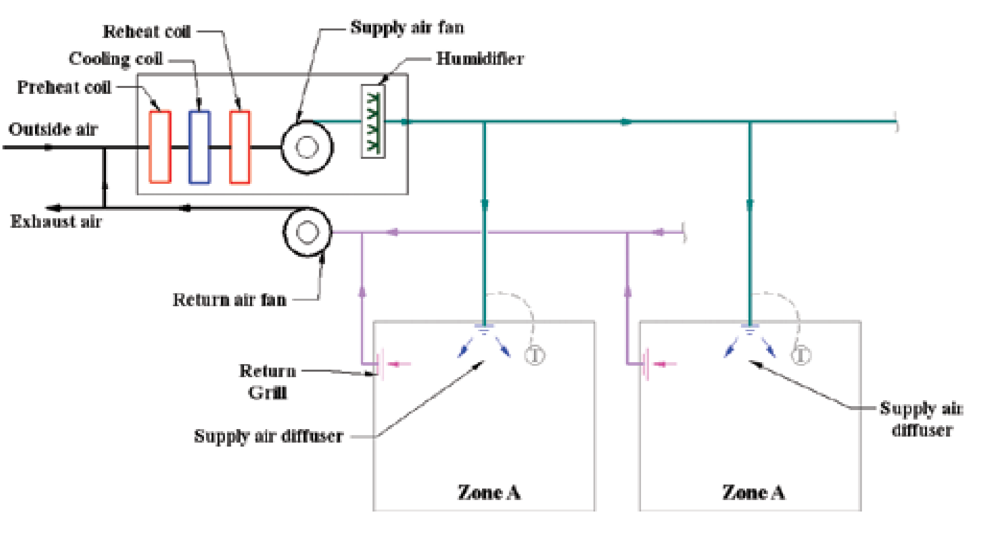

Figure 4. All-air HVAC system for single zone.

In a single zone all-air HVAC system, one control device such as thermostat located in the zone controls the operation of the system, as shown in **Figure 4**. Control may be either modulating or on–off to meet the required thermal load of the single zone. This can be achieved by adjusting the output of heating and cooling source within the packaged unit.

Although few buildings can be a single thermal zone, a single zone can be found in several applications. One family residential buildings can be treated as single zone systems, while other types of residential buildings can include different thermal energy based on the occupation and building structure. Movements of occupants affect the thermal load of the building, which results in dividing the building into several single zones to provide the required environmental condition. This can be observed in larger residences, where two (or more) single zone systems may be used to provide thermal zoning. In low-rise apartments, each apartment unit may be conditioned by a separate single zone system. Many sizeable single story buildings such as supermarkets, discount stores, can be effectively conditioned by a series of single zone systems. Large office buildings are sometimes conditioned by a series of separate single zone systems.

6.1.2. Multi-zone

In a multi-zone all-air system, individual supply air ducts are provided for each zone in a building. Cold air and hot (or return) air are mixed at the air handling unit to achieve the thermal requirement of each zone. A particular zone has its conditioned air that cannot be mixed with that of other zones, and all multiple zones with different thermal requirement demand separate supply ducts, as shown in **Figure 5**. Multi-zone all-air system consists of an air handling unit with parallel flow paths through cooling coils and heating coils and

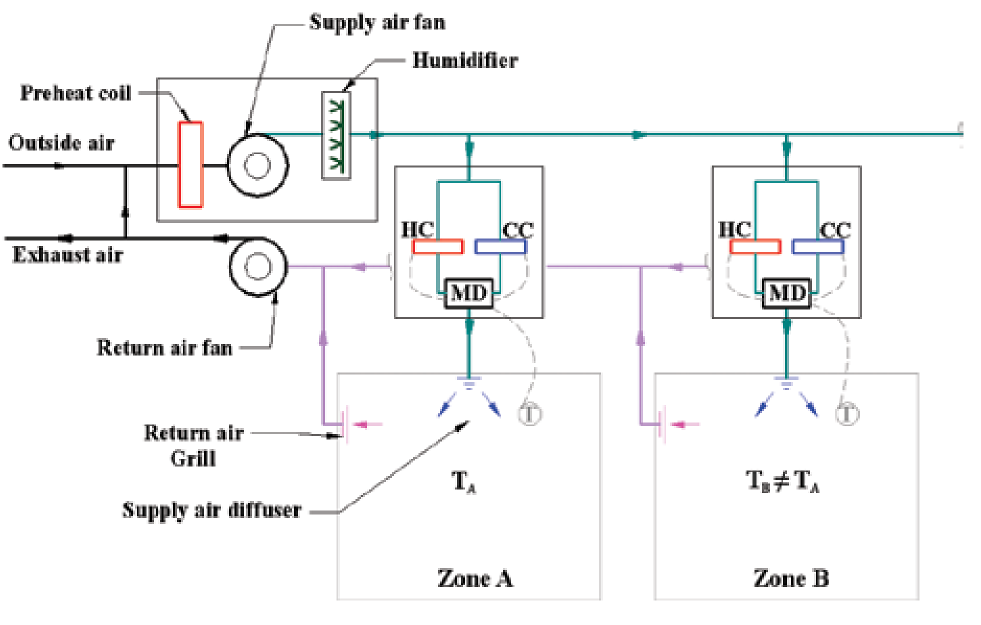

Figure 5. All-air HVAC system for multiple zones.

internal mixing dampers. It is recommended that one multi-zone serve a maximum of 12 zones because of physical restrictions on duct connections and damper size. If more zones are required, additional air handlers may be used. The advantage of the multi-zone system is to adequately condition several zones without energy waste associated with a terminal reheat system. However, leakage between the decks of air handler may reduce energy efficiency. The main disadvantage is the need for multiple supply air ducts to serve multiple zones.

6.1.3. Terminal reheat

A terminal reheat all-air system is a multiple zone, which considers an adaptation of single zone system, as shown in **Figure 6**. This can be performed by adding heating equipment, such as hot water coil or electric coil, to the downstream of the supply air from air handling units near each zone. Each zone is controlled by a thermostat to adjust the heat output of heating equipment to meet the thermal condition. The supply air from air handling units is cooled to the lowest cooling point, and the terminal reheat adds the required heating load. The advantage of terminal reheat is flexible and can be installed or removed to accommodate changes in zones, which provides better control of the thermal conditions in multiple zones. However, the design of terminal reheat is not energy-efficient system because a significant amount of extremely cooling air is not regularly needed in zones, which can be considered as waste energy. Therefore, energy codes and standards regulate the use of reheat systems.

6.1.4. Dual duct

The dual duct all-air system is a terminal-controlled modification of the multi-zone concept. A central air handling unit provides two conditioned air streams such as a cold deck and a hot deck, as shown in **Figure 7**. These air streams are distributed throughout the area served

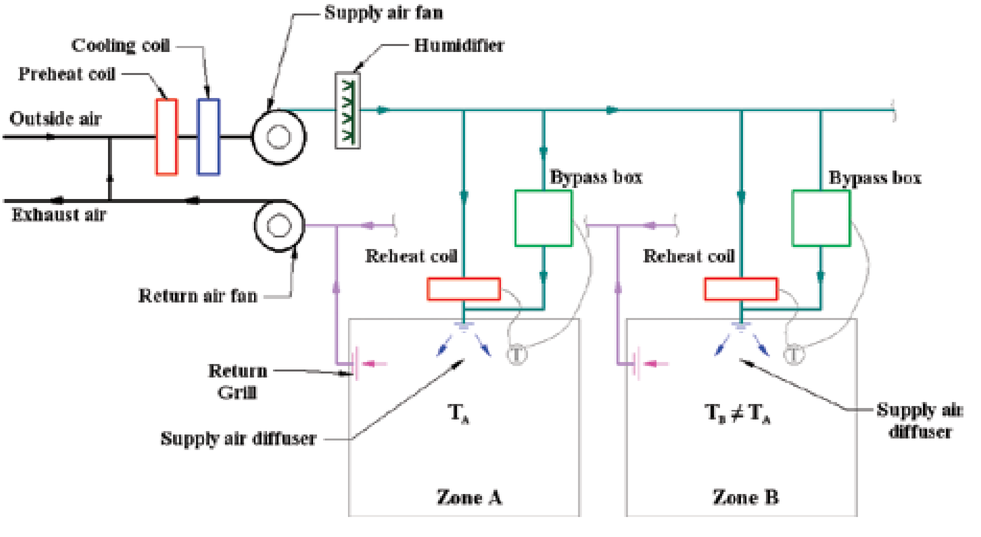

Figure 6. Single duct system with reheat terminal devices and bypass units.

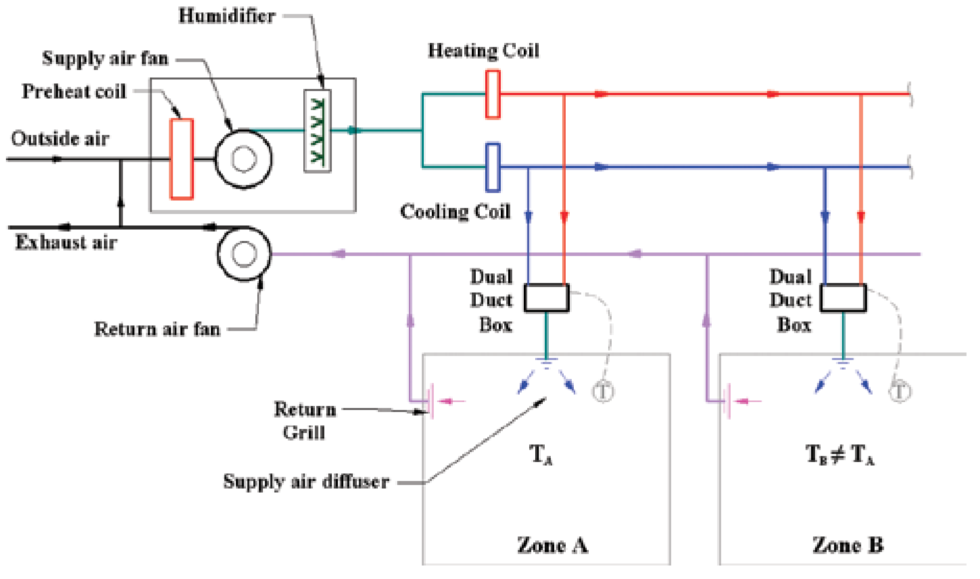

Figure 7. All-air HVAC dual-duct system.

by the air handling unit in separate and parallel ducts. Each zone has a terminal mixing box controlled by zone thermostat to adjust the supply air temperature by mix the supply cold and hot air. This type of system will minimize the disadvantages of previous systems and become more flexible by using terminal control.

6.1.5. Variable air volume

Some spaces require different airflow of supply air due to the changes in thermal loads. Therefore, a variable-air-volume (VAV) all-air system is the suitable solution for achieving thermal comfort. The previous four types of all-air systems are constant volume systems. The VAV system consists of a central air handling unit which provides supply air to the VAV terminal control box that located in each zone to adjust the supply air volume, as shown in **Figure 8**. The temperature of supply air of each zone is controlled by manipulating the supply air flow rate. The main disadvantage is that the controlled airflow rate can negatively impact other adjacent zones with different or similar airflow rate and temperature. Also, part-load conditions in buildings may require low air-flow rate which reduces the fan power resulting in energy savings. It may also reduce the ventilation flow rate, which can be problematic to the HVAC system and affecting the indoor air quality of the building.

6.2. All-water systems

In an all-water system, heated and cooled water is distributed from a central system to conditioned spaces [4, 5]. This type of system is relatively small compared to other types because the use of pipes as distribution containers and the water has higher heat capacity and density than air, which requires the lower volume to transfer heat. All-water heating-only systems include several delivery devices such as floor radiators, baseboard radiators, unit heaters,

http://dx.doi.org/10.5772/intechopen.78942

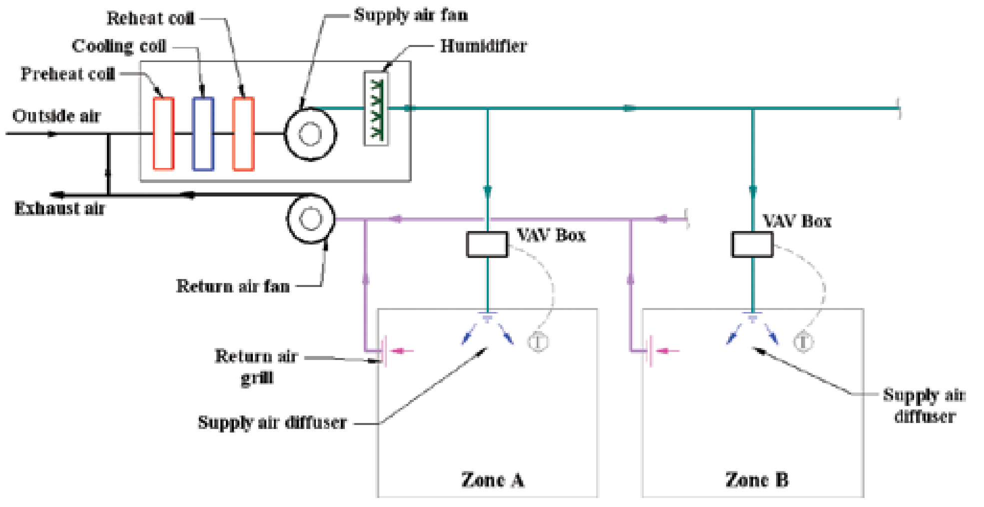

Figure 8. All-air HVAC systems with VAV terminal units.

and convectors. However, all-water cooling-only systems are unusual such as valance units mounted in the ceiling. The primary type that is used in buildings to condition the entire space is a fan-coil unit.

6.2.1. Fan-coil units

Fan-coil unit is considerably small unit used for heating and cooling coils, circulation fan, and proper control system, as shown in **Figure 9**. The unit can be vertically or horizontally installed. The fan-coil unit can be placed in the room or exposed to occupants, so it is essential to have appropriate finishes and styling. For central systems, the fan-coil units are connected to boilers to produce heating and to water chillers to produce cooling to the conditioned space. The desired temperature of a zone is detected by a thermostat which controls the water

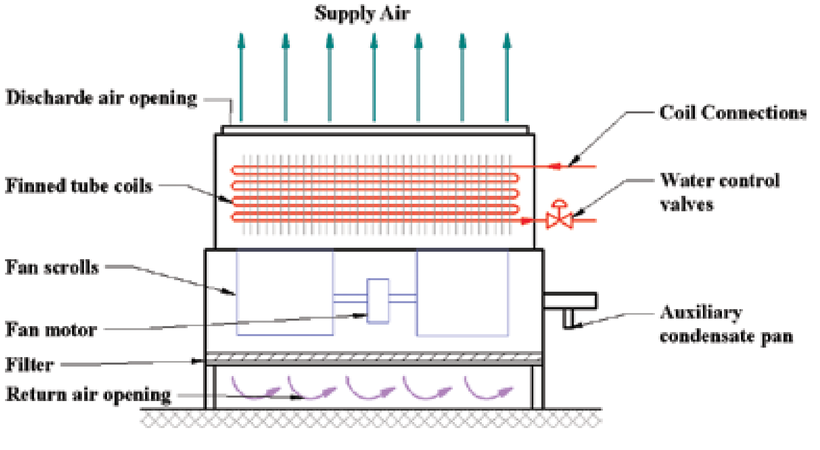

Figure 9. All-water system: fan-coil units.

flow to the fan-coil units. In addition, occupants can adjust fan coil units by adjusting supply air louvers to achieve the desired temperature. The main disadvantage of fan-coils is ventilation air and only can be solved if the fan-coil units are connected to outdoor air. Another disadvantage is the noise level, especially in critical places.

6.3. Air-water systems

Air-water systems are introduced as a hybrid system to combine both advantages of all-air and all-water systems [5]. The volume of the combined is reduced, and the outdoor ventilation is produced to properly condition the desired zone. The water medium is responsible for carrying the thermal load in a building by 80–90% through heating and cooling water, while air medium conditions the remainder. There are two main types: fan-coil units and induction units.

6.3.1. Fan-coil units

Fan-coil units for air-water systems are similar to that of all-water systems except that the supply air and the conditioned water are provided to the desired zone from a central air handling unit and central water systems (e.g., boilers or chillers). The ventilation air can be separately delivered into space or connected to the fan-coil units. The major types of fan-coil systems, are 2 pipes or 4-pipes systems, as shown in **Figure 10**.

6.3.2. Induction units

Induction units are externally similar to fan-coil units but internally different. An induction unit induces the air flow in a room through cabinet by using high-velocity airflow from a

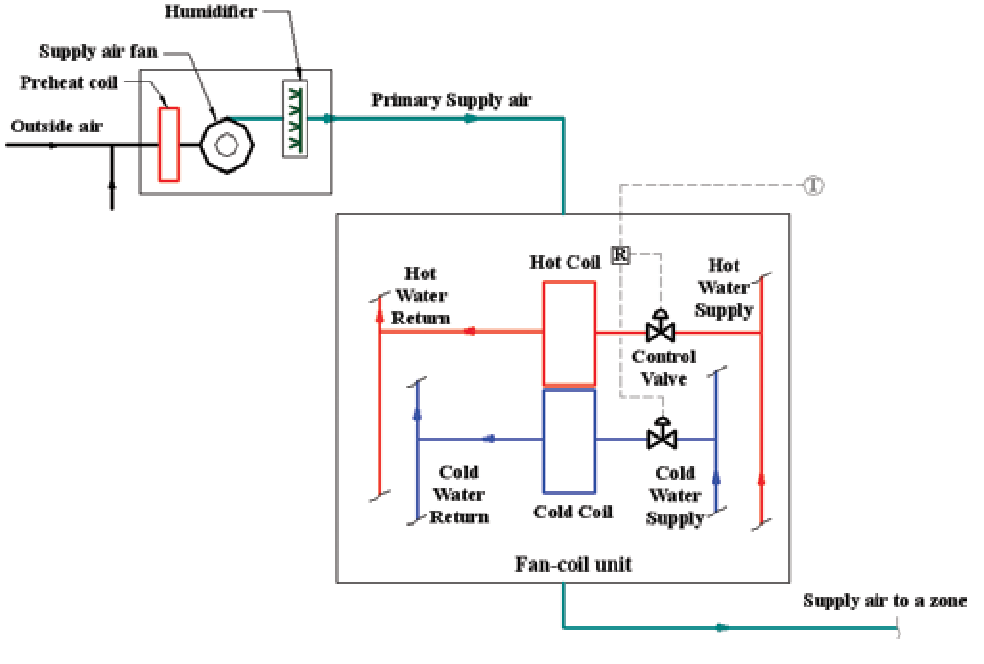

Figure 10. Air-water HVAC system using fan coil units with 4-pipes configuration.

http://dx.doi.org/10.5772/intechopen.78942

central air handling unit, which replaces the forced convection of the fan in the fan-coil by the induction or buoyancy effect of the induction unit, as shown in **Figure 11**. This can be performed as mixing the primary air from the central unit and the secondary air from the room to produce a suitable and conditioned air into the room/zone.

6.4. Water-source heat pumps

Water-source heat pumps are used to provide considerable energy savings for large building under the extreme cold weather [6]. A building of various zones can be conditioned by several individual heat pumps since each heat pump can be controlled according to the zone control. A centralized water circulation loop can be used as a heat source and heat sink for heat pumps. Therefore, heat pumps can act as the primary source of heating and cooling. The main disadvantage is the lack of air ventilation similar to the all-water systems as in fan-coil units. For a heating process, the boiler or solar collectors will be used to supply heat to the water circulation, while a cooling tower is used to reject heat collected from the heat pumps to the atmosphere. This system does not use chillers or any refrigeration systems. If a building requires a heating process for zones and cooling process for other zones at the same time, the heat pump will redistribute heat from one part to another with no need for a boiler or cooling tower operation,

6.5. Heating and cooling panels

Heating and cooling panels are placed on floors or walls or ceilings where can be a source of heating and cooling [7]. It also can be called as radiant panels. This type of system can be constructed as tubes or pipes impeded inside the surface where the cooling or heating media is circulated into the tubes to cool or heat the surface. The tubes are contacted to the adjacent large surface area to achieve the desired surface temperature for cooling and heating process. The heat transfer process is mainly by the radiation mode between the

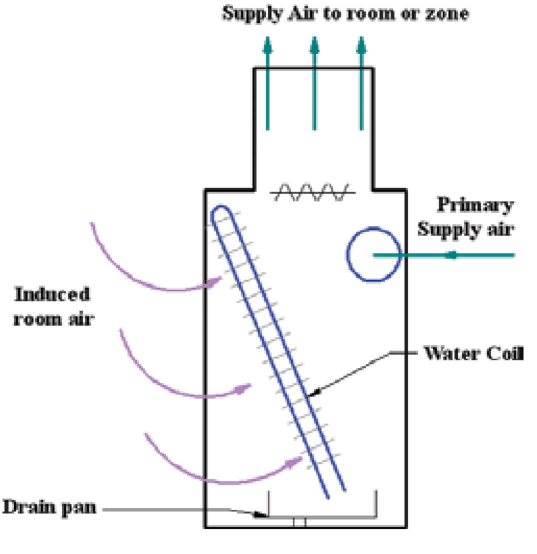

Figure 11. Air-water HVAC system using induction units.

occupants and the radiant panels, and the natural convection mode between the air and panels. Temperature restriction is recommended for radiant floor panels, a range of 66–84°F, to achieve thermal comfort for occupants (ASHRAE Standard 55). Radiant ceiling or wall panels can be used for cooling and heating process. The surface temperature should be higher than the air dew point temperature to avoid condensation on the surface during the cooling process. Also, the maximum surface temperature is 140°F for ceiling levels at 10 ft. and 180°F for ceiling levels at 18 ft. This temperature is recommended to avoid too much heating above occupants' heads.

The installation of such systems is often expensive compared to other types as mentioned above, but they can be useful and has a lower running cost mainly because of the surface temperature restriction. A control signal is connected to the thermostat of each zone to manipulate the medium temperature to condition the space. The used medium can be refrigerant or water mixing with inhibited glycol (anti-freeze) instead of plain water to prevent icing inside the tubes for the cooling process. The main advantage is no space required, only a few inches for the panels to be installed and no more collected dirt in the standard ceiling or the ductwork. Many designs are available to produce attractive panels.

7. Local HVAC systems

Some buildings can have multiple zones or have a large, single zone, which needs central HVAC systems to serve and provide the thermal needs [4, 5]. However, other building may have a single zone which needs equipment located inside the zone itself, such as small houses and residential apartments. This type of system is considered as local HVAC systems since each equipment serving its zone without crossing boundaries to other adjacent zones (e.g., using an air conditioner to cool down a bedroom, or using an electrical heater for the living room). Therefore, a single zone requires only one-point control point connected to a thermostat to activate the local HVAC system. Some buildings have multiple local HVAC systems as proper equipment serving specific single zones and controlled by the one-point control of the desired zone. However, these local systems are not connected and integrated to central systems, but still part of a large full-building HVAC systems. There are many types of local HVAC systems as shown in **Figure 12**.

7.1. Local heating systems

A single zone will require a complete, single package of heating system which contains heat source and distribution system. Some examples include portable electric heaters, electric resistance baseboard radiators, fireplaces and wood stoves, and infrared heaters [8].

7.2. Local cooling systems

Local cooling systems can include active systems as air-conditioning systems that provide cooling, a proper air distribution inside a zone, and control of humidification, and natural systems as convective cooling in open window, evaporative cooling in fountains [5, 6].

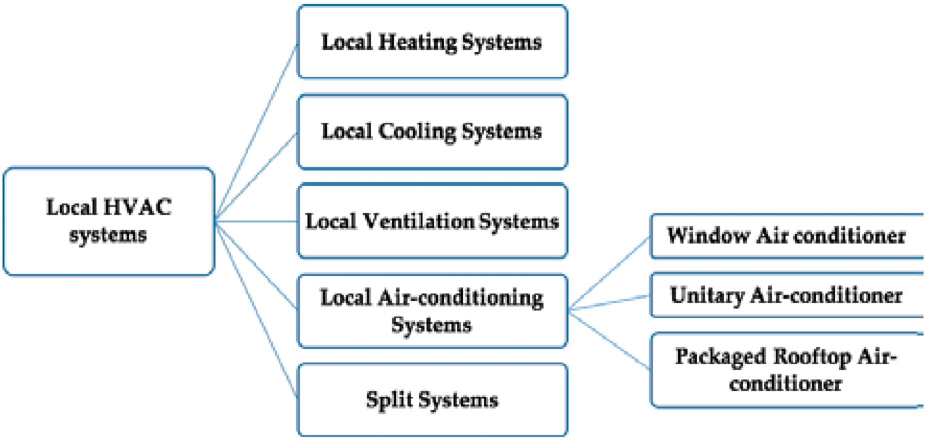

Figure 12. Horizontal hierarchy representation of the main types of local HVAC systems.

7.3. Local ventilation systems

Local ventilation systems can be forced systems by using devices such as window fan to allow air movement between outdoor and a single zone without changing in the thermal environment of the zone. Other systems used for ventilation are air circulation devices such as desk or paddle fans to improve thermal comfort of the space by allowing the heat to be transferred by conventional mode [5, 6].

7.4. Local air-conditioning systems

A local air conditioning system is a complete package that can contain cooling and heating source, a circulation fan, a filter, and control devices. There are three main types listed below [5, 6].

7.4.1. Window air-conditioner

This system is a packaged device consisting of a vapor compression refrigeration cycle that contains a compressor, a condenser, an expansion valve, and an evaporator, in addition to a fan, a filter, control system and housing. Window air-conditioners can be installed in a framed or unframed opening in building walls and in window openings without any ductwork and distribution the cooling or heating air effectively inside the conditioned space. The air conditioning contains both evaporator and condenser where the condenser is located outside the space while the evaporate is inside the space, however, it serves the entire single zone with the thermal requirements. The heating process can be achieved by adding electric resistance coil in the air conditioning or reversing the refrigeration cycle to act as a heat pump. Many feature designs are produced to provide aesthetical values and improve the quality and response.

7.4.2. Unitary air-conditioner

It is similar to window air conditioners from the equipment perspective, but it is designed for commercial buildings. It is installed on the exterior wall of the building and generally located near the floor-wall intersection, as shown in **Figure 13**. Every single zone will contain one unitary air-conditioner as in each guest room in many hotels.

7.4.3. A packaged rooftop air-conditioner

It consists of a vapor compression refrigeration cycle; heat source such as heat pump and electric resistance; an air handler such as dampers, filter, and fan; and control devices, as shown in **Figure 14**. This system may be connected to ductwork and serve a large-size single zone that cannot be served by unitary or window air conditioners.

7.5. Split systems

The split systems contain two central devices [5, 6]: the condenser, located outdoor, and the evaporator, located indoors. The two devices are connected by a conduit for refrigerant lines and wiring. This system solves some issues of small-scale single-zone systems since the location and installation of window, unitary or rooftop air conditioners may affect the esthetic value and architectural design of the building. The split systems can contain one condenser unit and connected to multiple evaporator units to serve multiple zones as possible under same conditions or different environmental conditions.

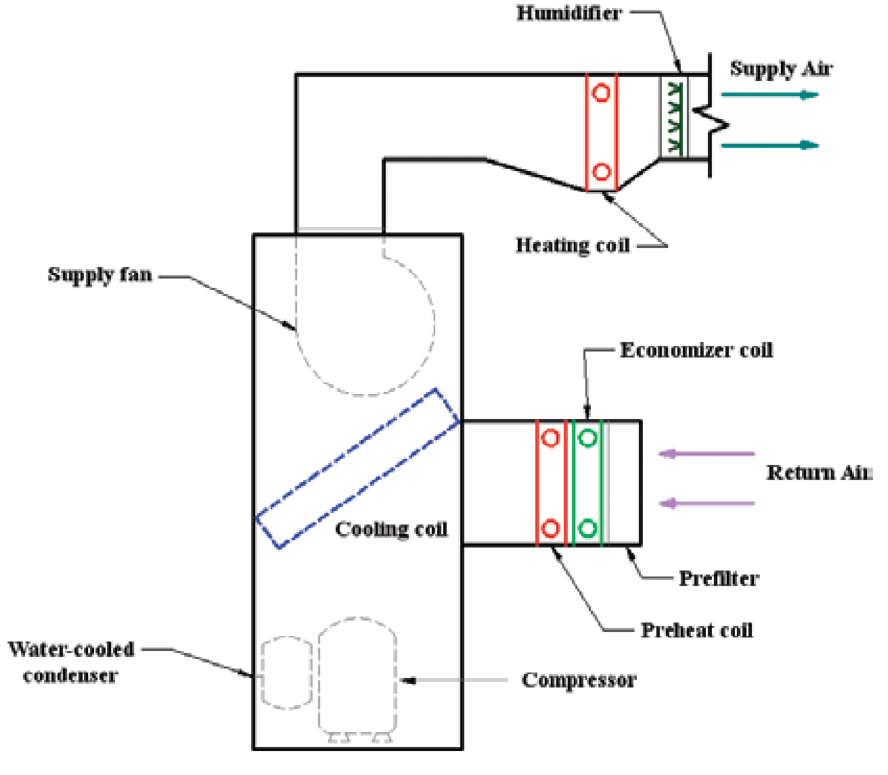

Figure 13. Unitary air-conditioner package.

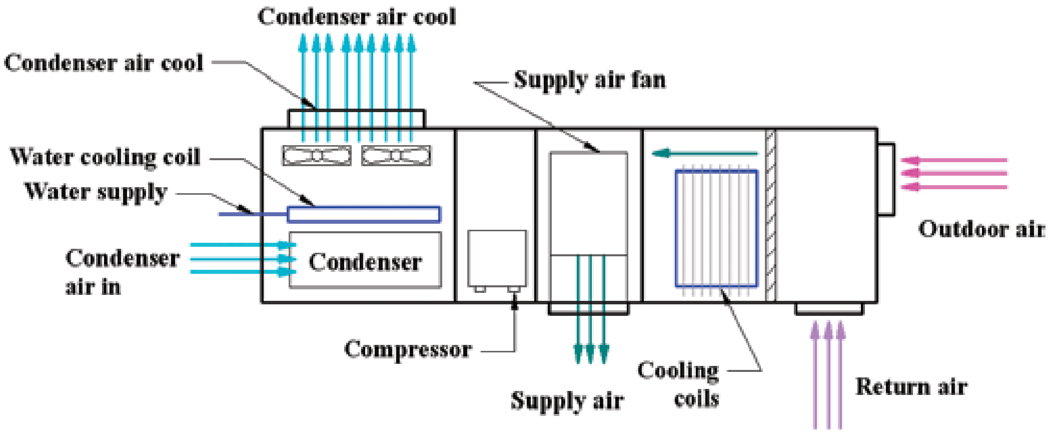

Figure 14. Packaged rooftop air-conditioning unit.

8. Conclusions

This chapter presents the types of HVAC systems. HVAC systems have several requirements including primary equipment such as heating equipment, cooling equipment, and delivery equipment; space requirement such as HVAC facilities, equipment room, and vertical shaft; air distribution; and piping. Type of HVAC systems can be divided into central HVAC systems and local HVAC systems. This classification depends on zone types and the location of HVAC equipment. The central HVAC systems can serve multiple and single zones and locate away from the building, which needs distribution devices. They also can be sub-classified into all-air HVAC systems, air-water systems, all-water systems, water-source heat pumps, and heating and cooling panel systems. The local HVAC systems are mostly placed inside or adjacent to the living spaces and serve one single zone. They consist of local heating systems, local air-conditioning systems, local ventilation systems, and split systems.

Author details

Shaimaa Seyam

Address all correspondence to: shaimaa.seyam@mail.utoronto.ca

M.A.Sc. at the University of Toronto, Toronto, Ontario, Canada

References

[1] ASHRAE Handbook. HVAC Systems and Equipment. Atlanta, GA: American Society of Heating, Refrigerating, and Air Conditioning Engineers; 1996. pp. 1-10

[2] American Society of Heating, Refrigerating & Air-Conditioning Engineers. Heating, Ventilating, and Air-Conditioning: Systems and Equipment: 2000 ASHRAE Handbook: Inch-Pound. Amer Society of Heating; 2000

[3] Sugarman SC. HVAC Fundamentals. 2nd ed. CRC Press, The Fairmont Press, Inc.; 2005

[4] American Society of Heating, Refrigerating & Air-Conditioning Engineers. ASHRAE Handbook. Fundamentals: SI ed. Amer Society of Heating, Atlanta, GA; 2009

[5] Haines RW, Myers ME. HVAC Systems Design Handbook. McGraw-Hill Education; 2010

[6] ASHRAE Handbook. Fundamentals. Atlanta: American Society of Heating, Refrigerating and Air Conditioning Engineers; 2001. p. 111

[7] Mumma SA. Ceiling panel cooling systems. ASHRAE Journal. 2001;**43**(11):28

[8] Brumbaugh JE. Audel HVAC Fundamentals: Volume 1: Heating Systems, Furnaces, and Boilers. Vol. 17. Canada: John Wiley & Sons, Wiley Publishing, Inc.; 2004

Chapter 5

Numerical Approach for the Design of Cost-Effective Renovation of Heating System Control in Buildings

Alessandro Carbonari, Massimo Vaccarini and
Emanuela Quaquero

Additional information is available at the end of the chapter

http://dx.doi.org/10.5772/intechopen.78613

Abstract

This chapter focuses on advanced tools for transient energy simulation of existing buildings. Budget constraints often hinder the possibility of implementing large-scale retrofit projects. As a consequence, designers must work out low-cost renovation, which asks for a deep knowledge of the current state of the buildings. Furthermore, the performances of heating plants in existing buildings can be enhanced through the improvement of the control of the system. These types of retrofit actions can be carried out with a limited budget, but asks for the availability of very accurate transient energy simulation tools, which can compare the current and the renovated scenarios. On top of them, cost–benefit analyses can be developed. In this chapter, a model of a small hospital is developed in the Dymola/Modelica environment. The high flexibility of the transient simulation model and the very good agreement between numerical estimations and measurements are shown. Then, one scenario regarding enhanced regulation of the heating system by means of a customized ambient temperature control system is developed, and the expected energy savings are estimated.

Keywords: advanced simulations, heating systems, control systems, Modelica, Dymola

1. Introduction

Buildings are responsible for a considerable amount of energy consumption [1]. Also, the studies by IPCC [2] and the European Community [3] are among the latest to uncover the very big energy-saving potentials in buildings. Once a building is accurately addressed in its current state, an informed analysis about the benefits that can be determined by several potential retrofit scenarios can be carried out [4]. In this process, the selection of the most suitable simulation tool is of utmost importance. Indeed, dynamic simulation tools should be developed, so that potential energy and money savings under real conditions of use can be estimated [5]. These outcomes will then be used to support cost–benefit analyses, where several prospective retrofit scenarios are compared to select the best one. An interesting example is the application of dynamic optimization methods to design retrofit actions that could improve comfort conditions in museums. This enhancement was able to solve the problems that an incorrect sizing of original HVAC systems had determined on comfort conditions [6]. In fact, building management systems (BMSs) are becoming increasingly important as they are an efficient means because they can both make buildings consume less and improve indoor air quality [7]. However, the implementation of these systems is still limited, even because of the need for setting BMS parameters at the design stage; this asks for the availability of dynamic simulators [7]. Indeed, dynamic models are of crucial importance in implementing an effective control strategy [8]. Our study was based on the open-source Modelica "Buildings" library v1.3 [9], which offers several advantages, among which the following can be cited:

1. the possibility to simulate advanced control systems and to customize the model, so as to accurately simulate even non-standard arrangements of building systems;
2. users are allowed to exploit, but also extend and adjust the library components, in order to suit the specific simulation requirements of the building under analysis [10].

Furthermore, the Modelica libraries are constantly being improved, and the latest releases published not only include new components [11] but also solve numerical problems that may arise during simulations. The model reported in this chapter was developed in the Dymola programming environment. The potentials of Dymola-like simulation tools were reported several years ago, when barely a few thermal models were developed in this programming environment [12]. Dymola brought in relevant innovations in terms of equation-based methods using program-neutral model description and domain-independent solution methods [12]. Since then, Dymola, which is based on the Modelica language, has been improving over time. It can show detailed dynamics of feedback control loops when evaluating different alternatives without interfering with real operating conditions [13]. Its open-source "Buildings v1.3" library allows the simulation of advanced control algorithms. Most existing building simulation programs are developed for building and HVAC system design and retrofit analyses, not for studying advanced (local and supervisory) control algorithms, which is one of the features offered by Dymola [14]. It has very good potentials even in the model calibration stage, too. As accurate and reliable simulation programs of control systems will soon be needed, because the expensive oversizing of plants can no longer be afforded, a detailed design of plants and buildings is necessary, and Modelica is the right language to simulate realistic operating conditions. Even more urgent is the need for the integrated simulation of heating, ventilation, and air-conditioning of existing buildings, in particular when not every zone is served by all the plants, but service conditions are variable depending on the age of the building block [15]. Our choice to use Modelica-based simulation is supported by a number of previous studies in which the performance of this tool has proved to be satisfactory, despite the complexity of the domains under analysis. In one case in which a French railway station building was modeled and its thermal and electrical loads estimated, the validation deviations were below 10% [16]. The same tool was suitable for accurately modeling single components of building equipment, such as a slinky-coil geothermal heat pump system [17] and mechanical air supply systems in subway stations [18]. Once the parameters are calibrated through comparison with real measured performance, the model can be used as the basis for the simulation of system regulation and control alternatives [19]. The refurbishment of the existing building stock is a further opportunity to improve the environmental sustainability of NHS buildings that should not be neglected [20]. Building energy management systems are becoming increasingly important as they are an efficient means to ensure that buildings consume less while offering improved indoor working and living environments [7]. When these approaches are adaptive, further energy savings may also be possible. One of these possibilities involves adapting the system to the user's temperature demand profile [21]. To create the demand profile, the users are asked to provide feedback about their thermal comfort simply by pushing a button. The system then calculates a usage profile for each room and controls the room temperature according to this usage profile. Simulations of advanced control strategies must rely on a reliable model of the object of analysis. To that end, a systematic, evidence-based methodology for calibrating these analyses may be carried out [22]. Mean Bias Error (MBE) and Cumulative Variation of Root Mean Squared Error (CVRMSE) are suggested by [22, 23] as good indices for driving the calibration of energy models.

Section 2 of this chapter deals with the description of the audited building and the development of its Dymola/Modelica simulation model, whose calibration will be performed in Section 3. The capability of the simulation model to assess the savings that can be derived from an even slight enhancement of the currently installed control subsystems will be provided in Section 4. Conclusions are proposed in Section 5.

2. Building description and model

2.1. Materials and methods

The existing stock of buildings has become the major field for real estate investments and for any related enhancement actions. When budget constraints hinder the possibility of implementing large-scale retrofit projects, low-cost renovation is the only feasible solution. The approach requires a thorough energy audit [24]. Once a building is accurately addressed in its current state, an informed analysis about the benefits that can be determined by several potential retrofit scenarios can be carried out [4]. In this process, the selection of the most suitable simulation tool is of utmost importance. The availability of transient simulation models is still more critical, in case both thermal comfort and energy behavior must be considered in the choice of the best combined retrofit and energy-saving actions [25]. To that end, in this chapter, a model of a small hospital is developed in the Dymola/Modelica environment. The model, developed in the following paragraphs, will be shown to have the level of detail that is necessary to analyze the behavior of each device and subsystem belonging to the building. Development, calibration, and the possibility to simulate the behavior of the buildings after the implementation of—even minor—retrofit solutions will be discussed. This approach is called a lumped parameter modeling. It supports features such as advanced control integration, multi-physics, and the integration of specific components and/or boundary conditions. At these boundaries, specific conditions in terms of heat flow, airflow, and mass transfer (water and pollutants) must be assigned in order to model the real dynamics [10]. The software builds on the Modelica language, an industry-driven, open, non-proprietary language and associated libraries, modeling, simulation, and optimization environments [26]. Equation-based languages allow a model builder to declare a set of algebraic equations, ordinary differential equations, and finite state machines that define the physics of a component or the logic of a control sequence. These equations need not be explicit or ordered. Then, a model translator analyzes these equations and rearranges and solves the systems of equations symbolically using computer algebra to reduce the number of variables that need to be solved iteratively during the time integration. Later, an executable code is generated, generally in the form of a C-code, and linked to numerical solvers. Using the same model architecture, different codes can be generated for simulation, for embedded systems, and for optimization. In addition, model linearization and state initialization are generally supported by equation-based simulation programs. This high-level model formulation leads to more flexible and intuitive model use as the composition of the system models can be done schematically using a causal model instead of a signal-flow chart. The decomposition of the system model does not need to follow primary and secondary HVAC system-loop structures or other non-intuitive constraints that may be imposed by a simulation engine. Since the model formulation is independent of the solution scheme of the simulation engine, it is easier to exchange between users and is more concise and faster to develop [9]. In addition, since domain-specific libraries can be developed separately from the simulation engines, the effort for engine development can be spread across various application domains [10].

2.2. Pilot/case study

A community clinic was as a pilot. It is a seven-storey building located in Sant’Elpidio, a Mare (Fermo, Italy), whose occupancy pattern has varied in the past (**Figure 1**). In this chapter, the simulation model will be calibrated and validated with respect to two scenarios. This choice was dictated by the awareness that the clinic has undergone several organizational rearrangements over recent years, which have determined variations in terms of occupancy

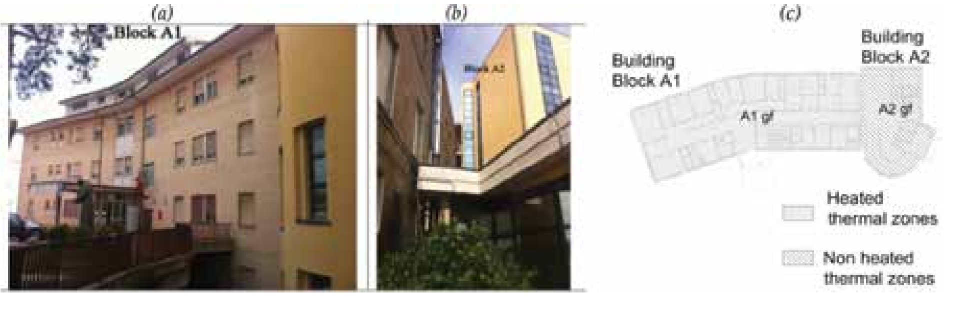

Figure 1. Front view of block A1—Partially hidden by block A2 (a), rear view of block A2 at the point where it connects with block A1 (b), and plan of the ground floor (c).

levels, number, and typology of heated and non-heated thermal zones. The first scenario is relative to the building at the beginning of the year 2013, from January to March (**Table 1**). In this period, the medical ward was open on the second floor, and the clinics were mainly accommodated on the first floor. The second scenario is relative to the months from January to March 2015, when the medical ward had been closed and the first floor, hosting the clinics, had been slightly renovated. The building is made up of two different blocks. The first (A1) was built in the 1970s (**Figure 1a**) and hosts all the wards and clinics of the hospital. The second block (A2) was built in the 1980s and serves the rest of the building through a large staircase, a lift, and some waiting rooms (**Figure 1b**). A representative plan of the building is depicted in **Figure 1c**, on which the two thermal zones "A1 gf" and "A2 gf" on the ground floor are explicitly labeled; the first zone is heated while the second is not. The layout of all the other floors is quite similar to this one. A reinforced concrete frame superstructure bears both blocks of the building. The insulation level of the envelope is quite low, due to the age of the external walls, windows, and roof. As a general rule, the performance of block A2 is slightly better than that of block A1.

Zone Id.	Net surface (m^2)	Gross volume (m^3)	Conditioning status from January to March 2013		Conditioning status from January to March 2015	
A1 2bg	475	1478	Heated		Heated	
A1 1bg	326	1124	Heated		Heated	
A1 gf	488	1683	Heated		Heated	
A1 l1	481	1660	Heated		Heated	
A1 l2	481	1659	Heated		Not heated	
A2 2bg	95	295	Heated		Heated	
A2 att	114	227	Heated		Not heated	
A1 att	545	1091	Not heated		Not heated	
A2 3bg	760	3040	Not heated		Not heated	
A2 2bgH	310	964	Not heated		Not heated	
A2 1bg	362	1249	Not heated		Not heated	
A2 gf	201	693	Not heated		Not heated	
A2 l1	201	693	Not heated		Not heated	
A2 l2	201	693	Not heated		Not heated	
Overall building	**5040**	**16,550**	**Net surface (m^2)**	**Gross volume (m^3)**	**Net surface (m^2)**	**Gross volume (m^3)**
Heated			2460	8127	2066	6934
Not heated			2580	8423	2974	9616

Table 1. A list of thermal zones in the SEM community clinic relative to the months from January to march 2013 and from January to march 2015.

However, in both cases, energy performance is definitely worse than the standards and regulations currently in force. There is no mechanical air supply, and hence the indoor air quality is provided by infiltration and incidental air leakage through the building envelope. During the several on-site surveys, the personnel of the clinic witnessed that they usually open the windows when they feel that the indoor air quality is no longer adequate. As a result of the surveys, two instances of the clinic's model, which will be described in the following subsection, were developed. Each of them refers to one of the two simulation scenarios that were developed for the years 2013 and 2015. The difference between these model instances consisted mainly in the input parameters (e.g., occupancy of the rooms, use of equipment and lighting, heating system operation in the different thermal zones). Also, at the end of 2013, the heat generator was replaced with a new system (ref. Section 2).

The whole building is served by a hydronic heating system, whose central plant is located on the third floor below grade, inside block A1. The 2013 scenario consists of two cast-iron heating boilers installed in the central plant, fired by natural methane gas. Both these devices are fitted with high/low/off-burner control [27]. One methane gas primary heat generator of the "Ecoflam Ecomax NC 630" type with a capacity of 682 kW power was installed in 2006. Its full load overall efficiency is 92.3%, whereas the overall efficiency at a reduced (30%) load is 90.2%. A secondary redundant "Riello RTQ 400" heat generator was automatically turned on, in case the primary generator was no longer able to satisfy the energy needs. Its maximum capacity is 511 kW; its full load overall efficiency is equal to 91.8%, whereas its 30% load efficiency is 92.9%. However, due to a recent reduction in the building's energy requirements, the second heat generator was kept merely as a backup unit, to activate should there be a failure in the primary generator. In the whole building, cast-iron panel radiators are installed as heat emitters. The complete heating circuit is made up of two principal circuits: primary and secondary. The former contains the two boilers, whereas the latter distributes hot water to the building. This circuit is controlled so as to vary the water flow rate in the secondary circuit, while a constant flow rate is maintained in the primary one. The secondary circuit is, in turn, broken down into two independently operated parallel sub-circuits. The first secondary sub-circuit serves block A1 of the building, while the second secondary sub-circuit serves block A2. Three circulation pumps were installed: one along the primary circuit and two along the two secondary sub-circuits (block A1 is served by a 1350-W circulator pump of the "UPC 65-120" type, while block A2 is served by a 375-W circulation pump, which is called "UPC 50-60"). Two different types of control drive the distribution system. In the primary circuit, a flow temperature regulation is applied. It is achieved by driving the burner firing rate of the boiler according to a function relating the outdoor temperature to the required water flow temperature. The two pumps along the secondary sub-circuits run at a constant speed in the short run, but during the heating season, their speed may be manually varied by the technical staff to meet changeable energy needs. Furthermore, 2 three-way motorized mixing valves are installed upstream of the pumps of the two secondary sub-circuit branches, allowing the cooler return water to be variably mixed with the warmer primary circuit water. The mixing valves rely on a feedback signal of the real water flow temperature, which is kept constant. The connection between the primary and the secondary circuit was made by means of one supply and one return headers, located in a technical room on the third floor below grade, about 60 m from the central plant room. The two main distribution pipes of the secondary circuit serve the two blocks according to different distribution patterns. The water pipe serving block A1 is laid horizontal on the third floor below grade and feeds several vertical supply and return pipes serving all the floors. This vertical piping was built according to the two-pipe system distribution scheme, that is, every vertical pipe supplies hot water to the radiators it meets while rising through the seven floors, and a second pipe returns the water to the main return pipe on the third floor below grade, until it reaches the return header. The flow pipe serving block A2 rises through all seven floors of the block, and, on each floor, it feeds a manifold station, which has as many outlets as necessary to supply hot water to all the panel radiators on that floor. There is no local control in the heated zones of block A2. The return pipe follows the same path as the flow pipe and is located on the same technical shaft and framing cavities. In the 2015 scenario, the heat generator was replaced with respect to the 2013 scenario. The new heat generator is a modular, condensing "Riello Condexa Pro 3" boiler fired by natural gas and is made up of four heat exchange modules, each of which has a capacity of 115 kW. These modules are driven by an integral control package that provides basic sequence control for the multiple operations of the burners. The full load efficiency of the boiler at a design temperature differential of 80–60°C will be 98.6%, while its efficiency at a design temperature differential of 50–30°C will be 108.6%. In addition, the boiler that had been working as the primary heat generator in the 2013 scenario (i.e., heat generator "Ecoflam Ecomax NC 630" with 682 kW power) was downgraded to become the secondary boiler of the heating circuit in the 2015 scenario. As a consequence, the boiler which had been working as a secondary boiler in the 2013 scenario was disposed of.

2.3. Data collection for calibration

In order to perform the calibration and validation of the Dymola model (Section 3.2), two scenarios were considered and the relative data were collected. Consumption figures measured during the year 2013 (**Table 2**) were derived not only from the bills invoiced by the utility company but also from energy metering, which monitors the energy delivered to the building (**Table 3**). This was accomplished by means of a KWS (i.e., for measuring hot water) "Coster" energy meter, which is a Woltmann-type turbine, approved by PBT, the German meteorological institute. This meter is fitted with a pulse transmitter for remote transmission of measured flow rate. Readings were collected approximately every 15 days and then interpolated and grouped as reported in **Table 3**.

In addition, indoor environmental conditions were monitored by means of a HOBOTM wireless Temperature/RH Monitoring Kit. This was made up of one receiver, one router node,

	Jan13	Feb13	Mar13	Apr13	May13	Jun13	Jul13	Aug13	Sep13	Oct13	Nov13	Dec13
Tot (m^3)	7538	11,292	7965	5313	1826	1790	1474	957	1050	1972	4852	7945
H (m^3)	6026	9781	6454	3802	0	0	0	0	0	0	3341	6434

Table 2. Methane gas consumption invoiced by the utility company during the year 2013.

	Apr14	May14	Jun14	Jul14	Aug14	Sep14	Oct14	Nov14	Dec14	Jan15	Feb15	Mar15
Tot (m^3)	3388	1137	1004	730	710	864	1008	3768	5962	4540	9237	5751
H (m^3)	2479	0	0	0	0	0	0	2859	5053	3631	8328	4842

Table 3. Total methane gas consumption (Tot) and heating (H) measured by the meter from April 2014 until march 2015.

and two wireless temperature and relative humidity nodes, arranged on the ground floor (**Figure 2a**). It uploads real-time data onto a laptop running the "HOBOware 3.0 Pro" software program.

The HOBO data router directs any data recorded by the data nodes to the HOBO data receiver as well as the commands coming from the latter to HOBO data nodes, thus extending the communication range. The two temperature probes were placed in the entrance hall of block A2 and in the corridor of block A1 (**Figure 2b**). The router was placed inside a staff room (on the same floor) at a distance of 6 and 11 m, respectively, from the two temperature probes. A 5-min time step was used for logging the data. These data were then averaged at hourly time steps so as to set up the final dataset to be used for validation. The laptop Internet connection was supported by a UMTS Gateway. These sensors were installed on February 10, 2015, and were kept in place until the end of March.

2.4. Thermal model of the building

Figure 3 shows the schematic model of the hospital as implemented in Dymola/Modelica. It is made up of four main components, each including a set of models relating to separated groups of subsystems. More specifically, the heading thermal zones include the models of the thermal zones of the hospital. The ventilation component includes the models that simulate the air change due to natural ventilation in the various thermal zones.

The central plant component groups all the models of the heat generation. The heating unit component includes the heating system's distribution from the secondary circuit to the thermal zones and all heat emitters. All the models were developed using the "Modelica" library and the "Buildings" library—release 1.3. The thermal zones component (**Figure 4a**) includes both heated and non-heated thermal zones. Each thermal zone was simulated using the Buildings, Rooms, MixedAir class (**Figure 4b**) [10]. It is a model with completely mixed air, which is able to consider all the heat transfer phenomena that can reasonably occur in any room. Heat conduction was computed according to the specific arrangements found for each building component of the thermal zones. In the MixedAir data record labeled "Parameters," every component had to be assigned the proper type of opaque constructions and windows as well as geometrical properties and size.

The convection coefficients were assigned as 3.0 $W/(m^2{\cdot}K)$ for room-facing surfaces and 10.0 $W/(m^2{\cdot}K)$ for exterior-facing surfaces. In every thermal zone (**Figure 4b**), one heat port was used to add a sensible convective heat flow to the room air and another heat port was used to add a radiative heat flow. Both contributions were supplied by the panel radiators under the heating unit component. The heat port connected to air volume was coupled with a temperature sensor to measure the indoor air temperature of the room. The fluid port

Figure 2. Location of the temperature probes on the ground floor (a) and picture of one sensor node in the corridor (b).

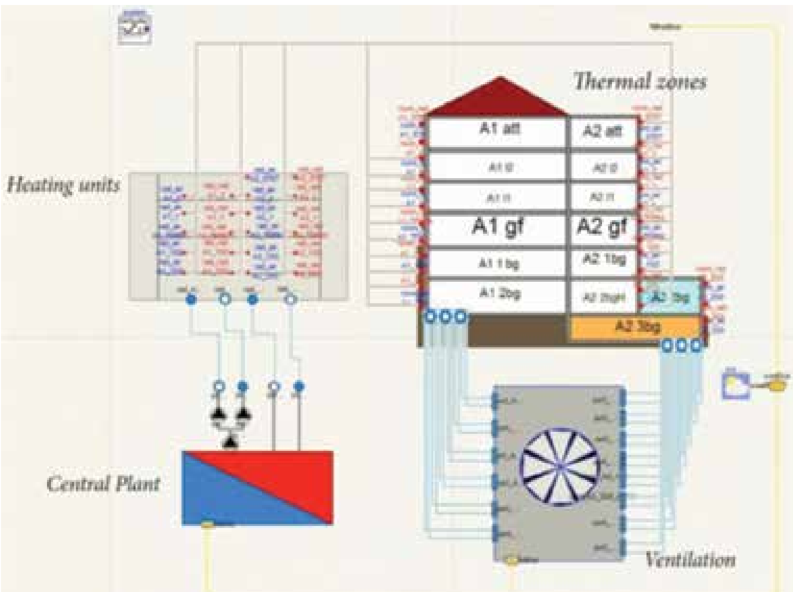

Figure 3. Top layer diagram of the hospital model.

placed at the bottom left of each thermal zone was used to couple the room with models that compute overall leakage through the envelope, which is implemented under the ventilation component. Two connectors were needed to model both the inlet and outlet connectors of the air circulating in the rooms. One of the two Realinput ports was used to account for the radiant, convective, and latent input to the room, due to three contributions: sensible gain due to people, equipment, and sensible gain due to lighting. Three classes of the type "Modelica.Blocks.Sources.constant" were used to input the average number of people occupying each thermal zone, the number of pieces of equipment, and the number of light fixtures. A component (IntGai) was inserted in the middle between the three inputs and the MixedAir component, in order to sum the three contributions and multiply by the metabolic rate emitted by each person [28], the average gain due to equipment, and the average power of light fixtures. Finally, all the thermal zones located below grade were connected to a

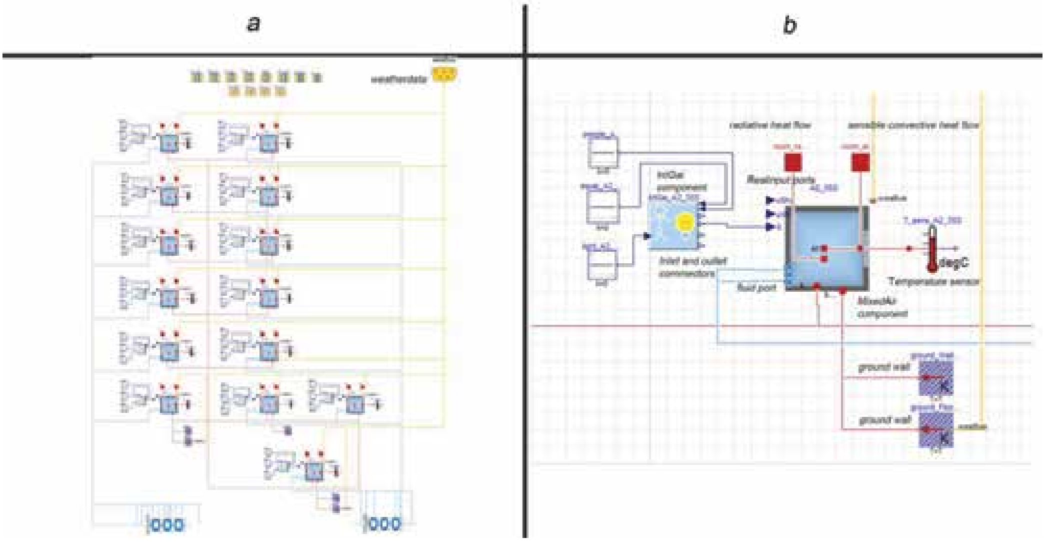

Figure 4. A schematic diagram of the thermal zones component (a) and zoomed view on one of the thermal zones (b).

custom-made component (ground wall), inside which a model was implemented, so as to estimate depth-dependent earth temperature. To that end, a well-established model suggested by the study was adopted [29]:

$$T(t) = T_m + \Delta T \cdot \cos(\omega t) \tag{1}$$

where T_m is the yearly average ambient temperature and ΔT is its amplitude, which is half the total variation during the year, both computed from the weather file. ω is the frequency, which depends on penetration depth (d), soil's thermal conductivity (k), density (ϱ), specific heat (c), and period (P).

These values were determined according to the suggestions in ISO EN 13370 [30]. This class requires all the above-listed parameters and the average depth of the below-grade walls to be defined by the user. An input connector comes from the weather data and subsequently computes the estimated temperature of the surface between the walls and the soil. The red lines on the pictures are connectors for heat ports that equate temperature T and conserve heat flow rates between the connected ports. The bright blue lines are fluid connectors that equate pressure and conserve mass flow rate. The yellow connector leaving the Weatherdata component was used to couple the external surface of each wall with the weather data arranged in the form of a TMY3 file. For calibration purposes, a tailored weather file related to a location close to the site under study was needed. This weather file was built by combining a weather file downloaded from Energy Plus (Ancona 161,910 (IGDG)) with historical weather data obtained from the "wunderground.com" database from the weather station called LIBP [31]. Two modified weather files were built in this way: one for the period January–March 2013, for which historical energy consumption data were used for calibration, and another relative to the period January–March 2015, for which environmental measures were also collected.

In the ventilation set of models (**Figure 5a**), 14 fans with a controlled mass flow rate obtain outdoor air from an air source whose temperature is prescribed to be the same as the outdoor air, by means of a direct connection to the weather data component. Every mass-controlled fan is connected with a fluid port, in order to push that outdoor air into each of the hospital's thermal zones, whose flow rate is varied according to the thermal zone's glazed surface and volume, so as to generate an amount of air change rate that includes two contributions. The first is provided by air infiltration through the windows and the second is due to the opening of windows by users. Air infiltration through the windows was assumed according to the suggestions in the Italian standard UNI 7979. This standard is no longer in force, but it was considered useful for the purpose of our simulation, where an overall average air exchange with the outdoor environment is needed to be estimated. In addition, this standard is taken as a reference by an energy simulation software program that is usually used for energy audits of buildings and that was also applied to the building analyzed in this chapter [32]. In fact, this software is based on the technical standard UNI 7979 and estimates air infiltration rates through windows according to their category: A1, A2, A3, and non-classified. These categories are defined by means of laboratory tests according to the rate of air exchange through a window at a given pressure gradient between its two sides. In the building analyzed in this study, some windows were very old and were assigned to the "non-classified" category; only the windows installed in block A2 were considered better and were assumed to belong to the A1 category, which is the worst category contemplated by the abovementioned standard. Air infiltration rates of the same amount as defined by the standard were then set for air infiltration: on average, 5 $m^3/(h \cdot m^2)$ in the non-classified category and 2.5 $m^3/(h \cdot m^2)$ in the A1 category. These values were multiplied by the glazed surface in each thermal zone and were set as the first contribution from the ventilation component. The second contribution, due to the air change rate resulting from the opening of windows, was set at 0.3 vol/h, as suggested by the Italian technical standard UNI TS 11300-1 [33], whose approach for load estimation in buildings is in accordance with the international standard UNI EN ISO 13790 [34]. More importantly, when this value was applied to the energy audit phase of the building,

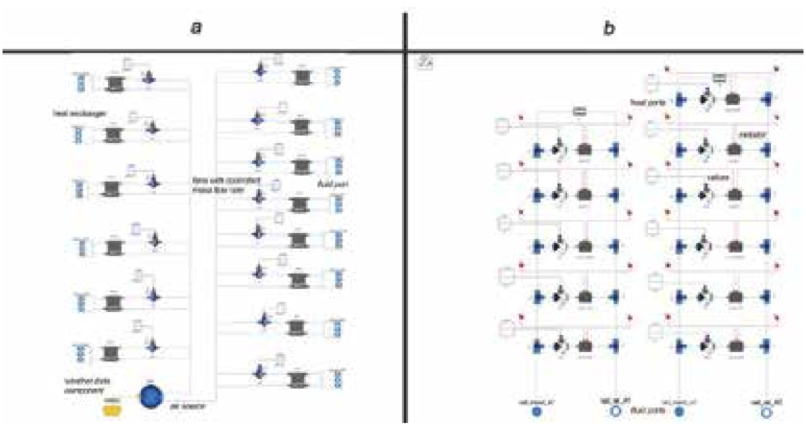

Figure 5. A schematic diagram of the ventilation set of models (a) and a schematic diagram of the heating unit set of models (b).

it provided a very good agreement (error < 5%) between estimated and measured overall consumption [32]. In order to facilitate the simulation of the renovation envisaged for the air supply system, a heat exchanger was interposed between each fan and each fluid port, whose purpose was to keep the directions of the air flows opposite to each other. The third group of components includes heat generation, together with the primary and secondary circuits, which are implemented in the central plant component (**Figure 6a**). The Ecoflam Ecomax NC 630 primary boiler, which served the hospital until October 2013, was inserted in the model. All the parameters were set according to the boiler datasheet. More specifically, of the three choices available, the "QuadraticLinear" efficiency curve was used to develop the efficiency plot suggested by the manufacturer, which is 92.3% at full load (100%) and 90.2% at partial load (30%). Interpolation was assumed to be linear. As a consequence, the coefficient array of the "QuadraticLinear" efficiency curve was assigned through the entries {1,2} = {0.893, 0.03}, which are the intercept and slope of the linear relationship, respectively. As the boiler is fuelled by natural gas whose net calorific value had been estimated equal to 34.54 MJ/m^3 by the utility company, the "fuel type" parameter in the Dymola model was set at "Natural gas, lower heating value." In accordance with estimations made by the burner manufacturer, the density was set at 0.715 kg/m^3. Starting from these values, enthalpy was calculated as 48.3·106 J/kg and carbon dioxide emission as $2.75\ kg_{CO_2}/kg_{CH_4}$. The boiler pump was modeled by means of a controlled mass flow rate pump, whose input was set at the real constant value, given that fluid circulation through the primary circuit is kept constant. The value of this constant was set in accordance with the flow/power curve of the pump datasheet. Two instances were generated, in order to estimate the amount of heat wasted by the flow and return pipes running from and to the secondary circuits.

At the bottom of the boiler, a group of objects were connected, in order to adjust the boiler's heat delivery into the flow water, hence its temperature, according to outdoor air temperature,

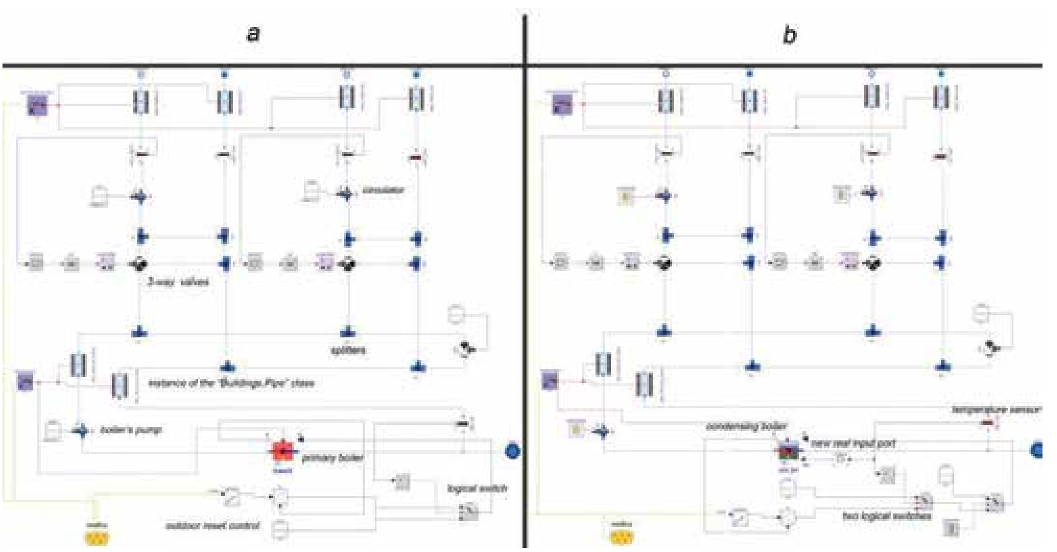

Figure 6. A schematic diagram of the central plant set of models relative to the 2013 scenario (a) and to the 2015 scenario (b).

that is to say in order to set up an outdoor temperature reset control. A safety control device (logical switch) was interposed between the PID output and the boiler input, thereby setting a return water temperature threshold. If the return water temperature is higher than 90°C, the switch will set the boiler input to zero; otherwise, the boiler input will be sent to the PID output ("PID.y"). Four main splitters connect the primary and secondary circuits, in particular, the primary loop with the flow and return pipes of the two secondary circuits. Mixing of the water flowing into and returning from the secondary sub-circuits was carried out by 2 three-way valves. Further pipe components capable of controlling the amount of heat waste were also added even to these parts of the circuits and were coupled to the ground wall component. The only component in this group that was replaced within the time period considered for performing the simulations was the boiler. In fact, the Ecoflam Ecomax NC 630 primary boiler was replaced with a new condensation boiler in November 2013.

Therefore, considering that no class is available in the Modelica.buildings library to simulate a condensation boiler, a new class was developed in order to simulate the 2015 scenario.

The same class as before was used, but it was enhanced in order to be able to take into account the condensation phenomenon relative to the shape of the efficiency curve, the amplified efficiency plot due to condensation, and the dependence of efficiency on return water temperature. No general efficiency relationship was available in the boiler datasheet provided by the manufacturer, which listed no more than a few efficiency values at its maximum load and specified supply and return water temperatures. For that reason, the efficiency curve was defined according to a model that includes both return temperature (T) and load (y) as independent variables [35]:

$$\eta = a(1) \cdot T + a(2) \cdot T\text{^}2 + a(3) \cdot T^3 + a(4) \cdot T\text{^}4 + a(5) \cdot y + a(6) \cdot T \cdot y + a(7) \cdot y \cdot T\text{^}2 + a(8) \quad (2)$$

where a(i) is the coefficient array, whose entries were set according to the suggestions found in relevant literature in the field [36]. To that end, a new curve type was added to those already available in the boiler class, and the coefficients were defined in the form of the array a(i) = {8.663,−0.2866,0.003865,−0.000018676,−11.102,0.2822,−0.00177,7.626}.

In addition, the efficiency estimated by means of Eq. (2) is based on the gross calorific value of the fuel, while the model class in Dymola refers to the net calorific value of the fuel. As a consequence, a multiplication factor as high as 1.11 [27] was used to amplify the efficiency estimated by means of Eq. (2), so that it could include the additional input of heat at return pipe level, determined by the condensation of the vapor produced by fuel combustion.

This approach gave back an estimation of the boiler efficiency. Another change in the boiler class consisted in the generation of a new port for the return water temperature of the heating system that could be used by the enhanced class of the boiler, in order to consider this variable while computing Eq. (2). This new element is depicted in **Figure 6b**, where the temperature sensor placed along the return pipe is connected to the new real input port "T_{in}" entering the class of the modified boiler. The third change concerns the fact that this model included not only one switch but two logical switches. One was used as a safety device, similar to the 2013 model. The other switch was needed to simulate the highly varying rate of the boiler in 2013.

The last group of components was labeled as heating units (**Figure 5b**). One radiator was coupled to the heat ports of each room implemented under the group thermal zones. Among the main parameters, the exponent for heat transfer and the fraction of radiant heat transfer were set according to the datasheet. The valves controlling water flow into the radiators were set fully open, because there is no control at this level in the building. The water flow and return between the heating units group and the central plant group were coupled by means of four fluid ports.

3. User profiles and model calibration

3.1. User profiles and available data

The main difference between the periods January–March in 2013 and 2015 was noticed in terms of the overall monthly consumption. In 2013, seven thermal zones were heated, compared with six thermal zones in 2015 having a smaller extension in terms of net area and gross volume. As a consequence, the corresponding consumption of methane gas during the same months was lower in 2015. The two thermal zones called "A1 l2" and "A2 att" had been closed in the middle of 2013. In November 2013, the old primary boiler was replaced by the new condensation one. Therefore, this contributed to a further reduction in the amount of fuel consumed, and it partially explains why the consumption records listed in **Table 3** are smaller than those listed in **Table 2**. Finally, in January 2015, the heating system was switched off for some time, perhaps due to refurbishment; the system was operational again from February 2015. Another difference between the two simulated scenarios was dependent on the types of data available. As regards 2013, only the consumption readings were monitored. In 2015, the temperature plots in the two zones were also collected. Hence, the profiles for the presence of people in the hospital and the number of light fixtures that were on were managed differently. In 2013, the average daily values were considered. The owner of the community clinic supplied the estimated number of staff members, patients, and other visitors. For each category, a reasonable number of hours of daily permanence in the hospital and the right type of activity were assumed. Finally, the overall thermal gains derived from these assumptions were averaged over the whole simulation period and uniformly distributed throughout the day. This type of analysis was later refined for the 2015 scenario. Dedicated schedules including presence profiles were given as inputs in the simulation. The unit internal gains were estimated on the basis of the figures provided by ASHRAE [28]. The number of hours each fixture or piece of equipment was turned on per working day was determined on the basis of information provided by the hospital staff. In 2015, even temperature plots were given as input for calibration against measured temperature plots. Another parameter that was kept fixed was the air change rate (0.3 vol/h), because previous energy simulations showed that this value gave back the best agreement between the real and the simulated overall consumption of this building [32]. A further contribution was added to this air change rate due to the window permeability. Other relevant parameters were varied for calibration purposes. In particular, the water flow rate in the heating system was used for calibrating the 2013 scenario model. Similarly, the radiator exponent for heat transfer was adjusted in order to match real and simulated consumption figures in the year 2013. In the 2015 scenario, the radiator parameters were kept unvaried with respect to the year 2013. The water flow rate was recalibrated for 2015, because the maintenance team reported that from time to time the rate of the pumps was manually adjusted to the real needs of the building.

3.2. Calibration and validation

The 2013 scenario of the Dymola model is calibrated with respect to the consumption figures recorded from January to March. Some adjustments were then made to the model, in order to recalibrate it with respect to the changes made in 2015. Calibration was performed by means of a comparison between the simulated and monitored data on monthly consumption and indoor air temperature in two thermal zones of the building. In the months January–March 2013, eight readings of measured consumption were available (10 and 25 January, 5, 15, and 25 February; 5, 15, and 25 March 2013). In 2015, six readings of measured consumption were available (5, 15, and 30 January; 27 February, and 13 and 31 March 2015). The modeling uncertainty was measured by means of the indicators: Mean Bias Error (MBE) and Cumulative Variation of Root Mean Squared Error (CVRMSE) values, calculated using the following formulae [27, 28]:

$$MBE = \frac{\Sigma_{i=1}^{N_p}\left(M_i - S_i\right)}{\Sigma_{i=1}^{N_p} M_i} \tag{3}$$

$$CVRMSE = \frac{\sqrt{\Sigma_{i=1}^{N_p}\frac{\left(M_i - S_i\right)^2}{N_p}}}{M_p} \tag{4}$$

where M_i is the list of measured data, S_i is the set of simulated data, N_P is the size of the database, and the average value of the measured data (M_P) will be calculated as

$$M_p = \frac{\Sigma_{i=1}^{N_p} M_i}{N_p} \tag{5}$$

The model calibration was carried out as an iterative process. The first set of parameters was the flow rate provided by the three pumps: the one belonging to the main heating circuit and the two included in the distribution subsystem. These parameters are represented as a three-element array listed in **Table 4**. It can be noticed that MBE and CVRMSE in the case of the initial model were equal to −0.19 and 0.22, respectively. In simulations relative to cases 2–5 listed in **Table 4**, both the water flow rate arrays and the radiator exponent were calibrated in order to improve MBE and CVRMSE with respect to the results obtained from the first simulation scenario. All the MBE indices are negative, so the model always estimated lower consumption than the real data. In **Figure 7a**, a comparison is shown between the cumulative real and simulated consumption plots from January to March 2013, where a very good matching between the two series is qualitatively demonstrated.

Year	Scenario Id	Stage of the calibration process	MBE	CVRMSE (monthly)
2013	1	Base model 2013: water flow = {1.0,1.0,1.0}; radiator exp. = {1.24}	−0.19	0.22
	2	Modified model 1: water flow = {0.3,0.9,0.4}; radiator exp. = {1.24}	−0.05	0.10
	3	Modified model 2: water flow = {0.3,0.9,0.4}; radiator exp. = {1.3}	−0.04	0.10
	4	Modified model 3: water flow = {0.3,0.8,0.4}; radiator exp. = {1.24}	−0.05	0.10
	5	Modified model 4: water flow = {0.3,0.8,0.4}; radiator exp. = {1.3}	−0.04	0.09
2015	6	Base model 2015	0.109	0.28
	7	Modified model 5: water flow: changeable; radiator exp. = {1.3}	0.003	0.13

Table 4. Analysis of the estimation error on methane gas consumption in the whole building.

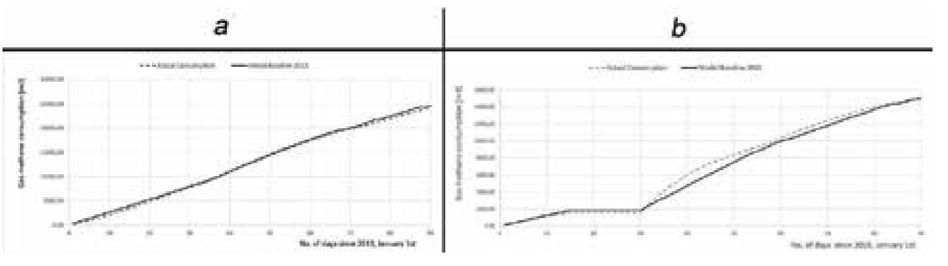

Figure 7. Comparison between cumulative simulated and measured consumption at the community clinic in 2013 (a) and 2015 (b).

The modified model 4 was then adjusted and simulated over the 2015 scenario. The results are listed in line no. 6 of **Table 4**. They are still too far from the 5 and 15% thresholds recommended by technical standards. Considering the very disturbed plot for methane gas consumption in this period (**Figure 7b**), changeable water flow rates were assigned to the three pumps. These are expressed as the ratio of the maximum flow rate admissible for each pump: 0.025 of the maximum flow rate until January 15; turned off until January 30; 1.5 of the maximum at the restart (only on January 31); 100% of the maximum rate until February 15; 0.9 of the maximum rate until February 28; 0.02 of the maximum rate until March 31. The last line in **Table 4** shows that the indices in Eqs. (3) and (4) were again constrained within the required limits. This result is even better if we consider the high variability in consumption and in the operational rate of the system in the period under consideration. As a second validation, the hourly temperature plots monitored in the period from February 10 to March 31 were compared with the plots estimated by the Dymola model in the same rooms. **Figure 8** depicts the very good agreement between them. The real and simulated plots relative to "A2 gf" are in very good

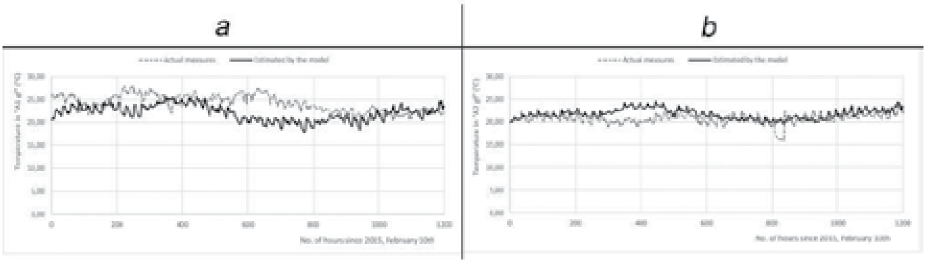

Figure 8. Comparison between real and simulated plots in "A1 gf" (a) and "A2 gf" (b).

agreement, and the average percentage deviation is around 5%. The deviations between the plots in "A1 gf" are still quite reasonable, although the average deviation this time is higher, being about 21%. This was deemed to be a good result, considering that no information had been recorded about real occupation and user behavior during the monitoring period.

4. Action for energy enhancement

4.1. Improved control of the regulation system

As a demonstration of the potential of this model, this paragraph provides an example of the enhanced control system that was integrated in the 2013 scenario. The first scenario was preferred because this baseline is relative to a period during which the heating system was running regularly and assessing to what extent low-cost energy refurbishment action is more expressive because the old heat generator was installed. The assumption made about low-cost actions for energy performance improvement is relative to the installation of an enhanced control system. The community clinic may be equipped with a temperature probe in the most representative rooms, and the rate of the water supply valves might be controlled according to the feedback provided by such records. Two temperature sensors were placed on the ground floor of block A1 and on the second level below the grade of block A2. These two components were connected to two "Real.output" ports, which were then connected to two real input ports within the central plant component (**Figure 9a**). Between of these real inputs and the three-way valves, a hysteresis cluster of components was inserted that sets indoor temperatures between 19 and 21°C. Finally, the new fuel consumption was assessed.

4.2. Discussion of the results

As a result of the simulation performed within the scenario described, the new cumulative fuel consumption of the boiler plotted in **Figure 9b** was calculated. The final value is 18% lower than the benchmark, and such a value represents the average percentage savings that can be obtained each month as a result of the abovementioned enhancement of the control system. This value is strongly dependent on the lowest and highest thresholds set for temperature control in the hysteresis cluster of components and on the control logics chosen

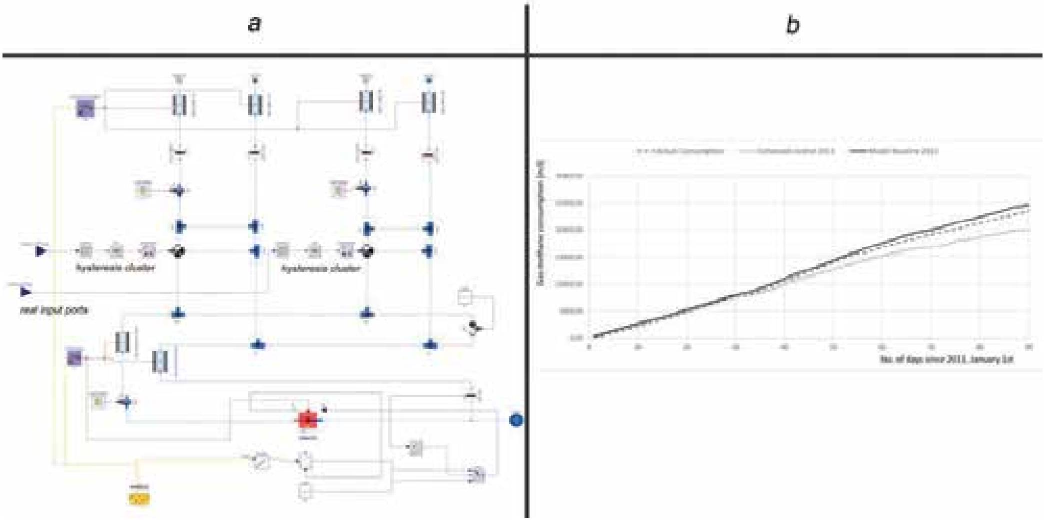

Figure 9. The Dymola model relative to the 2013 scenario with enhanced regulation (a) and the energy savings achievable by that renovation solution (b).

for running the heating system. However, the generally valid conclusion is that, once the baseline model has been calibrated for the reference scenario, the benefits deriving from even tailored control policies can be simulated. In the case under analysis, the control subsystem enhancement was relative to a very slight change with respect to the reference scenario. Moreover, it was tailored to the building under analysis, in that only two sensors were placed in two rooms, rather than in every room of the building. Therefore, neither can be classified as a standard control system nor can it be simulated by means of standard whole building analysis tools. In fact, this scenario can be simulated in this model, which is also capable of providing detailed results, such as the temperature difference that this control would generate between floors.

5. Conclusions

In this chapter, the energy model of a typical small public building was developed. It can be considered as representative of a popular category of public buildings that cannot undergo extensive refurbishment because of budget limitations. Hence, the only option is to implement low-cost retrofit solutions that can make energy savings possible by means of reduced investments. This scheme applies to any case in which budget constraints prevent the adoption of complete refurbishment of the audited object. Therefore, in this case, an accurate assessment of potential energy savings is necessary under real dynamic conditions. The case study considered in this chapter was modeled in the Dymola/Modelica environment and was shown to be very flexible, adaptable, and capable of modeling any kind of technology that can reasonably be found in buildings, thanks to its open “Buildings” library. In addition, it was able to provide estimations about the improvements that may be determined by retrofit actions,

http://dx.doi.org/10.5772/intechopen.78613

even if relative to low-cost enhancement regarding minor devices of existing subsystems and components. Hence, this software tool may be considered as a valid support for performing reliable cost–benefit analyses for the energy retrofit of buildings.

Author details

Alessandro Carbonari[1]*, Massimo Vaccarini[1] and Emanuela Quaquero[2]

*Address all correspondence to: alessandro.carbonari@univpm.it

1 Department of Civil and Building Engineering and Architecture (DICEA), Università Politecnica delle Marche, Ancona, Italy

2 Department of Civil and Environmental Engineering and Architecture (DICAAR), Università di Cagliari, Cagliari, Italy

References

[1] Perez-Lombard L, Ortiz J, Pout C. A review on buildings energy consumption information. Energy and Buildings. 2008;**40**:394-398

[2] IPCC. Summary for Policymakers—Contribution of Working Group III to the Fourth Assessment Report of the Intergovernmental Panel on Climate Change. Cambridge: Cambridge University Press; 2007

[3] European Commission. Action Plan for Energy Efficiency. Realising the Potential. Brussels: European Commission; 2006

[4] Taillandier F, Mora L, Breysse D. Decision support to choose renovation actions in order to reduce house energy consumption—An applied approach. Building and Environment. 2016;**109**:121-134

[5] Silenzi F, Priarone A, Fossas M. Hourly simulations of an hospital building for assessing the thermal demand and the best retrofit strategies for consumption reduction. Thermal Science and Engineering Progress. In press. DOI: 10.1016/j.tsep.2018.01.015

[6] Silva HE, Henriques FMA, Henriques TAS, Coelho G. A sequential process to assess and optimize the indoor climate in museums. Building and Environment. 2016;**104**:21-34

[7] Tomazic S, Logar V, Kristl Z, Krainer A, Skrjanc I, Kosir M. Indoor-environment simulator for control design purposes. Building and Environment. 2013;**70**:60-72

[8] Gorni D, Castilla MdM, Visioli A. An efficient modelling for temperature control of residential buildings. Building and Environment. 2016;**103**:86-98

[9] Wetter M. Modelica library for building heating, ventilation and air-conditioning systems. In: Proceedings of 7th International Modelica Conference; 20-22 September 2009; Como, Italy

[10] Wetter M, Zuo W, Nouidui TS. Modeling of heat transfer in rooms in the modelica "buildings" library. In: Proceedings of 12th Conference of International Building Performance Simulation Association, 14-16 November 2011; Sydney, Australia

[11] Hernandez-Albaladejo G, Urquia A. Modelling of low-temperature solar thermal systems with Modelica. IFAC Papers OnLine 51-2. 2018. pp. 783-788

[12] Sahlin P, Eriksson L, Grozman P, Johnsson H, Shapovalov A, Voulle M. Whole-building simulation with symbolic DAE equations and general purpose solvers. Building and Environment. 2004;**39**:949-958

[13] Wetter M. Modelica-based modelling and simulation to support research and development in building energy and control systems. Journal of Building Performance Simulation. 2009;**2**(2):143-161

[14] Bünning F, Sangi R, Müller D. A Modelica library for the agent-based control of building energy systems. Applied Energy. May 2017;**193**(1):52-59

[15] Trčka M, Hensen JLM, Wetter M. Co-simulation of innovative integrated HVAC systems in buildings. Journal of Building Performance Simulation. 2009;**2**(3):209-230

[16] Traore I, Gavan V, Riffonneau Y, L'Henoret B, Drouet E. Development of a generic and scalable modelica based model of a typical French railway station building. In: Proceedings of BS 2013; 25-28 August 2013; Chambery, France. ISBN 9782746662940

[17] Sangi R, Müller D. Dynamic modelling and simulation of a slinky-coil horizontal ground heat exchanger using Modelica. Journal of Building Engineering. March 2018;**16**:159-168

[18] Vaccarini M, Carbonari A, Casals M. Development and calibration of a model for the dynamic simulation of fans with induction motors. Applied Thermal Engineering. 2017;**111**:647-659

[19] Monfet D, Zmeureanu R. Calibration of a central cooling plant model using manufacturer's data and measured input parameters and comparison with measured performance. Journal of Building Performance Simulation. 2013;**6**(2):141-155

[20] Short CA, Cook M, Cropper PC, Al-Maiyah S. Low energy refurbishment strategies for health buildings. Journal of Building Performance Simulation. 2010;**3**(3):197-216

[21] Adolph M, Kopmann N, Lupulescu B, Muller D. Adaptive control strategies for single room heating. Energy and Buildings. 2014;**68**:771-778

[22] Raftery P, Keane M, Costa A. Calibrating whole building energy models: Detailed case study using hourly measured data. Energy and Buildings. 2011;**43**:3666-3679

[23] ASHRAE. ASHRAE Guideline 14-2002: Measurement of Energy and Demand Savings. American Society of Heating. Atlanta, GA: Refrigeration and Air Conditioning Engineers. 2002

[24] European Committee for Standardization. Energy Audits—Part 2: Buildings. EN 16247-2:2014; 31st July 2014

[25] Buratti C, Moretti E, Belloni E, Cotana F. Unsteady simulation of energy performance and thermal comfort in non-residential buildings. Building and Environment. 2013;**59**:482-491

[26] Mattsson SE, Hilding E. Modelica—An international effort to design the next generation modeling language. In: Boullart L, Loccufier M, Mattsson SE, editors. 7th IFAC Symposium on Computer Aided Control Systems Design; April 1997; Gent, Belgium

[27] Day AR, Ratcliffe MS, Shepherd KJ. Heating Systems, Plant and Control. Oxford: Blackwell Science; 2003. ISBN: 978-0-632-05937-9

[28] American Society of Heating Refrigerating and Air-Conditioning Engineers. 2009 Ashrae Handbook: Fundamentals. 2009. ISBN-13: 978-1933742540, ISBN-10: 1933742542

[29] Athienities AK, Santamouris M. Thermal Analysis and Design of Passive Solar Buildings. James and James Publisher; 2002. ISBN: 1-902916-02-6

[30] European Committee for Standardization. Thermal performance of buildings. Heat transfer via the ground—Calculation methods. EN ISO 13370:2007; 15th December 2007

[31] Available from: http://www.wunderground.com [Accessed: May 2015]

[32] Carbonari A, Giuliani M, Ruffini S, Lemma M. Measured and estimated breakdown of energy consumption in a community clinic. In: Proceedings of KGH 2014; ISBN: 9788681505755

[33] Italian Organization for Standardization. Prestazioni energetiche degli edifici—Parte 1: Determinazione del fabbisogno di energia termica dell'edificio per la climatizzazione estiva ed invernale. UNI, UNI TS 11300-1:2008; 28th May 2008

[34] International Organization for Standardization. Energy performance of buildings—Calculation of energy use for space heating and cooling. ISO 13790:2008; 1st March 2008

[35] Aganovic A. Analysis of dynamical behavior of the boiler room [Master's thesis]. Norwegian University of Science and Technology, Department of Energy and Process Engineering; Mechanical Engineering Faculty in Sarajevo in Standard Exploitation Conditions; Submitted on August 2013

[36] Cockroft J, Samuel A, Tuohy P. Development of a methodology for the evaluation of domestic heating controls—Phase 2 of a DEFRA Market Transformation Programme Project. ESRU Report. Carried out under Contract to BRE Environment. University of Strathclyde; 4th July 2007

The Solution of Private Problems of Optimization for Engineering Systems

Andrei Melekhin

Additional information is available at the end of the chapter

http://dx.doi.org/10.5772/intechopen.80520

Abstract

The author has developed a mathematical model of process of heat exchange in heat exchange surfaces of apparatuses with the solution of multicriteria optimization problem, an optimal range of managed parameters influencing the process of heat exchange with minimal metal consumption and the maximum heat output fin heat exchanger, the regularities of heat exchange process with getting generalizing dependencies distribution of temperature on the heat-release surface of the heat exchanger engineering systems of buildings, defined convergence of the results of research in the calculation on the basis of theoretical dependencies and solving mathematical model.

Keywords: mathematical model, heat exchanger, air heating systems of buildings, ribbed surface, thermal imaging survey

1. Introduction

The conduct of practical studies to optimize basic parameters in engineering systems of buildings is urged by power-saving requirements.

The given practical problem of improving engineering systems is to optimize the design of the heat exchanger in air heating systems of buildings.

Air heating systems of buildings are resource-consuming systems, for this reason, improving their resource efficiency appears to be of great significance.

Heating of air is provided by heat exchangers, which have been studied quite thoroughly. The studies involved different authors to deal with particular aspects of improving heat exchange elements [1].

The main properties of heat exchangers, such as amount of heat exchange, area of heat exchange, metal capacity and cost of an apparatus depend largely on the size of ribbing, so the efficiency of the design is determined by the optimal height of the rib [2, 3].

One of the authors of this paper, Khrustalev, looked into the criterion to assess the efficiency of heat exchanger design. The paper also suggests theoretical dependencies to calculate technical characteristics of heat exchangers. However, these dependencies do not allow optimization on several parameters [4–6].

A.A. Melekhin in his previous papers studied the multicriterion optimization of the rib in heat exchangers based on two criteria; however, other parameters were not considered [7].

In the given paper the author makes a thermodynamic analysis and optimizes heat exchangers of air-cooling, at the same time these improvements are not based on the complex approach [8].

The occurrence of new methods, namely a complex method, allows combining mathematical modeling with visualization of heat fields, and as a result, obtaining optimal parameters of heat exchangers for the given systems.

The purpose of the given study is improving the efficiency of heat exchangers by optimizing their parameters and design.

To achieve this goal we set and solved the following tasks:

- we have developed a mathematical model of multicriterion problem to optimize heat exchange on the ribbed heat exchanging surfaces.
- using the mathematical model we developed, we have determined the mechanism of heat exchanging process and have derived dependencies of temperature distribution on heat exchange surfaces in heating systems of buildings during the heating season;
- we have made a comparison of the obtained results with the results based on the established theoretical dependencies;
- we have reduced the metal capacity of the heat exchanger by improving its heat engineering characteristics.

The novelty of the given paper lies in the following:

- we have elaborated a new complex research technique, based on multi-criterion problems with generic dependencies, obtained from empirical data.
- we have obtained functional dependence of process parameters on heat exchanging surfaces on optimal geometrical parameters of the heat exchanger.

The practical value of the paper is in the following:

- we have derived semiempirical equations for computing and designing air heating systems in buildings;
- we have reduced metal capacity of heat exchangers which are used in air heating systems of buildings.

2. Materials/methods

In order to set optimal parameters for the heat exchanger and balance its design with technological elements the author conducted actual studies with the help of the complex method. It comprises optimization of parameters for heat exchanging process based on multicriterion multiparameter mathematical models and experiments with thermal field visualization.

The optimization problems are solved using the method of non-linear optimization in computing complex IOZO NM 3.0b [9].

Besides, the solution of such problems is also possible with the help of non-linear optimization program Generalized Reduced Gradient (GRG2), designed by Leon Lasdon, University of Texas at Austin and Allan Waren, Cleveland State University, and based on the method of conjugate gradients—iterative method for unconstrained optimization in multidimensional space. The main advantage of this software package is that it is able to solve the quadric optimization problem within finite number of moves. So, first the author describes the method of conjugate gradients to optimize the quadric functional, then he derives iterative formulas and estimates convergence rate. Next, the author demonstrates how the method of conjugate gradients is generalized to optimize arbitrary functional, looks at different variations of the method, and assesses convergence. The shortcoming is that controllable and non-controllable parameters and criteria are constrained [10].

It is possible to use as a mathematical model a two-criterion problem of clusterization with fuzzy constraints. The fuzzy constraints can be set by specific preference functions. The solution is made in Boolean variables with the help of stochastic search, improved by heuristics. The algorithm is implemented in the form of a universal software module [11].

Solution of multicriterion multiparameter nonlinear optimization problem of engineering systems in buildings suggested applying software package IOSO NM version 3.0b, where the author entered empirical data from thermal imaging. A special feature of this software is its compatibility with Microsoft Excel and other programs. IOSO package allows setting controllable and noncontrollable parameters, optimal criteria, and constraints for the process. Further, IOSO program establishes optimal process parameters by using the data from Excel.

Preliminary IOSO procedure is forming the initial experiment plan, which can be passive (using the previously obtained information about variable parameters, optimization criteria and constraints), as well as active, when the set is generated in the initial search field in accordance with the preset partition law. Each vector of variable parameters for optimization and constraints implies direct use of mathematical model of the object studied. The number of points in the initial experiment plan depends on the problem dimension and the chosen variant of approximation function.

3. Results and discussion

To find the minimum mass of the ribs of the heat-exchange apparatus with the maximum of its heat productivity developed mathematical model of multi-criteria optimization problem

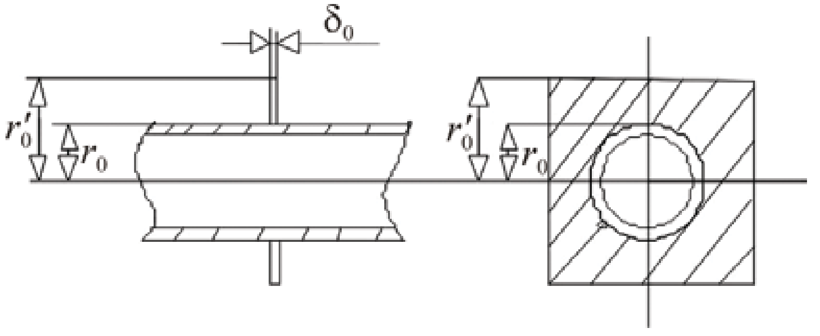

Figure 1. Radial edge.

parameters heat-giving elements of the heat-exchange apparatus systems of air heating of buildings, which is solved using the method of nonlinear optimization [12, 13].

Formulation of the mathematical model has been made for the outer surface of the radial ribs (**Figure 1**).

The temperature on the surface of the ribs defines heat output, and the height of the rib - metal heat-exchange apparatus, so as the optimality criteria for staging a mathematical model selected [14]:

1. the temperature on the surface of the ribs (J1);
2. the height of the ribs (J2).

As unmanaged parameters taken: the radius of the carrier pipe, of a thickness of edges, the thermal conductivity of the ribs, the location of the beam in a heat exchanger, step ribs, the number of ribs, the number of the Nusselt number for the air, the Reynolds number for the air, the coefficient of heat transfer from the wall to the air, etc. ($x_1 \ldots x_n$).

In work the estimation of influence of these parameters on the process of heat exchanger.

As of controlled parameters are: ambient air temperature, the temperature of the heat-carrier ($U_1 \ldots U_n$) as the most influence on the heat transfer process.

In the process of heat exchange occurs between the warm water and the environment, which depend on parameters of water and air. Parameters that characterize these changes are within the permissible limits, established for the process.

The dependence of optimization criteria [15] and process parameters:

$$\begin{aligned} J_1 &= J_1(x_1, \ldots\ x_{21}; U_1, U_2) \to \text{max}, \\ J_2 &= J_2(x_1, \ldots\ x_{21}; U_1, U_2) \to \text{min}. \end{aligned} \tag{1}$$

Restrictions on the parameters of the process, is within the following limits:

$$x_i^{\text{min}} \le x \le x_i^{\text{max}}, \tag{2}$$

$$J_i^{\min} \leq J_i\ (x_i) \leq J_i^{\max}, \tag{3}$$

$$r = r_0;\ \ \vartheta = \vartheta_0;\ \ r = r_0';\ \ \frac{d\vartheta}{dr},\ \ \delta_0,\ \ \lambda_{c_2} = \text{const}. \tag{4}$$

The task of searching for the optimal height of the ribs is to find x϶ D in cases, when

$$\begin{aligned} &J_1(x_1,\ \ \dots\ x_{21}, U_1, U_2) \to \max, \\ &J_2(x_1,\ \ \dots\ x_{21}, U_1, U_2) \to \min. \end{aligned} \tag{5}$$

Thus, the problem can be formulated as follows: it is required to find such controlled parameters of the element heat exchanger (fins), which are optimal from the perspective of the selected criteria under the given constraints.

The basis of mathematical model equations Bessel, describing the temperature distribution on the outer surface of the ribs.

Modified Bessel equation for the radial fin of rectangular profile is:

$$r^2 \frac{d^2\vartheta}{dr^2} + r\frac{d\vartheta}{dr} - m^2 r^2 \vartheta = 0, \tag{6}$$

$$m = \frac{2\alpha}{\lambda_{c_2}\delta}, \tag{7}$$

where, m—the dimensionless complex; α—heat transfer coefficient from the outer surface to the air, W/(m^2 * °); λ_{c_2}—thermal conductivity of fin, W/(m * °); δ—thickness of fin, m.

The heat transfer coefficient from the outer surface to the air, W/(m^2 *grad.):

$$\alpha = \frac{\text{Nu}_\text{в} \cdot \nu_\text{в}}{h}, \tag{8}$$

where $\text{Nu}_\text{в}$—the Nusselt number for air; $\nu_\text{в}$—coefficient of kinematic viscosity of air, m^2/s; h—fin height, m.

The Nusselt number for turbulent regime of the air movement:

$$\text{Nu}_\text{в} = 0,096 \cdot \text{Re}_\text{в}^{0,72} \cdot \left(\frac{d_\text{н}}{h_\text{р}}\right)^{0,54} \cdot \left(\frac{h}{h_\text{р}}\right)^{-0,14}, \tag{9}$$

where R—step rib, m; d—outside diameter of pipe, m; h—height of fin, m; Re_B—Reynolds number for air.

Given the heat transfer coefficient:

$$\alpha_{2np} = \alpha_2 \cdot \left(\frac{F_\text{р} \cdot \theta_0}{F_{pc} \cdot \theta_1} + \frac{F_\text{п}}{F_{pc}}\right), \tag{10}$$

where α_2—heat transfer coefficient, W/(m$^{2*\circ}$); θ_0—the difference between the temperatures of the surfaces of the ribs and of air, degrees; θ_1—the difference in temperature between the core tube surface and air, °; F_{π}—surface area between the ribs, m^2; F_{pc}—area finned surface, m^2; F_{p}—area of fins, m^2.

The general solution is determined by the ratio:

$$\theta = C_1 J_0(mr) + C_2 K_0(mr). \tag{11}$$

The constant $K_1,\ K_0,\ J_0,\ J_1$ is calculated in accordance with boundary conditions described above.

$$\theta_0 = C_1 J_0(mr_0) + C_2 K_0\left(mr_0'\right), \tag{12}$$

$$0 = C_1 J_1(mr_0) + C_2 K_1(mr_0). \tag{13}$$

Calculating C_1, C_2 we find the temperature distribution along fin height for the radial fin of rectangular shape (grad.):

$$\theta(r) = \frac{\theta_0\left(K_1\left(mr_0'\right) \cdot J_0(mr), +J_1\left(mr_0'\right)K_0(mr)\right)}{J_0(mr_0)K_1\left(mr_0'\right) + J_1\left(mr_0'\right)K_0(mr_0)}, \tag{14}$$

where θ_0 is the temperature on the surface of the carrier pipe, degrees.

To estimate the heat flux from the surface of the ribs used in the work the dependence proposed by Bessel:

$$q_0 = 2\pi_0 r\delta_0\lambda m\theta_0\left[\frac{J_1\left(mr_0'\right)K_1(mr_0) - K_1\left(mr_0'\right)J_1(mr_0)}{J_0(mr_0)K_1\left(mr_0'\right) + J_1\left(mr_0'\right)K_0(mr_0)}\right]. \tag{15}$$

Thus, the problem can be formulated in the following way: it is required to find such managed parameters element of heat exchanger (the height of the edges), which are optimal from the point of view you are the chosen criteria under certain constraints.

The basis of mathematical model based on Bessel equation describing the distribution of temperature on the outer surface of the ribs [4].

For the staging of the mathematical model are determined boundary conditions of the process of heat transfer in the work of the air heating systems, described in the dependencies (2–4).

To create the most resource-efficient heat exchangers in the article the low temperature and middle temperature of the heating system of the buildings with the following parameters the heat-carrier from +45 to +95°. With these parameters the heat exchanger of the most metal-consuming.

To identify the most critical conditions of heat exchange on the surface of the ribs considered by the turbulent mode of movement of the heat-carrier temperature of ambient air from −35 up to 10°. The analysis of use of brands fans in systems of air heating of buildings. Set the maximum speed of the air entering the heat exchanger—7 kg/(m^2•°), which would consider in selecting the data of heat exchangers. Solution of the task is carried out with the help of the method of conjugate gradients—iterative method for unconstrained optimization of the multidimensional space, of the solution of a quadratic optimization problem for a finite number of steps.

As a software complex for solving multiparameter nonlinear multiobjective optimization of engineering systems of buildings used IOSO NM [9].

A feature of this complex is compatible with Microsoft Excel and other programs. Empirically obtained data are compiled in Excel. In the program IOSO are controllable and uncontrollable parameters, optimality criteria, restrictions on the parameters of the process. Next, the program IOSO generates optimal process parameters selection method from Excel [8].

Preliminary procedure IOSO is the formation of the initial experiment plan that could be implemented as a passive way (using information about various parameters, the optimization criteria and constraints obtained earlier) and active way, when too much is generated in the initial search area in accordance with a given distribution law. For each vector of variable

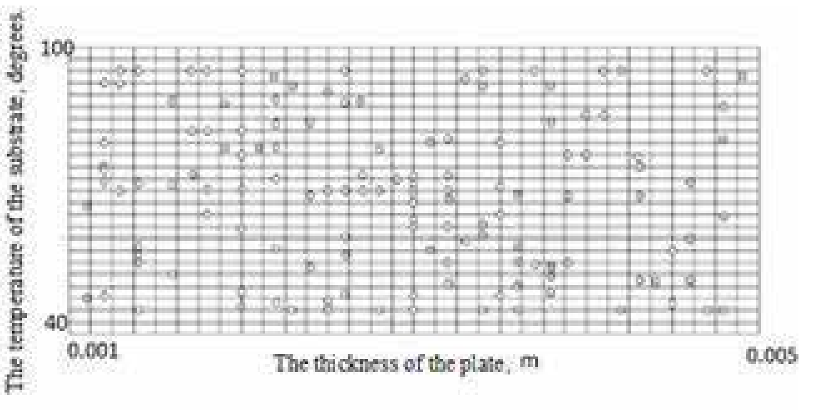

Figure 2. The temperature of the substrate surface (°) from the thickness of the plate (m) (all solutions).

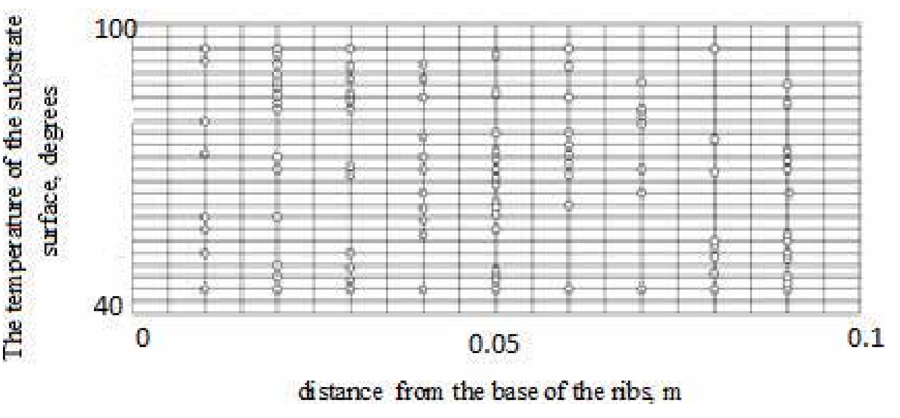

Figure 3. The temperature of the substrate surface (°) from a distance from the base of the ribs (m) (all solutions).

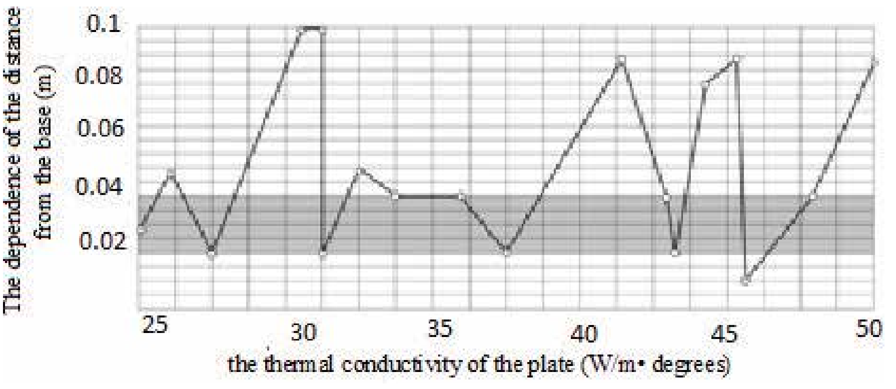

Figure 4. The dependence of the distance from the base (m) of the fin from the thermal conductivity of the plate (W/m• °) (optimal solution).

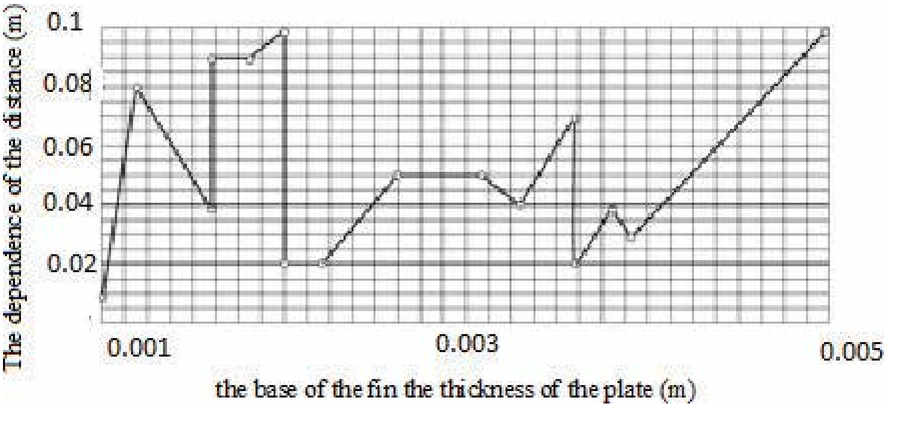

Figure 5. The dependence of the distance (m) from the base of the fin the thickness of the plate (m) (optimal solution).

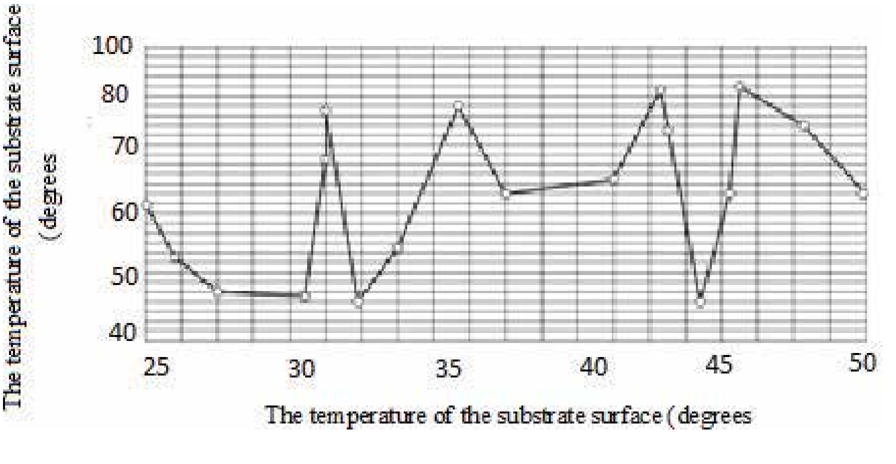

Figure 6. The temperature of the substrate surface (°) from the thermal conductivity of the plate (W/m• °) (optimal solution).

parameters, the values of the optimization criteria and constraints are determined by direct appeal to the mathematical model of the investigated object. The number of points constituting the initial plan of the experiment depends on the dimension of the problem and the selected approximation functions.

Figures 2–8 shows the Pareto-optimal set of values when solving multi-criteria parameter optimization of a fin heat exchanger by using design software IOSO NM obtained the optimal values. For ease of understanding the obtained values of the graphs for each controlled parameter.

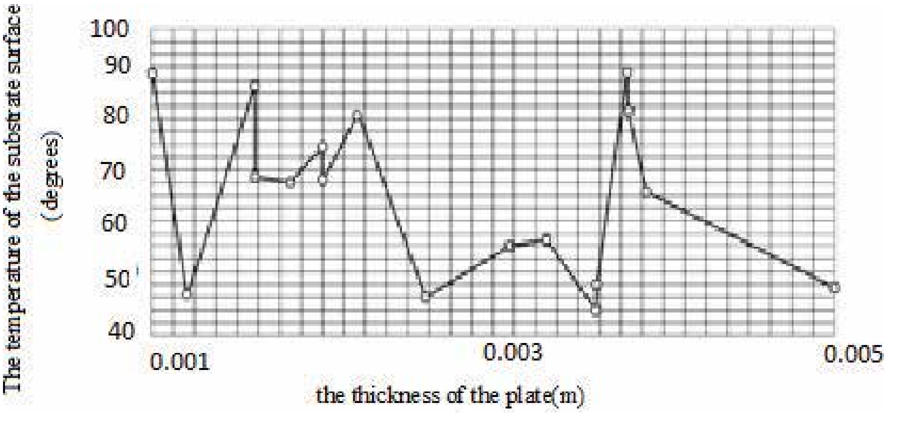

Figure 7. The temperature of the substrate surface (°) from the thickness of the plate (m) (optimal solution).

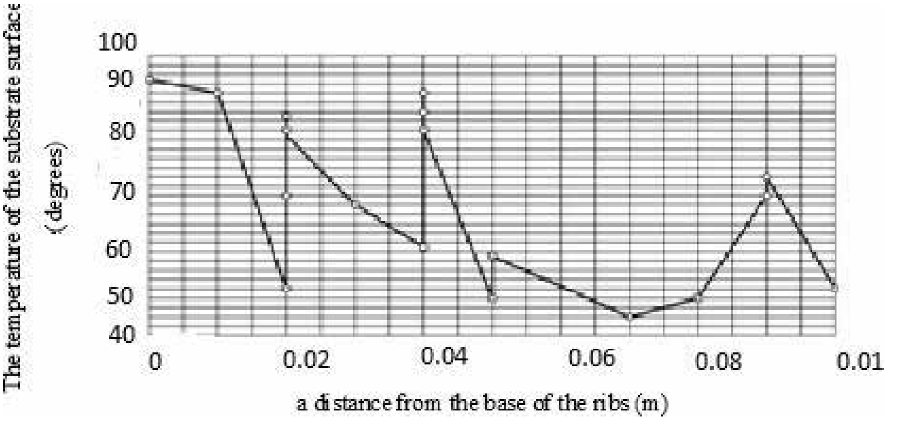

Figure 8. The temperature of the substrate surface (°) from a distance from the base of the ribs (m) (the optimal solution).

4. Conclusion

Improving the energy efficiency of engineering systems of buildings and structures, reduction of energy consumption through the optimization of their operation, introduction of energy saving technologies and optimization of structural elements of engineering systems is important.

As applied problems of improvement of engineering systems of buildings considered an example of optimization of heat exchanger element air heating system of the building.

Finding the best managed of the parameters of the heat exchanger element air heating system of a building is possible with the developed by the author of a comprehensive method of research based on multi-criteria parameter optimization with the introduction of empirically obtained data.

When developing a mathematical model of the heat exchanger element air heating system of a building used for the basic equations of heat and mass transfer.

The decision of tasks of optimization carried out using the method of nonlinear optimization in design-software complexes IOZO.

The aim of the study is to increase the efficiency of engineering systems of buildings by optimizing the parameters of the elements of heat exchangers used in air heating systems of buildings.

To achieve this goal the author posed and solved the following tasks:

- developed a mathematical model of multicriteria optimization problems of the process of heat transfer on finned heat transfer surfaces of the apparatus;
- the regularities of process of heat exchange with the receipt of the generalized dependency of the temperature distribution on the heat-transfer surface of heat exchanger air heating systems of the buildings at work during the heating period using the developed mathematical model;
- a comparison of the obtained results with the known theoretical dependencies;
- reduced metal heat exchanger optimized thermal performance.

Author details

Andrei Melekhin

Address all correspondence to: melehin2006@yandex.ru

Moscow State University of Civil Engineering (National Research University), Moscow, Russia

References

[1] Bejan A. Convection Heat Transfer. 4th ed. New York, NY, USA: John Wiley & Sons; 2013

[2] Liu S, Saker M. A comprehensive review on passive heat transfer enhancements in pipe exchangers. Renewable and Sustainable Energy Reviews. 2013;**19**:64-81

[3] Hasan MI, Rageb AMA, Yaghoubi M. Investigation of a counter flow microchannel heat exchanger performance with using nanofluid as a coolant. Journal of Electronics Cooling and Thermal Control. 2012;**2**(2):35-43; 2013;**58**:68-76

[4] Khrustalev BM, Nesenchuk AP, et al. Heat and Mass Transfer. Part 1. Minsk: Belarusian National Technical University; 2007

[5] EU. The Vilkas, Maiminas AS. Solution: Theory, Information, Modeling. Moscow: Radio and Communication; 1981

[6] Himmelblau D. Applied Nonlinear Programming. Translation from English Publishing House "World". Moscow: World; 1975

[7] Melekhin AA, Melekhin AG. Optimization of parameters of heat exchangers of air heating systems. Applied Mechanics and Materials. 2014;**672–674**:1471-1480; Switzerland; 1662-7482

[8] Salimpour MR, Bahrami Z. Thermodynamic analysis and optimization of air-cooled heat exchangers. International Journal of Heat and Mass Transfer. New York: Springer. 2011;**47** (1):35-44

[9] Egorov IN, Kretinin GV, Leschenko IA, Kuptcov SV. Multi-objective optimization using IOSO technology. In: 7th ASMO UK/ISSMO Conference on Engineering Design Optimization; Bath, UK; 7–8 July, 2008

[10] The tool Microsoft Excel Solver uses an algorithm of nonlinear optimization Generalized Reduced Gradient (GRG2), developed by the Leon Lasdon (University of Texas at Austin) and Allan Waren (Cleveland State University)

[11] Burke EK, Landa Silva JD, Soubeiga E. Hyperheuristic approaches for multiobjective optimization. In: Proceeding of the MIC 2003; Kyoto, Japan; 2003

[12] Kashevarova GG, Permyakova TB. Numerical Methods for Solving Problems of Construction of the Computer. Perm: Publishing house of PSTU; 2007

[13] Kashevarova GG, Martirosyan AS. Software implementation of the algorithm the statistical straggling of the mechanical properties of materials in the design of structures. Advanced Materials Research. Switzerland: Trans Tech Publication. 2013;**684**:106-110

[14] Lapidus AS. Selection of criteria for the engineering and economical optimization of heat exchangers. International Journal of Chemical and Petroleum Engineering. New York: Springer. 1977;**13**(2):160-165.

[15] Sobol IM, Statnikov RB. The Choice of Optimal Parameters in Problems with Many Criteria. Moscow: Science; 1981

Chapter 7

Improving the Vehicular Engine Pre-Start and After-Start Heating by Using the Combined Heating System

Igor Gritsuk, Vasyl Mateichyk, Miroslaw Smieszek, Vladimir Volkov, Yurii Gutarevych, Valery Aleksandrov, Roman Symonenko and Valeriy Verbovskiy

Additional information is available at the end of the chapter

http://dx.doi.org/10.5772/intechopen.79467

Abstract

The chapter focuses on the use of the combined thermal development system with phase-transitional thermal accumulators. The peculiarity of the combined system is that it uses thermal energy of exhaust gas, coolant and motor oil for rapid pre-start and after-start heating of the vehicular engine. The structure of the combined thermal development system and a mathematical model have been developed to study the impact of the system parameters on the heating processes of the engine. The results of experimental and estimation studies of thermal accumulator materials and the combined heating system of the vehicular engine are shown. For a truck engine 8FS 9.2/8, it is shown that the use of the combined system reduces the time of coolant and motor oil thermal development by 22.9–57.5% and 25–57% accordingly compared with the use of a standard system. The peculiarities of forming and using the system depend on operational and climatic conditions and the category of the vehicle.

Keywords: vehicular engine, phase-transitional thermal accumulator, thermal development system, heating processes, mathematical model

1. Introduction

One of the promising ways to improve engine cooling systems is the introduction of modern technology into their design in order to increase efficiency and adapt to operating conditions, etc. These measures include a variety of methods of analysis, design, experimental studies, both at the system level and at the component level. These suggested methods are particularly relevant to those modes of vehicular engines that require significant efforts for their thermal development under cold operating conditions. They are as follows: pre-start and after-start heating of the engine, keeping the engine heated for a successful start under cold operating conditions. Apart from ease of use, the decisive factors are low cost of devices for engine thermal development, state legislation and standards, the need for full power immediately after the engine starts, improved fuel economy and reduced emissions during pre-start and after-start thermal development. The limiting factors are weight and size characteristics of the devices and their compact installation space according to modern vehicle design. In this regard, the most relevant is the development of complex systems for solving these problems in both the design of the engine and the vehicle. In this case one of the promising ways is the development and the study of the combined heating system with phase-transitional thermal accumulator (TA) to carry out pre-start and after-start heating of the engine under cold operating conditions.

2. Creating the scheme of the ICE and vehicle combined heating system and its operating principle

To create the ICE and vehicle heating system, a combination of phase-transitional thermal accumulators was used (combination by function). Thermal accumulator is a device for accumulating thermal energy based on physical or chemical process associated with heat absorption and release [1–11]. The main processes are: accumulation-release of internal energy when heating–cooling solids or liquids, phase transitions with absorption-release of latent heat, the process of sorption–desorption or a reverse chemical reaction occurring with heat release-absorption. Accumulation of thermal energy or heat accumulation is a process of accumulating thermal energy, when its supply is maximum, for later use when the need arises. The process of accumulating energy is called charging, the process of its use is called discharging [1–5]. Substances used to accumulate thermal energy are called heat accumulating materials. The amount of accumulated energy depends on the temperature at which heat accumulating material is heated and its specific heat capacity. The main operating procedures in thermal accumulators, namely the accumulation of thermal energy, are based on the reverse phase-transitional process of melting-solidification. In this case, phase change material is used as the heat accumulating material. The implementation of this method is more difficult because of the need to make the design more complicated. However, much greater amount of heat per unit of volume is accumulated in such thermal accumulators. The process of charging and discharging can be performed in a narrow temperature range, which is very important when there is a need for thermal accumulators to work at small temperature differences. In vehicles the use of thermal accumulators is advantageous to facilitate the engine start and heating the vehicle interior during cold weather. The heat is accumulated during engine operation and can be stored for several days. To do this, thermal accumulator is placed in a Dewar flask (thermos) which provides the best thermal insulation.

In [1, 2], the main stages of creating the combined heating system (CHS) of the vehicular engine and the vehicle are shown. To ensure the required temperature condition during pre-start and after-start heating of the internal combustion engine (ICE) and the vehicle under cold operating conditions, a scheme and components of the CHS are formed on the basis of vehicular engine main systems. The suggested CHS consists of the following subsystems: rapid heating of the engine (RHE), the utilization of thermal energy of exhaust gases (EG) by phase-transitional TA (UTETA), contact thermal accumulator (CTA), thermal accumulator for storing motor oil (TASMO), thermal accumulator for storing a coolant (TASC), TA of EG cleaning system (TAEGCS). The CHS itself is a part of a cooling system (CS), lubrication system (LS) and exhaust system of the vehicular engine. It performs some functions of the systems and has a significant influence on the operation of the vehicular engine [1–4]. It is the CHS that provides pre-start and rapid after-start heating of a coolant and motor oil, exhaust gases cleaning system (EGCS) of the engine to the temperature at which the engine can be loaded and then to an operating temperature. The operating temperature is maintained for a long time within specified limits.

The elements of the combined heating system, such as the subsystems of rapid heating of the engine, the utilization of thermal energy of exhaust gases by phase-transitional TA, contact thermal accumulator and thermal accumulator for storing a coolant are the components of the engine cooling system. TA of EG cleaning system is a component of the engine exhaust system. The elements of the combined heating system, such as the subsystems of rapid heating of the engine, the utilization of thermal energy of exhaust gases by phase-transitional TA, contact thermal accumulator and thermal accumulator for storing motor oil are the components of the engine lubrication system. All the above-mentioned subsystems can work together within and according to the algorithm of the combined heating system operation or separately from each other performing their inherent functions [1, 5].

The combined heating system generally works on the principle of thermal energy of EG accumulation by phase-transitional thermal accumulator of the utilization of thermal energy of EG subsystem. It also implies the accumulation of engine thermal energy by contact thermal accumulator in the form of convection and thermal radiation of the vehicular engine during its operation. The "free" thermal energy generated during the fuel combustion is emitted into the atmosphere and is not used usefully.

Figure 1 shows the implementation of the combined heating system for the vehicular engine. EG thermal energy accumulation of the vehicular engine 1 by phase-transitional thermal accumulator, namely by the subsystem of the utilization of thermal energy of exhaust gases 20, is made possible by parallel installing the engine silencer 18 in the EG heat exchanger (HE) 6. The circulation of a heat carrier between TA 20 and exhaust gases heat exchanger 6 is provided by a modulating pump 21. The heat carrier passing through HE 6 in the exhaust manifold is heated by thermal energy of EG to a temperature of 150–190°C (a process fluid with a boiling point of 220°C was used as the heat carrier). Heat exchanger 6 is installed in a bypass, in parallel with the main EG manifold of the vehicular engine. Such a decision was made in order to ensure the disconnection of the heat exchanger 6 after phase-transitional TA 20 of the subsystem of the utilization of thermal energy is fully charged. The switching of EG flow is carried out by electromagnetic gas valves 30 and 25 with an electric drive based on control system commands. The EG flow adjustment is carried out following a special algorithm [4, 9, 10] according to a developed cycle of heating the engine. From the heat exchanger 6 the heat carrier delivers the heat into phase-transitional TA 20 of the subsystem of the utilization of thermal energy. In an

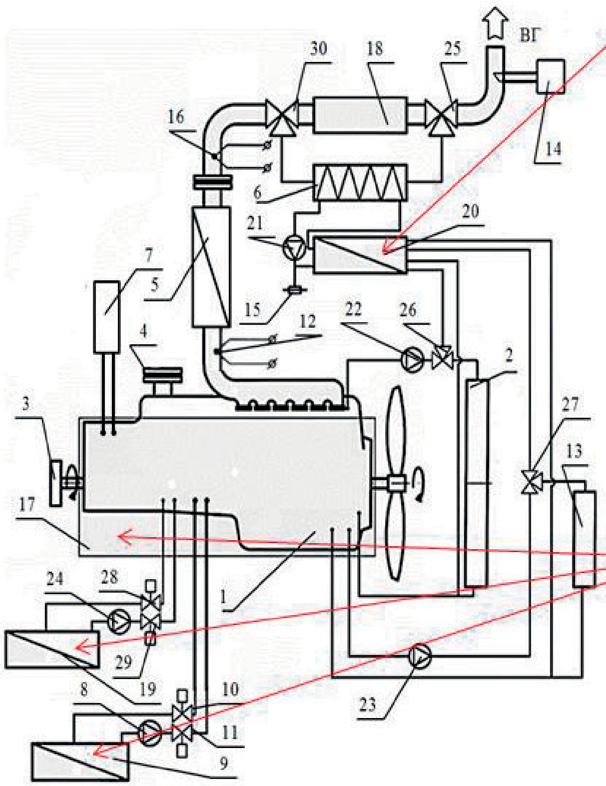

Title	Specification
Heat accumulating material properties:	high-density polyethylene
Density, kg/м³ ρ_s / ρ_l	925 / 800
Temperature of phase transition, K	408
Specific heat of phase transition, kJ/kg	230
Specific heat capacity, kJ/(kg·K), C_s / C_l	2.5 / 3.3
Thermal conductivity, WT/(м·K), λ_s / λ_l	0.25 / 0.04
Heat accumulating material weight, kg	18.5
Weight of thermal accumulator with HAM, kg	32.75
TA dimensions, mm	164x280x480
Thermal insulating material	double layer of polyethylene foam coated on both sides with layers of aluminum foil
TA frame material	stainless steel
TA heat exchanger material	brass
TA heat capacity, kJ/K	46.25

Title	Specification
Heat accumulating material properties (according to the relevant standards):	Paraffin - a mixture of high-molecular hydrocarbons C_{18}-C_{35}
State	Solid
Melting temperature, °C (K)	45-52 (318- 325)
Boiling temperature, °C (K)	350 (623)
Latent heat of melting, K	35
Specific heat of phase transition, kJ/kg	190
Thermal insulating material	double layer of polyethylene foam coated on both sides with layers of aluminum foil

Figure 1. The scheme of the combined heating system of the engine and the vehicle, and specifications of phase-transitional TA and its HAM.

insulated tank of TA with three heat exchangers (for TA charging and heating of the engine coolant and motor oil) the heat carrier cools down and gives off the accumulated thermal energy to a phase-transitional heat accumulating material (HAM).

In the process of HAM energy accumulation the most efficient is the process of a phase transition of the material (TA filler), i.e., the change of its physical state which requires a large amount of EG energy. The most energy-intensive process is the phase transition of HAM. All the other processes of HAM energy accumulation do not require such a large amount of energy. The peculiarities of phase-transitional TA 20 at different periods of thermal energy accumulation and release are detailed in [1, 5, 10, 11].

Contact thermal accumulator 17 of the vehicular engine (**Figure 1**) is a multi-layered case. To ensure close fitting it is mounted on the outside of the cylinder block and the engine oil pan [8]. The peculiarity of the contact thermal accumulator design 17 is the availability of individual sections of container-based phase-transitional HAM that are fitted to the outside of the cylinder block and the oil pan. They are covered by several layers of thermal insulation material [1, 5, 9].

Using contact thermal accumulator 17 does not require significant changes in the design of the vehicular engine and its systems. It is easily installed, is easy to maintain and does not require additional energy. The contact thermal accumulator operation is based on the change of the phase state of heat accumulating material when the energy is emitted and absorbed during convection and thermal radiation of the cylinder block and the engine oil pan. Due to contact thermal accumulator, an insulating function of the engine is performed and the minimum loss of thermal energy in the form of convection and thermal radiation is achieved during engine operation. In this way it is also possible to avoid thermal stresses in the engine during its heating at low temperatures. The contact thermal accumulator operation provides a long-term maintenance of the set coolant and motor oil temperatures when the engine is switched off, unlike the well-known TA by means of which the ICE is heated after stop [1, 5, 9].

The peculiarity of the thermal accumulator for storing motor oil design 19 (**Figure 1**) is an additional phase-transitional contact TA in an accumulation vessel membrane for motor oil. It is similar in design and operating principle to contact thermal accumulator 17, but is mounted on the accumulation vessel case for draining motor oil. Due to thermal accumulator for storing motor oil 19 the minimum loss of thermal energy is achieved. It is released by motor oil after its draining by electromagnetic hydraulic valves 28 and 29 in the insulated vessel with TA during long-term stop of the vehicular engine. When motor oil is pumped backwards into the engine oil pan by the modulating pump 24 it is possible to rapidly heat the engine components and lubrication system parts. They are as follows: a crankshaft area, an oil channel and an oil case of the vehicular engine. The motor oil temperature in thermal accumulator for storing motor oil 19 is controlled by the built-in motor oil temperature sensor.

The peculiarity of the thermal accumulator for storing a coolant design 9 (**Figure 1**) is an additional phase-transitional contact TA in the accumulation vessel membrane for the coolant. It is similar in design and operating principle to thermal accumulator for storing a coolant 19, but is mounted on the accumulation vessel case for draining the coolant. Due to thermal accumulator for storing a coolant 9 the minimum loss of thermal energy is achieved. It is released by the coolant after its draining by electromagnetic hydraulic valves 10 and 11 in the insulated vessel 9 with TA during long-term stop of the vehicular engine. When the coolant is pumped backwards into the engine cooling system by the modulating pump 8 it is possible to rapidly heat the engine components and cooling system parts. They are as follows: a coolant case and the ICE cylinder head. The coolant temperature in thermal accumulator for storing a coolant 9 is controlled by the built-in coolant temperature sensor.

EG thermal energy for rapid heating of a catalytic converter 5 in the exhaust system is accumulated in TA of exhaust gases cleaning system during engine operation. A rapid heating of catalytic converter composition 5 after starting the engine occurs when EG pass through TA of exhaust gases cleaning system.

The interior of the vehicle is heated by the heat exchanger 7 during engine operation when the coolant circulates in the engine cooling system through the heat exchanger.

In addition to the above-mentioned components, the combined heating system also includes standard components of the engine and its cooling and lubrication systems (**Figure 1**). They are as follows: a cooling system radiator 2, an engine output shaft 3 an intake manifold 4, EG temperature sensor 12; a lubrication system radiator 13; gas analysis equipment 14 (in the form of appropriate sensors); a tank for expanding the heat carrier 15; EG temperature sensor 16. The circulation of the coolant and motor oil in the combined heating system is provided by modulating pumps 22 and 23. The coolant and motor oil regulation is provided by electromagnetic hydraulic valves 26 and 27.

Pre-start and after-start heating of the coolant and motor oil is possible with standard heating of the engine and (or) in the following modes of the combined heating system operation. The examples are: when operating only the rapid heating of the engine subsystem in the process of after-start heating of the engine, when operating the rapid heating of the engine subsystem with the utilization of thermal energy of exhaust gases by phase-transitional TA, the combined functions of contact thermal accumulator (thermal accumulator for storing motor oil and (or) thermal accumulator for storing a coolant) or joint operation of contact thermal accumulator + thermal accumulator for storing motor oil + thermal accumulator for storing a coolant and the utilization of thermal energy of exhaust gases by phase-transitional TA. Storing thermal energy, accumulated by the coolant and motor oil, is possible with standard ICE assembly and (or) in the following modes of the combined heating system operation. The examples are: when operating the rapid heating of the engine subsystem with the utilization of thermal energy of exhaust gases by phase-transitional TA, when operating only contact thermal accumulator or thermal accumulator for storing motor oil (thermal accumulator for storing a coolant), the combined functions of contact thermal accumulator (thermal accumulator for storing motor oil and (or) thermal accumulator for storing a coolant) or joint operation of contact thermal accumulator + thermal accumulator for storing motor oil + thermal accumulator for storing a coolant and the utilization of thermal energy of exhaust gases by phase-transitional TA.

If it is necessary to start the engine after a long stop, the combined heating system is involved. It works according to its own algorithms and includes electric modulating pumps 21, 22, 23 of the rapid heating of the engine subsystem. They circulate the coolant and motor oil in the vehicular engine and phase-transitional TA for the utilization of thermal energy of exhaust gases. Passing through TA, the coolant gets thermal energy accumulated by HAM and transfers it by the coolant to the engine cooling system and by motor oil to the lubrication system and to the engine design elements. The right choice of TA 20 thermal capacity allows you to quickly heat the ICE from low ambient temperature (−20°C) to the coolant and motor oil temperatures at +40–60°C. The choice of TA thermal capacity by HAM weight is based on a calculation of the heat balance of the engine with the combined heating system and the vehicle. It helps determine the amount of thermal energy required for heating the coolant and motor oil, cylinder block, cylinder head, connecting branch pipes and manifolds considering heat loss [1, 5, 10, 11].

After receiving thermal energy from the coolant and motor oil, the engine elements transfer it to the combustion chamber. It positively affects the process of ICE start which occurs after the combined heating system sensors record the coolant and motor oil temperatures at +40–60°C. After that the ICE starts running and it is possible to load the engine. After starting the ICE, the combined heating system continues its work and facilitates more rapid and efficient heating of the working engine up to the coolant and motor oil temperatures at +85°C. This is achieved due to further use of the accumulated heat in TA and thermal energy from the working engine. After reaching the coolant and motor oil temperatures of +85°C, the combined heating system maintains it within the limits set, i.e., 85 ± 5°C and then the engine standard system (SS) starts working (in the meanwhile, the combined heating system stops working).

Taking into consideration the data from temperature sensors, the control system of the combined heating system calculates the optimal rotational speed of circulation pumps 21, 22, 23. It gives commands to the system valves directing the flow of working fluids through certain CSPSH elements. The combined heating system functioning is based on the analysis of temperature values of the coolant and motor oil heat carriers [1, 5, 10, 11].

During a stop and storage of the heat accumulated by contact thermal accumulator 17 of the engine being shut off, the contact thermal accumulator operation implies giving off HAM phase-transitional heat of contact thermal accumulator backwards to provide long-term maintenance of the coolant and motor oil temperatures. In low ambient temperature and when phase-transitional TA 20 for the utilization of thermal energy of exhaust gases subsystem is charged, when the heat accumulated by contact thermal accumulator 17 is insufficient, the engine 1 heating is carried out similarly as described above.

During a long stop of the engine, when it is necessary to maintain the coolant and motor oil within the "hot heating" for a long time, thermal accumulator for storing motor oil 19 and (or) thermal accumulator for storing a coolant 9 are used (**Figure 1**), in which the coolant and motor oil are drained from lubrication system and cooling system of the engine. If it is necessary to start the engine when phase-transitional TA 20 for the utilization of thermal energy of exhaust gases subsystem is charged, thermal accumulator for storing motor oil (thermal accumulator for storing a coolant) is combined with lubrication system (cooling system) of the engine by using valves 28 and 29 (9 and 11). By using the circulation pump 24 (8), motor oil (the coolant) goes to the engine cylinder block. Further heating of the engine 1 is carried out similarly as described above. By using motor oil and coolant temperature sensors, working capacity of the combined heating system is controlled in relation to heat capacity of its components and subsystems and its further use.

3. Objects of experimental studies

The research on using the CHS in vehicles was based both on experiments and numerical modeling.

The results of experimental studies conducted by the authors under the ITS information conditions are detailed in [1, 5, 10, 11–13] (**Figure 2**). The authors developed a mathematical model [1, 5, 10, 11–13] for the estimation studies (**Figure 3**). It is based on a systems approach used in the processes of the vehicular thermal development when using phase-transitional thermal accumulators [1, 4–19].

Figure 2. The truck during pre-start and after-start heating of the ICE and the vehicle interior.

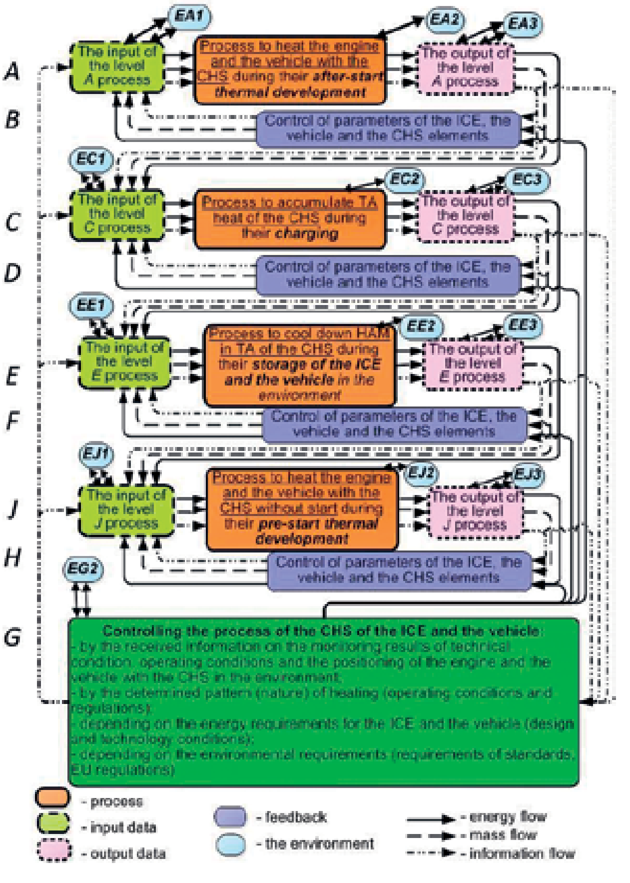

Figure 3. The flowchart of "combined heating system of the engine and the vehicle."

4. The study results of the influence of the combined heating system different options on engine thermal development indicators

The general process of pre-start and after-start heating (PSASH) during engine and vehicle operation can be split into the following components: pre-start and after-start processes of thermal development and industrial (commercial) process of the ICE and vehicle operation. The engine pre-start heating without actual start and the operation of the engine in an idling mode can be only realized using the developed heating system. It is a set of subsystems, elements and means of thermal development and maintenance of the thermal state of the engine and the vehicle using the combined heating system based on phase-transitional thermal accumulators. During after-start thermal development of the engine and the vehicle, it is possible to heat them either without using the combined heating system (engine and vehicle standard systems) or using the CHS. During industrial (commercial) process of engine and vehicle operation, the heating system is used only when it is not possible to maintain the thermal state of the engine and the vehicle in a corresponding range under operating conditions. After-start heating of the engine and the vehicle can be carried out in various modes of vehicle operation (both steady and transitional modes of the engine operation when the vehicle is stopped and when in motion). These modes are: (1) heating in an idling mode; (2) heating in an idling mode with electrical consumers switched on; (3) heating in an idling mode with gradual heating in motion; (4) heating in motion. The study of the vehicle heating according to the above-mentioned modes is detailed in [1, 16–19].

The article presents the study results of thermal development of the truck engine 8FS 9.2/8 in operation. The investigation was conducted in the mathematical model of the “combined heating system of the engine and the vehicle” for option 1 - Heating in an idling mode. In evaluating different options of the CSPSH operation the following considerations were taken into account. The combined heating system is a combination of five independent subsystems: the utilization of thermal energy of EG (with TA), rapid heating of the engine, contact thermal accumulator, thermal accumulator for storing motor oil and thermal accumulator for storing a coolant [1, 16–19]. The first two subsystems, working together, provide the work of TA with accelerated circulation of the coolant, motor oil and standard systems of the truck engine 8FS 9.2/8 during pre-start and after-start heating of the truck. Contact thermal accumulator provides long-term storage of accumulated heat in the coolant and motor oil in the cylinder block using an insulated membrane. Thermal accumulator for storing motor oil and thermal accumulator for storing a coolant provide long-term storage of accumulated heat by motor oil and the coolant in separate insulated tanks with TA. The results of pre-start and after-start heating of the engine were assessed and compared in the study depending on the combined heating system different options or their combination.

Based on the developed algorithms for pre-start and after-start heating of the engine coolant and motor oil, 19 combinations of options were suggested to analyze the sets of components of the developed combined heating system (**Table 1**) [1, 2, 5, 12, 15–19]. Thus, for all options during pre-start and after-start heating of the engine with CSPSH mode parameters of its work were estimated. They are as follows: heating the coolant and motor oil from T_{amb} to

# of option	The combined heating system components (the definition of the option)	Structural and technology features and the use of the combined heating system option according to its purpose
1	2	3
1	Engine standard systems without the combined heating system—SS without the CHS	Engine pre-start heating is impossible to do. After-start heating is carried out by the elements of cooling and lubrication systems of the standard engine. To ensure the maintenance of $T_c \approx 50°C$ and $T_{MO} \approx 50°C$ when the engine is not running, the elements of cooling and lubrication systems of the standard engine can only be used.
2	Engine standard systems with the combined heating system—SS with the CHS	Engine pre-start heating is impossible to do. For rapid after-start heating, only additional electric modulating pumps for the coolant and motor oil of the rapid heating of the engine subsystem are used. To ensure the maintenance of $T_c \approx 50°C$ and $T_{MO} \approx 50°C$ when the engine is not running, the elements of cooling and lubrication systems of the standard engine can only be used.
3	Phase-transitional thermal accumulator—TA	Engine pre-start and rapid after-start heating is carried out by phase-transitional TA. Besides, additional electric modulating pumps for the coolant and motor oil of the rapid heating of the engine subsystem (#2), the subsystem of the utilization of thermal energy of EG by phase-transitional thermal accumulator are also used. To ensure the maintenance of $T_c \approx 50°C$ and $T_{MO} \approx 50°C$ of the engine with phase-transitional TA when the engine is not running, additional electric modulating pumps for the coolant and motor oil of the rapid heating of the engine subsystem can be used.
4	Phase-transitional contact thermal accumulator—CTA	Engine pre-start and after-start heating is impossible to do. To ensure the maintenance of T_c > or ≈ 50°C and T_{MO} > or ≈ 50°C of the engine with phase-transitional CTA when the engine is not running, the elements of cooling and lubrication systems of the standard engine can be used.
5	Thermal accumulator for storing motor oil ($T_{HAM} = Tamb$) – TASMO ($T_{HAM} = Tamb$)	Engine pre-start and after-start heating is impossible to do. The maintenance of T_{MO} > or ≈ 50°C of the engine with TASMO when the engine is not running is possible with the elements of lubrication system of the engine with thermal accumulator for storing motor oil without HAM thermal development ($T_{HAM} = Tamb$). To ensure the maintenance of $T_c \approx 50°C$ when the engine is not running, the elements of cooling system of the standard engine can only be used.

# of option	The combined heating system components (the definition of the option)	Structural and technology features and the use of the combined heating system option according to its purpose
6	Thermal accumulator for storing motor oil (T_{HAM} = 85°C) – TASMO (T_{HAM} = 85°C)	Engine pre-start and after-start heating is impossible to do. The maintenance of T_{MO} > or ≈ 50°C of the engine with TASMO when the engine is not running is possible with the elements of lubrication system of the engine with thermal accumulator for storing motor oil with HAM thermal development (T_{HAM} = 85°C). To ensure the maintenance of T_c ≈ 50°C when the engine is not running, the elements of cooling system of the standard engine can only be used.
7	The combination of separate CHS components, namely: thermal accumulator + contact thermal accumulator (# 3 and # 4): TA + CTA	The combination of separate components of the combined heating system, namely: phase-transitional thermal accumulator and phase-transitional contact thermal accumulator. # 3 and # 4 describe structural and technology features and the use of the combined heating system option according to its purpose during engine pre-start and after-start heating and long-term keeping in an idling mode without the operation.
8	The combination of separate CHS components, namely: thermal accumulator + thermal accumulator for storing motor oil (T_{HAM} = *Tamb*): # 3 and # 5 – TA + TASMO (T_{HAM} = *Tamb*)	The combination of separate components of the combined heating system, namely: phase-transitional thermal accumulator and thermal accumulator for storing motor oil without HAM thermal development (T_{HAM} = *Tamb*). # 3 and # 5 describe structural and technology features and the use of the combined heating system option according to its purpose during engine pre-start and after-start heating and long-term keeping in an idling mode without the operation.
9	The combination of separate CHS components, namely: thermal accumulator + thermal accumulator for storing motor oil (T_{HAM} = 85°C): # 3 and # 6 – TA + TASMO (T_{HAM} = 85°C)	The combination of separate components of the combined heating system, namely: phase-transitional thermal accumulator and thermal accumulator for storing motor oil with HAM thermal development (T_{HAM} = 85°C). # 3 and # 6 describe structural and technology features and the use of the combined heating system option according to its purpose during engine pre-start and after-start heating and long-term keeping in an idling mode without the operation.
10	The combination of separate CHS components, namely: thermal accumulator + contact thermal accumulator + thermal accumulator for storing motor oil (T_{HAM} = *Tamb*): # 3, #4 and # 5 – TA + CTA + TASMO (T_{HAM} = *Tamb*)	The combination of separate components of the combined heating system, namely: phase-transitional thermal accumulator, phase-transitional contact thermal accumulator and thermal accumulator for storing motor oil without HAM thermal development (T_{HAM} = *Tamb*). # 3, # 4 and # 5 describe structural and technology features and the use of the combined heating system option according to its purpose during engine pre-start and after-start heating and long-term keeping in an idling mode without the operation.

# of option	The combined heating system components (the definition of the option)	Structural and technology features and the use of the combined heating system option according to its purpose
11	The combination of separate CHS components, namely: thermal accumulator + contact thermal accumulator + thermal accumulator for storing motor oil (T_{HAM} = 85°C): # 3, #4 and # 6 – TA + CTA + TASMO (T_{HAM} = 85°C)	The combination of separate components of the combined heating system, namely: phase-transitional thermal accumulator, phase-transitional contact thermal accumulator and thermal accumulator for storing motor oil with HAM thermal development (T_{HAM} = 85°C). # 3, # 4 and # 6 describe structural and technology features and the use of the combined heating system option according to its purpose during engine pre-start and after-start heating and long-term keeping in an idling mode without the operation.
12	Thermal accumulator for storing a coolant (T_{HAM} = $Tamb$) – TASC (T_{HAM} = $Tamb$)	Engine pre-start and after-start heating is impossible to do. The maintenance of T_c > or ≈ 50°C of the engine with TASC when the engine is not running is possible with the elements of cooling system of the engine with thermal accumulator for storing a coolant without HAM thermal development (T_{HAM} = $Tamb$). To ensure the maintenance of T_{MO} ≈ 50°C when the engine is not running, the elements of lubrication system of the standard engine can only be used.
13	Thermal accumulator for storing a coolant (T_{HAM} = 85°C) – TASC (T_{HAM} = 85°C)	Engine pre-start and after-start heating is impossible to do. The maintenance of T_c > or ≈ 50°C of the engine with TASC when the engine is not running is possible with the elements of cooling system of the engine with thermal accumulator for storing a coolant with HAM thermal development (T_{HAM} = 85°C). To ensure the maintenance of T_{MO} ≈ 50°C when the engine is not running, the elements of lubrication system of the standard engine can only be used.
14	The combination of separate CHS components, namely: thermal accumulator + thermal accumulator for storing a coolant (T_{HAM} = $Tamb$): # 3 and # 12 – TA + TASC (T_{HAM} = $Tamb$)	The combination of separate components of the combined heating system, namely: phase-transitional thermal accumulator and thermal accumulator for storing a coolant without HAM thermal development (T_{HAM} = $Tamb$). # 3 and # 12 describe structural and technology features and the use of the combined heating system option according to its purpose during engine pre-start and after-start heating and long-term keeping in an idling mode without the operation.
15	The combination of separate CHS components, namely: thermal accumulator + thermal accumulator for storing a coolant (T_{HAM} = 85°C): # 3 and # 13 – TA + TASC (T_{HAM} = 85°C)	The combination of separate components of the combined heating system, namely: phase-transitional thermal accumulator and thermal accumulator for storing a coolant with HAM thermal development (T_{HAM} = 85°C). # 3 and # 13 describe structural and technology features and the use of the combined heating system option according to its purpose during engine pre-start and after-start heating and long-term keeping in an idling mode without the operation.

http://dx.doi.org/10.5772/intechopen.79467

# of option	The combined heating system components (the definition of the option)	Structural and technology features and the use of the combined heating system option according to its purpose
16	The combination of separate CHS components, namely: thermal accumulator + contact thermal accumulator + thermal accumulator for storing a coolant (T_{HAM} = *Tamb*): # 3, # 4 and # 12 – TA + CTA + TASC (T_{HAM} = *Tamb*)	The combination of separate components of the combined heating system, namely: phase-transitional thermal accumulator, phase-transitional contact thermal accumulator and thermal accumulator for storing a coolant without HAM thermal development (T_{HAM} = *Tamb*). # 3, # 4 and # 12 describe structural and technology features and the use of the combined heating system option according to its purpose during engine pre-start and after-start heating and long-term keeping in an idling mode without the operation.
17	The combination of separate CHS components, namely: thermal accumulator + contact thermal accumulator + thermal accumulator for storing a coolant (T_{HAM} = 85°C): # 3, # 4 and # 13 – TA + CTA + TASC (T_{HAM} = 85°C)	The combination of separate components of the combined heating system, namely: phase-transitional thermal accumulator, phase-transitional contact thermal accumulator and thermal accumulator for storing a coolant with HAM thermal development (T_{HAM} = 85°C). # 3, # 4 and # 13 describe structural and technology features and the use of the combined heating system option according to its purpose during engine pre-start and after-start heating and long-term keeping in an idling mode without the operation.
18	The combination of separate CHS components, namely: thermal accumulator + contact thermal accumulator + thermal accumulator for storing motor oil (T_{HAM} = *Tamb*) + thermal accumulator for storing a coolant (T_{HAM} = *Tamb*): # 3, # 4, # 5 and # 12 – TA + CTA + TASMO+TASC	The combination of separate components of the combined heating system, namely: phase-transitional thermal accumulator, phase-transitional contact thermal accumulator, thermal accumulator for storing motor oil without HAM thermal development (T_{HAM} = *Tamb*) and thermal accumulator for storing a coolant without HAM thermal development (T_{HAM} = *Tamb*). # 3, # 4, # 5 and # 12 describe structural and technology features and the use of the combined heating system option according to its purpose during engine pre-start and after-start heating and long-term keeping in an idling mode without the operation.
19	The combination of separate CHS components, namely: thermal accumulator + contact thermal accumulator + thermal accumulator for storing motor oil (T_{HAM} = 85°C) + thermal accumulator for storing a coolant (T_{HAM} = 85°C): # 3, # 4, # 6 and # 13 – TA + CTA + TASMO (T_{HAM} = 85°C) + TASC (T_{HAM} = 85°C)	The combination of separate components of the combined heating system, namely: phase-transitional thermal accumulator, phase-transitional contact thermal accumulator, thermal accumulator for storing motor oil with HAM thermal development (T_{HAM} = 85°C) and thermal accumulator for storing a coolant with HAM thermal development (T_{HAM} = 85°C). # 3, # 4, # 6 and # 13 describe structural and technology features and the use of the combined heating system option according to its purpose during engine pre-start and after-start heating and long-term keeping in an idling mode without the operation.

Table 1. The options of the combined heating system components to analyze the efficiency of pre-start and after-start heating of the truck engine 8FS 9.2/8.

50°C, min., heating the coolant and motor oil from 50 to 85°C, min., maintaining $T_c \approx 50$°C and $T_{MO} \approx 50$°C min. The operating parameters were analyzed separately for the coolant and motor oil at different ambient temperatures, namely 20, 0 and −20°C.

Figures 4–6 show the results of pre-start and after-start heating according to the duration of thermal development of the truck engine coolant and motor oil using the combined heating system. **Figure 4** shows the duration of the coolant and motor oil heating from *Tamb* to 50°C, min. **Figure 5** shows the duration of the coolant and motor oil heating from 50 to 85°C, min. **Figure 6** shows the duration of maintaining $T_c \approx 50$°C and $T_{MO} \approx 50$°C, min. The comparison of indicators for every option of the combined heating system components and the technology for use was provided in absolute values (and in %). Every indicator for a corresponding option was compared with the similar one for a standard system of the engine ZMZ-66-06 (8FS 9.2/8) of the truck GAZ-66-11 (**Figures 4–6**). Based on the calculation results of pre-start and after-start heating of the coolant and motor oil according to the appropriate options of the combined heating system components (**Figures 4–6**), it is obvious that the use of the above-mentioned ways of heating according to the operating algorithms ensures both pre-start and rapid after-start heating of the engine ZMZ-66-06 (8FS 9.2/8) of the truck GAZ-66-11. It also increases the length of the long stop of the engine without idling. Meanwhile, according to the temperature values of the coolant and motor oil, the engine is in pre-start availability that corresponds to the thermal state to enable the engine load.

The indicators of the engine thermal state during pre-start heating of the coolant and motor oil of the ICE with the combined heating system were compared with the standard systems of the engine (option 1, **Table 1**) from *Tamb* to 50°C, min (**Figure 4**). The greatest reduction in the heating time was obtained in options 3, 7–11, 14–19 for all ambient temperatures, i.e., at *Tamb*

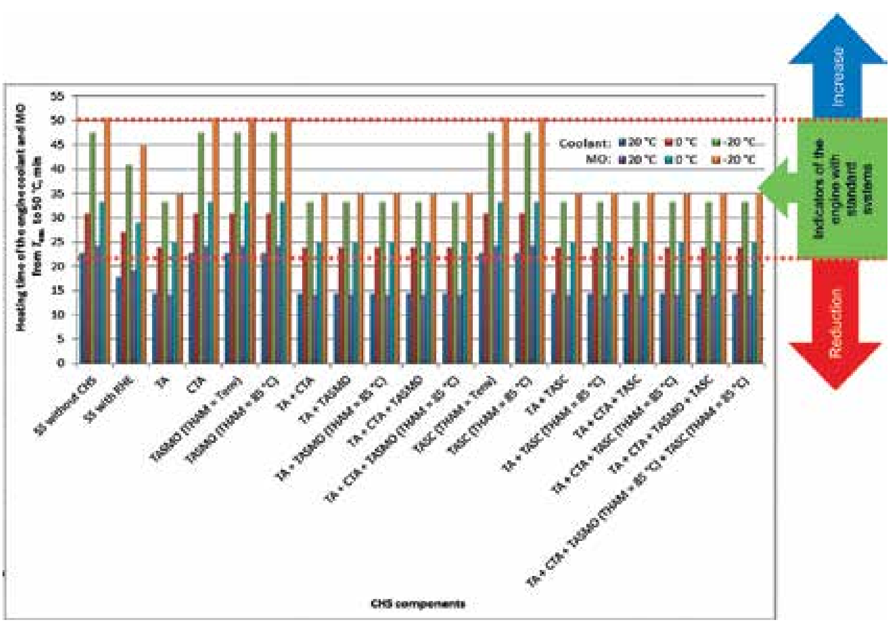

Figure 4. The influence of options of the combined heating system components on the heating time of the engine coolant and motor oil from *Tamb* to 50°C.

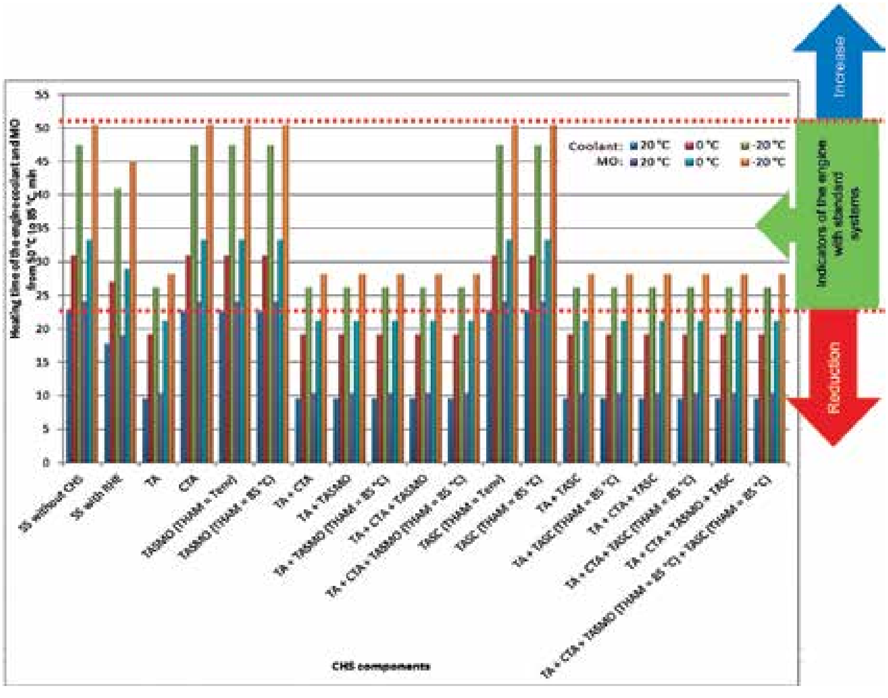

Figure 5. The influence of options of the combined heating system components on the heating time of the engine coolant and motor oil from 50 to 85°C.

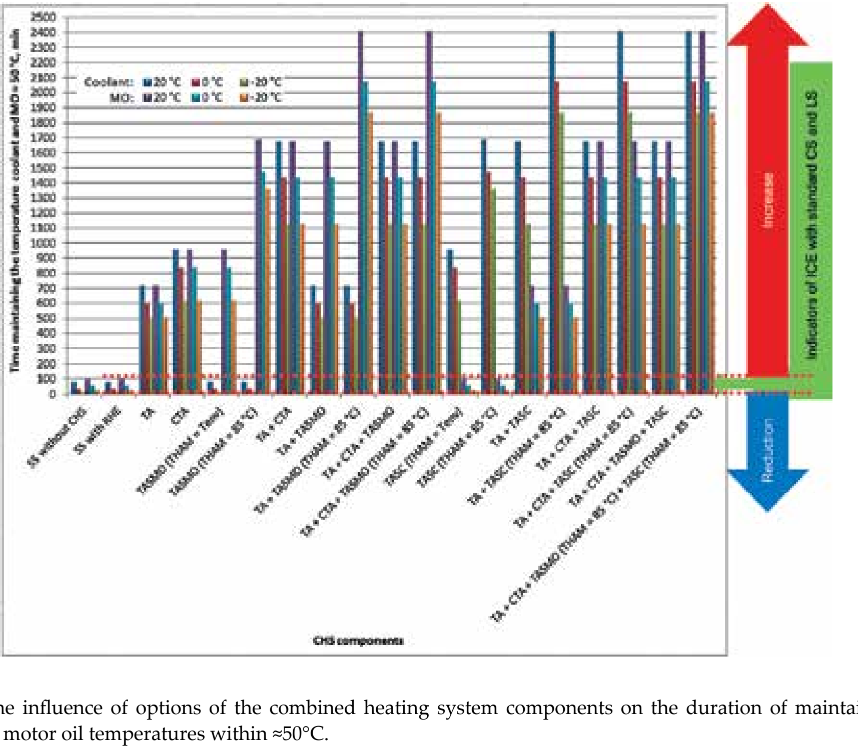

Figure 6. The influence of options of the combined heating system components on the duration of maintaining the coolant and motor oil temperatures within ≈50°C.

= 20 (0/−20)°C. These options are characterized by the operation of phase-transitional TA and the rapid heating of the engine subsystem at the same time. For relevant temperatures of *Tamb* = 20 (0/−20)°C, the duration of heating is reduced according to the values 14.4 (24/33.3) min for the coolant and 14.2 (25/35) min for motor oil. This option is compared with the standard systems of the engine (option 1), i.e., 22.8 (31/47.5) min for the coolant and 24.2 (33.3/50.5) min for motor oil. Thus, the duration of heating is reduced by 8.4 (7.1/14.2) min or by 36.9 (22.9/29.9)% for the coolant and by 10 (8.3/15.5) min or by 41.3 (25/30.8) % for motor oil.

The indicators of the ICE thermal state during rapid after-start heating of the coolant and motor oil of the engine with the combined heating system were compared with the standard systems of the engine (option 1, **Table 1**) from 50 to 85°C, min (**Figure 5**). The greatest reduction in the heating time was obtained in options 3, 7–11, 14–19 for ambient temperatures at *Tamb* = 20(0/−20)°C. These options are characterized by the operation of phase-transitional TA and the rapid heating of the engine subsystem at the same time. The duration of heating is reduced according to the values 9.7 (19.2/26.2) min for the coolant and 10.5 (21.2/28.2) min for motor oil. This option is compared with the standard systems of the engine (option 1), i.e., 22.8 (31/47.5) min for the coolant and 24.2 (33.3/50.5) min for motor oil. Thus, the duration of heating is reduced by 13.1 (11.8/21.3) min or by 57.5 (38/44.8)% for the coolant and by 13.7 (12.1/22.3) min or by 57 (36/44.2)% for motor oil.

The duration of maintaining the engine $T_c \approx 50$°C and $T_{MO} \approx 50$°C, min (**Figure 6**) within the combined heating system (option 1, **Table 1**) was compared with the standard systems. A substantial increase in long-duration stop of the engine with the combined heating system when the engine was not running in an idling mode was obtained. The duration of maintenance did not change in option 2 for the coolant and motor oil, in options 5 and 6 for the coolant, in options 12 and 13 for motor oil. According to **Figure 6**, the increase in the maintenance duration occurred in options 3–18 for both the coolant and for motor oil for ambient temperatures *Tamb* = 20 (0/−20)°C. The most significant increase in duration occurred in option 19 for the coolant and motor oil, in options 15 and 17 for the coolant, in options 9 and 11 for motor oil respectively. These options are characterized by simultaneous operation of phase-transitional TA and the rapid heating of the engine subsystem, contact thermal accumulator subsystem as well as thermal accumulator for storing motor oil and thermal accumulator for storing a coolant previously heated to $T_{HAM} = 85$°C. The duration of maintaining $T_c \approx 50$°C and $T_{MO} \approx 50$°C is increased according to the values from 720 (600/510) min to 2410 (2078/1870) min for the coolant and from 720 (600/510) min to 2410 (2078/1870) min for motor oil. This option was compared with the standard systems of the engine (option 1), i.e., 80 (40/20) min for the coolant and 100 (60/30) min for motor oil. Thus, the duration of maintaining the temperatures is increased from 640 (560/490) min. to 2330 (2038/1850) min or ranging from 9 (14/24) to 29.13 (50.95/92.50) times for the coolant and from 620 (540/480) min to 2310 (2018/1840) min or ranging from 6.2 (9/16) to 15.9 (33.63/61.33) times for motor oil for appropriate operating conditions.

The use of the combined heating system is generally effective (**Figures 4–6**) for pre-start and after-start thermal development of the vehicular engine and for maintaining it for a long time when it is not running under different climatic conditions. The peculiarities of the combined heating system components and the technology for use are chosen depending on operational needs, climatic conditions and the category of the vehicle.

http://dx.doi.org/10.5772/intechopen.79467

5. Estimating the indicators of optimum temperature (OT) of the engine and the vehicle under operating conditions

The estimation was based on the mathematical modeling of the "combined heating of the engine and the vehicle" system. The mathematical modeling was carried out for various components of the CHS used for the truck and a car. The options of operating conditions and methods of the engine and the vehicle heating were chosen in accordance with the provisions of [1, 5, 10, 11, 16–19].

The influence of various components of the CHS on pre-start heating of the engine was analyzed in terms of fuel consumption (kg/h). The results revealed the most significant components of the CHS, namely in options 2 and 3. For them, additional estimation studies were carried out to determine the specific indicators of the total influence of the CHS components on the coolant and MO heating time from $T_{amb.}$ to 50°C and from 50 to 85°C. All indicators were compared with thermal development indicators of the engine standard systems. **Figure 7(a)** shows the main indicators of the truck engine thermal development when heating the coolant and MO from $T_{amb.}$ to 50°C. The most significant components of the CHS were studied. They have the greatest influence on thermal processes in the engine coolant and MO. Thus, a phase-transitional TA has the greatest influence on the parameters of the engine coolant heating for all ambient temperatures +20 (0/−20°C) − 0.085 (0.134/0.168) kg/h; and for MO heating, respectively 0.085 (0.133/0.167) kg/h.

To estimate the total influence of the CHS components on the coolant and MO heating time, the most significant components were chosen, namely in options 3–6, 12, 13 and 19 (**Figure 7(b)**. All indicators were compared with the indicators of the engine standard systems. The total influence on thermal development processes implies the total time of pre-start (from $T_{amb.}$ to 50°C) and after-start heating (from 50 to 85°C) and the time of maintaining the coolant and MO temperature within ≈50°C in relation to the fuel consumed for thermal development. **Figure 7b** shows the main study results of the influence of the CHS components on the total time of the coolant and MO thermal development. It is determined in the specific indicators of fuel consumption, kg/h. The lowest fuel consumption indicators were obtained for the CHS with such components: TA + CTA + TASMO (T_{HAM} = 85°C) + TASC (T_{HAM} = 85°C). Phase-transitional TA indicators are worth mentioning as well. They are optimal for all options of the heating, both according to the options of the heating and the ambient temperatures.

In general, to provide the OT of the engine with the CHS, it is advisable to use all options of simultaneous influence on the coolant and MO.

To provide the temperature influence on the CC of the EGCS indicators, it is advisable to use TA installed in the exhaust system of the engine. When using TAEGCS, depending on the option of the engine heating, the time of reaching the temperature at the Light-off point (250°C/523 K) of the CC heating curve is 3–5 min of the CC operation for all options. This indicator is almost twice as good as the experimentally obtained indicators of the CC heating.

To ensure the compliance with the requirements for the heating periods of different areas of the vehicle interior and the driver, the use of the CHS is completely stipulated. In this case,

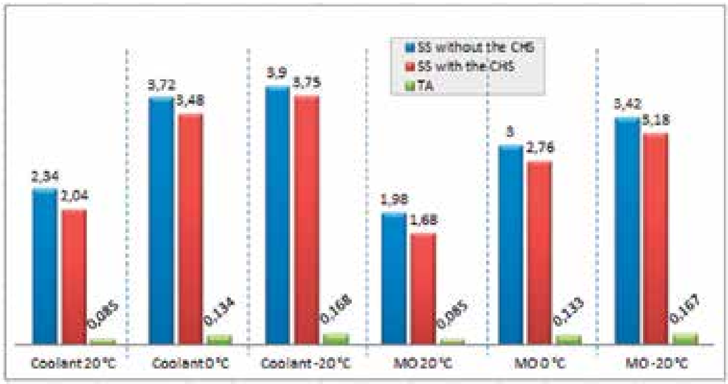

a

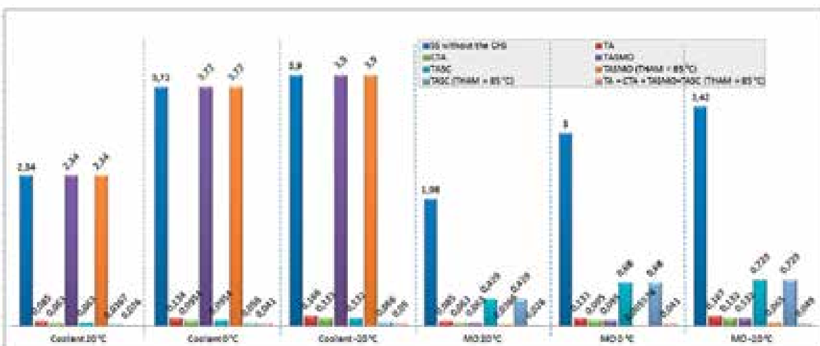

b

Figure 7. The results of investigating the influence of the CHS components on the coolant and MO heating time (a) and on the total time of the coolant and MO thermal development (b) in terms of fuel consumption (kg/h).

the interior and the driver are heated by the engine CS, that is, without changing the design of the vehicle. The results of the mathematical modeling of the interior heat transfer processes confirmed the feasibility of using the CHS. When using the CHS, the requirements are fully met in terms of the efficiency and safety of the heating system. It means that 15 min after the vehicle starts its motion at the ambient temperature to −25°C the requirements of the standard for heating the driver's head, legs, and body are fully met.

6. Summary

The development and the study of the engine combined heating system with phase-transitional thermal accumulators for pre-start and after-start heating under cold operating conditions were considered. To ensure optimal temperature condition of the ICE and the vehicle, general and individual tasks were determined. The combined heating system scheme of the ICE and the vehicle in operation was developed. The objects of experimental studies in operation were described. Using a systems approach to ensure optimal temperature condition of the vehicle in operation, the "combined heating system of the engine and the vehicle" and its application methods were developed. The results of significant impact of the

http://dx.doi.org/10.5772/intechopen.79467

combined heating system on thermal development indicators of the engine and the vehicle were obtained. The use of the combined heating system in the vehicular engine for different ambient temperatures enables to improve the indicators of the duration of coolant and motor oil thermal development. It is possible at: pre-start and after-start heating by 22.9–57.5% and 25–57%, and for a long storage ranging from 9 to 92 times and from 6.2 to 61 times, without the engine operation in an idling mode. The use of the combined heating system is generally effective for pre-start and after-start thermal development of the vehicular engine and for maintaining it for a long time when it is not running under different climatic conditions. The peculiarities of the combined heating system components and the technology for use are chosen depending on operational needs, climatic conditions and the category of the vehicle.

Thus, in order to ensure safety in terms of maintaining the OT of the engine and the vehicle, it is advisable to use the following options:

- heating from $T_{amb.}$ to 50°C - SS + RHE and phase-transitional TA;
- heating from 50 to 85°C - SS + RHE and phase-transitional TA;
- maintaining the coolant and MO temperature within ≈50°C when the vehicle is stopped – TA + CTA + TASMO (T_{HAM} = 85°C) + TASC (T_{HAM} = 85°C) and phase-transitional TA;
- by total specific indicators - TA + CTA + TASMO (T_{HAM} = 85°C) + TASC (T_{HAM} = 85°C) and phase-transitional TA.

To ensure the harmless environmental impact, it is expedient to use TAEGCS, TA + CTA + TASMO (T_{HAM} = 85°C) + TASC (T_{HAM} = 85°C) and phase-transitional TA.

To ensure the transportation comfort, it is expedient to use any means of thermal development in the engine CS. The best of them are – the vehicle - TA + CTA + TASMO (T_{HAM} = 85°C), the vehicle - TA + CTA + TASMO (T_{HAM} = 85°C) + TASC (T_{HAM} = 85°C) and phase-transitional TA.

In order to ensure the engine capacity at its start, that is the ability to have the load on the engine immediately after its start, it is expedient to use TAEGCS, the vehicle - TA + CTA + TASMO (T_{HAM} = 85°C) + TASC (T_{HAM} = 85°C) and phase-transitional TA.

In order to ensure specific efficient fuel consumption when maintaining the OT of engines and vehicles, it is expedient to use TA + CTA + TASMO (T_{HAM} = 85°C) + TASC (T_{HAM} = 85°C).

Definitions/acronyms

CC	catalytic converter
CHS	combined heating system
CS	cooling system
CTA	contact thermal accumulator
EG	exhaust gases
EGCS	exhaust gases cleaning system

HAM	heat accumulating material
HE	heat exchanger
ICE	internal combustion engine
LS	lubrication system
PSASH	pre-start and after-start heating
RHE	rapid heating of the engine
SS	standard system
TA	thermal accumulator
TAEGCS	TA of EG cleaning system
TASC	thermal accumulator for storing a coolant
TASMO	thermal accumulator for storing motor oil
UTETA	utilization of thermal energy of exhaust gases by phase-transitional TA

Author details

Igor Gritsuk[1]*, Vasyl Mateichyk[2], Miroslaw Smieszek[3], Vladimir Volkov[4], Yurii Gutarevych[5], Valery Aleksandrov[6], Roman Symonenko[7] and Valeriy Verbovskiy[8]

*Address all correspondence to: gritsuk_iv@ukr.net

1 Department of Operation of Ship Power Plants, Kherson State Maritime Academy, Kherson, Ukraine

2 Department of Ecology and Safety of Vital Functions, National Transport University, Kyiv, Ukraine

3 Department of Quantitative Methods, Rzeszow University of Technology, Rzeszow, Poland

4 Department of Technical Operation and Service Vehicles, Kharkiv National Automobile and Highway University, Kharkiv, Ukraine

5 Department of Engines and Thermal Engineering, National Transport University, Kyiv, Ukraine

6 Department of Physics, Mathematics and Materials Science, Donbas National Academy of Civil Engineering and Architecture, Ukraine

7 Research Laboratory for Fuel Use and the Environment, State Road Transport Research Institute, Kyiv, Ukraine

8 Gas Processing and Transportation Department, Institute of Gas of the National Academy of Sciences of Ukraine, Kyiv, Ukraine

References

[1] Gritsuk I, Volkov V, Gutarevych Y, Mateichyk V, Verbovskiy V. Improving engine pre-start and after-start heating by using the combined heating system. SAE Technical Paper 2016-01-8071; 2016. DOI: 10.4271/2016-01-8071

[2] Gritsuk IV. The Development and the Study of the Combined Heating System of Engines and Vehicles. Vol. 70. Kharkiv: The Herald of Kharkiv National Automobile and Highway University; 2015. pp. 23-32

[3] Vashurkin IO. Thermal Development and Start of ICE of Mobile Vehicles and Construction Machinery in Winter. Sant Peterburg: Nauka Publisher; 2002. 145p

[4] Klets D, Gritsuk I, Makovetskyi A, Bulgakov N. et al., Information Security Risk Management of Vehicles. SAE Technical Paper 2018-01-0015. 2018. https://doi.org/10.4271/2018-01-0015

[5] Volkov VP, Gritsuk IV, Gutarevych YF, Aleksandrov VD, Poddubnyak VY, Prilepskiy YV, Komov PB, Adrov DS, Verbovskiy VS, Krasnokutska ZI, Volkova TV. ICE Heating Systems: The Basics of Functioning. Donetsk: Landon-XXI; 2015. p. 314

[6] Morosuk T, Morosuk C, Bishliaga S. Thermodynamic analysis of traditional and alternative heating systems for Ukraine. In: Ulgiati S, Brown TM, Giampietro V, Herendeed RA, Mayumi K, editors. Advances in Energy Studies. Reconsidering the Importance of Energy. Padova: SG Editoriali; 2003. pp. 381-388

[7] Valero A et al. Structural theory and thermoeconomic diagnosis. In: Proceedings of Conference ECOS'99; Tokyo, Japan; 1999. pp. 368-379

[8] Balasanyan GA. The effectiveness of advanced integrated systems for energy supply based on cogeneration units of low capacity (theoretical basics, analysis, optimization) [Doctoral thesis of Technical Sciences]. Odesa: Technical Thermal Physics and Industrial Combined Heat and Power; 2007. 356p

[9] Karnauhov NN, Pustovalov IA, Yarkin AV. Thermal accumulator for maintaining ICE start temperature of construction machinery in winter. In: Motor Transport Enterprise. Moscow: 2010;**11**: pp. 45-48

[10] Patent for invention № 103729 Ukraine, (2013.01) F01P 3/22, B60H 1/04, B60K 11/00. The system of coolant optimal temperatures in ICE/Gutarevych YF, Mateichyk VP, Gritsuk IV, Volkov VP, Kagramanyan AO, Komov PB, Komov OB, Poddubnyak VY, Sergiyenko MI, Krasnokutska ZI/(Ukraine); Patent applicant and patent holder: National Transport University, State № ua 103729; app. 30.10.2012; publ. 10.04.2013, Bul. №7.- 17p.:il

[11] Patent for invention № 106525 Ukraine, F01P 3/22 (2013.01), B60H 1/04 (2013.01), "The system of coolant optimal temperatures in ICE"/Gutarevych YF, Mateichyk VP, Gritsuk IV, Volkov VP, Kagramanyan AO, Komov PB, Komov OB, Poddubnyak VY, Sergiyenko MI, Krasnokutska ZI, Yeroschenkov SA, Verbovskiy VS, Adrov DS, Makedonska LO, Komov AP,

Komov YO/(Ukraine); Patent applicant and patent holder: National Transport University, Kharkiv National Transport University, Ukrainian State Academy of Railway Transport, Donetsk Railway Transport Institute, State № ua 106525; app. 16.10.2012 application: a2012 11919, publ. 10.09.2014, Bul. №17.-17p.:il

[12] Gritsuk I, Volkov V, Mateichyk V, Grytsuk Y, et al. Information model of V2I system of the vehicle technical condition remote monitoring and control in operation conditions. SAE Technical Paper 2018-01-0024; 2018. DOI: 10.4271/2018-01-0024

[13] Hahanov V, Gharibi W, Litvinova E, Chumachenko S. et al., Cloud-Driven Traffic Monitoring and Control Based on Smart Virtual Infrastructure. SAE Technical Paper 2017-01-0092. 2017. https://doi.org/10.4271/2017-01-0092

[14] Gritsuk I, Aleksandrov V, Panchenko S, Kagramanian A. et al., Features of Application Materials While Designing Phase Transition Heat Accumulators of Vehicle Engines. SAE Technical Paper 2017-01-5003. 2017. https://doi.org/10.4271/2017-01-5003

[15] Dmytrychenko MF, Mateichyk VP, Gryschuk OK, Tsyuman MP. Systems Analysis Techniques for Automotive Engineering. Kyiv: NTU; 2014. p. 168

[16] Gritsuk I, Gutarevych Y, Mateichyk V, Volkov V, Improving the processes of preheating and heating after the vehicular engine start by using heating system with phase-transitional thermal accumulator. SAE Technical Paper 2016-01-0204; 2016. DOI: 10.4271/2016-01-0204

[17] Verbovskiy VS. The assessment of pre-start and after-start development of gas engine K-159 M2 using the combined system of pre-start heating. The collection of scientific papers. Donetsk. DonIZT UkrDAZT. 2014;**39**:93-99

[18] Gritsuk I, Mateichyk V, Tsiuman M, Gutarevych Y. et al., Reducing Harmful Emissions of the Vehicular Engine by Rapid After-Start Heating of the Catalytic Converter Using Thermal Accumulator. SAE Technical Paper 2018-01-0784. 2018. https://doi.org/10.4271/2018-01-0784

[19] Gritsuk I, Volkov V, Mateichyk V, Gutarevych Y. et al., The Evaluation of Vehicle Fuel Consumption and Harmful Emission Using the Heating System in a Driving Cycle. SAE International Journal of Fuels and Lubricants. 2017;**10**(1)236-248. https://doi.org/10.4271/2017-26-0364

Chapter 8

Techno-Economic Analysis of a Peltier Heating Unit System Integrated into Ventilated Façade

Lizbeth Salgado-Conrado, César Martín-Gómez,
María Ibáñez Puy and
José Antonio Sacristán Fernández

Additional information is available at the end of the chapter

http://dx.doi.org/10.5772/intechopen.76642

Abstract

This chapter aims to describe the conceptual design and operating mode of an innovative thermoelectric heating unit (THU) prototype in a heating mode. Firstly, the conceptual design of THU system and improvements are described to investigate the effects of design in the thermal performance. Secondly, the THU prototype was compared with a conventional air-conditioning system using the typical economic indicators (investment costs, maintenance costs and operational costs). The results indicate that the overall cost of this project was approximately 84,860 Euros, of which 69.27% of the total investment cost are for the engineering costs. By focused on the investment costs of the THU system, the results reveal that the conventional air-conditioning system is economically viable than a THU system. The analysis shows that the design has a direct effect on the costs. The maintenance costs show that THU v1.2 prototype is more economically viable in maintenance than the conventional air-conditioning system. Likewise, the operational costs show that THU v1.2 had a more stable thermal behaviour than the conventional air-conditioning system. Based on the results, the authors concluded that the THU system could be a viable option for a heating room.

Keywords: Peltier, façade, thermoelectric system, techno-economic analysis

1. Introduction

The thermoelectric generators, sometimes called Peltier modules, are semiconductors based on Peltier effect to pump heat. The advantage of this system is that it can be used in the heating or cooling mode in a simple way. Due to it, the use of the thermoelectric generators is having a growing interest in developing new prototypes in the military, industrial and commercial areas [1–5].

The studies related to the cooling mode have focused their efforts on developing prototypes [6–12] that dissipate the heat in small applications such as in lasers, personal computers, refrigerators, cryogenic prototypes, and so on, while heating modes are being applied mainly in architectural area. The essential concepts of Peltier modules applied in the architecture have been introduced by Khire et al. [13], who proposed an ABE system that uses solar energy to compensate for passive heat losses or gains in a building envelope. The authors discussed the design and optimization of Peltier modules with PV panels in their work. Under this context, Xu et al. [14] developed various ABE prototypes in a heating mode, using commercially available PVs and Peltier cells, and Liu et al. [15] designed an ASTRW system with thermoelectric technology and PV panels. Likewise, Vázquez et al. [16] described the basic principles of a new concept for an active thermal wall that improves the current practice for designing and installing air-conditioning for enclosed spaces. Irshad et al. [17] designed a solar TE-AD system that employs thermoelectric modules (TEMs) inside an air duct to provide thermal comfort. In [18], a solar thermoelectric cooled ceiling is combined with a displacement ventilation system. The prototype was tested in cooling and heating modes. Other interesting studies [19, 20] described the application of Peltier cells in active walls, active building windows and thermoelectric ventilators. Recently, Luo et al. [21–23] proposed a building integrated photovoltaic thermoelectric wall system, which is supported by the co-work of PV module for solar radiation transformation, air gap for thermal dissipation and thermoelectric radiant panel system for active radiant cooling/heating. This study focused on an efficient and accurate system model for the simulation of this system. Wang et al. [24] develop a thermoelectric heating system powered by renewable energy to reduce the CO_2 emission in buildings. According to results, the prototype minimises the energy demands and therefore reduces CO_2 emissions.

The studies related to the economic analysis of HVAC technologies emphasise energy saving in the heating/cooling system [25–27] and the energy demand in buildings [28, 29]. From the engineering point of view, the number of Peltier cells, the heat exchanger design and the auxiliary system (fans, back-up system, control system, etc.) are studied in order to reduce the investment, operational and maintenance costs [30–32]. The purpose of this study is to present the conceptual design of a THU integrated into ventilated façade and analyse its economic viability and its thermal performance. To accomplish this aim, the following items are proposed:

1. describe the conceptual design and the operating mode of an innovative THU prototype;
2. compare the thermal performance of a THU prototype with a conventional air-conditioning system using the typical economic indicators (investment costs, maintenance costs and operational costs).

This work contributes in identifying the key aspect that may increase the efficiency of the HVAC systems in ventilated façades. Also, this research completes the authors' previous work [33–37] about the theoretical design and construction of an active ventilated façade with Peltier modules. The authors are aware that a techno-economic analysis of a THU prototype has not yet been reported.

2. Technical description of the thermoelectric heating units

Since 2009, the authors have been working on alternative HVAC systems for buildings. Based on their previous experience as architects (not engineers) in the area of building services and energy systems [38], the authors have focused on the design of decentralised ventilated heating system for new and rehabilitated building envelopes. The result was the construction of a simplified inhabited housing unit (prefabricated module) with a thermoelectric heating system. A detailed report on this first THU version (v1.1) and its manufacture has been presented by the authors in previous works [33–36]. This section provides a brief description of this first version and presents the improvement of this prototype (THU v1.2). Both prototypes were installed in a prefabricated test room to analyse their performance under real conditions.

2.1. Thermoelectric system of THU version 1.1

Thermoelectric heating unit (THU v1.1) consists of three subsystems: a heating system, a ventilation system and a control system. The heating system was composed of 84 RC12–8 Peltier modules (Marlow Industries, Inc.) with a heat dissipation system. The Peltier modules were placed in groups of two thermoelectric modules, where the Peltier modules were connected in series and the groups were connected in parallel; altogether, they form 42 groups that require a voltage of 50 volts and have a heating capacity of 3 kW (3/4TR heating tonnage). The elements of heat dissipation system are composed of 84 heat pipes, 21 finned heat sinks, two axial fans (fixed on the façade) and two tangential fans (fixed on the internal chamber). A schematic diagram of THU v1.1 prototype is illustrated in **Figure 1**.

The prototype has a control system that supplies electric energy to the system, controls the auxiliary equipment (fans, sensors, actuators, etc.) and regulates the working operations (inside temperature). In addition, a protection equipment was included in case of accidents that basically consists of a PLC, sensors and actuators.

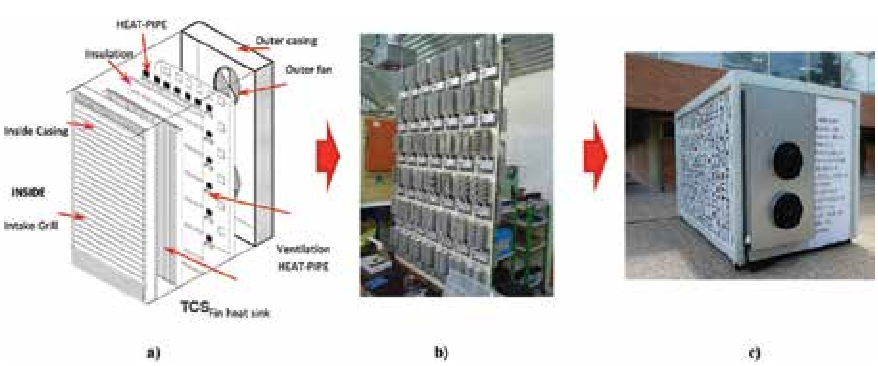

Figure 1. Schematic diagram of THU v1.1: (a) parts of the prototype, (b) heating system (heat pipes with Peltier cells) and (c) external view showing the electrical connection (down) and the ventilation grills (sideways).

2.2. Thermoelectric system of THU version 1.2

Recently, an improved prototype of the THU v1.1 was designed, named THU v1.2. This second version mainly consists of three subsystems: a heating system, a ventilation system and a control system. The heating system is composed of 20 Peltier modules (Marlow Industries, Inc.) with a heat dissipation system. All Peltier modules are connected in parallel, require a voltage of 20 volts and have a heating capacity of 1 kW (1/4TR heating tonnage). The elements of heat dissipation system are composed of 20 finned heat sinks and four tangential fans. This second version has more insulation, better heat dissipation and lower power consumption. **Figure 2** shows the outside and inside views of THU v1.2 prototype.

In order to know the economical and thermal viability of the THU v1.2 prototype, an identical test room was built for a conventional air-conditioning system, as shown in **Figure 3**. The conventional air-conditioning system uses inverter technology to regulate the voltage, current and frequency of an air conditioner so that it consumes only the necessary energy. The used model in this work is the air-conditioning split (1X1 MSZ-HJ35VA Mitsubishi Split) with a heating capacity of 3.6 kW (1TR heating tonnage).

To provide a consistent baseline for comparative analysis, the authors show the technical information for the THU prototype and conventional air-conditioning system (**Table 1**).

2.3. Design and operating principle

The exterior image in this project is based on an opaque ventilated façade with an active mechanism (air grilles) that adapts to different environmental conditions and seeks maximum efficiency at all times. The activation mechanism adjusts the air chamber ventilation of the façade and the heating system. This means that during winter months, the grilles are shut to enhance the accumulation of heat inside a room. However, in the summer months, the grilles are opened to extract the excess heat from the system. It is relevant to mention that the initial configuration of the active ventilated façade is in accordance with the requirements under the regulation of the ventilation of the cavity of the ventilated façade. As is shown in **Table 2**, an enclosure of a light sheet metal, as a light element with low thermal inertia that allows an immediate response to external environmental conditions and a ventilation capacity of 50CFM in the room was selected.

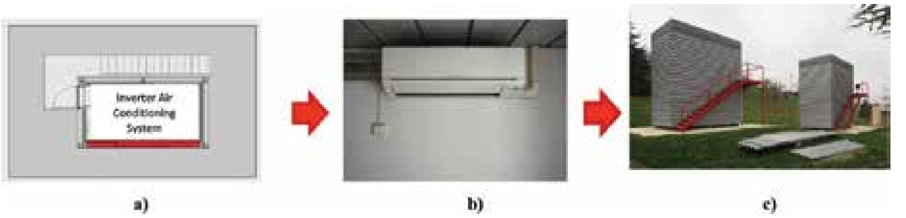

Figure 2. Integration of the thermoelectric system in THU v1.2: (a) top view, (b) inside view (air inlet and outlet and ceramic surface) and (c) outside view of the prototype with the grills to dissipate the heated/cooled air.

Figure 3. Schematic diagram of conventional system v2.0: (a) top view, (b) inside view and (c) outside view.

Parameter/component	THU v1.0	THU v1.2	Conventional system V2.0
Internal dimension (m)	4.0 × 2.4 × 2.5	3.75 × 2.10 × 2.0	3.75 × 2.1 × 2.0
Façade thickness (mm)	35	160	160
Dimension of chambers (cm)	100 × 10	100 × 10	No
U of the façade (W/m^2 K)	0.52	0.21	2.21
Double height	No	Yes	Yes
Roof thickness (mm)	35	127	127
U of the roof (W/m^2 K)	0.52	0.21	0.21
Floor thickness (mm)	19	195	195
U of the floor (W/m^2 K)	5.26	0.29	0.29

Table 1. Technical parameters of the prototypes.

The internal concept of the THU prototype consists of three layers, two air chamber and a HVAC system (thermoelectric system), as is shown in **Figure 4**. The first layer (external view) is composed of the metallic frame with two fans and a heat dissipation system. The fans allow the entrance of air to the external chamber (chamber connected to the outside environment), it passes through of the heat pipes and leaves external chamber eliminating the excess heat

Material	Thicknesses (mm)	Λ (W/mK)	R (m^{2}K/W)
Sheet metal	0.8	—	—
Ventilated air chamber/sealed	100	—	0.18
Inner sheet	177.5	0.163	4.62
Semi-rigid rockwool panel	80	0.034	1.91
Sandwich panel	35	0.028	1.25
Rockwool panel	50	0.035	1.40
Plasterboard	12.5	0.25	0.05

Table 2. Technical parameters of the active ventilated façade THU v1.2.

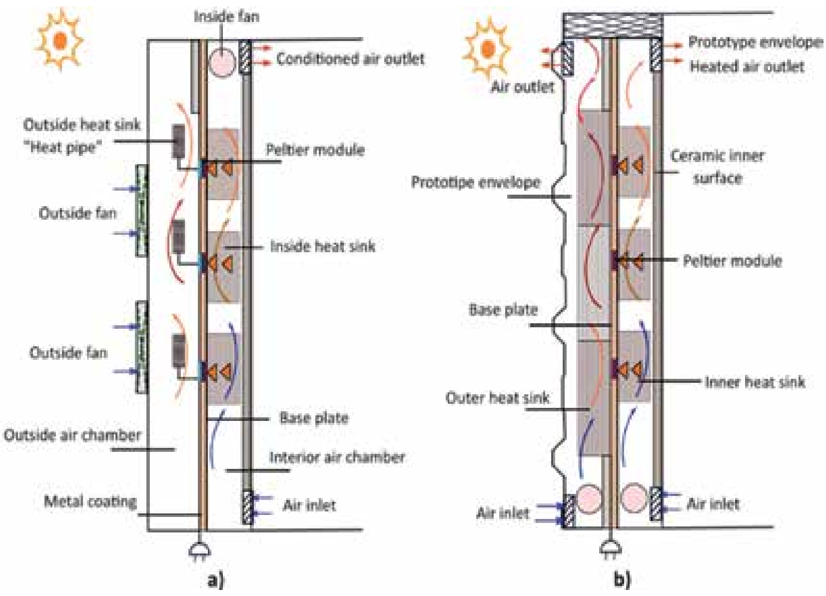

Figure 4. Schematic diagram of the design: (a) THU v1.1 prototype and (b) THU v1.2 prototype.

from the thermoelectric system. A relevant detail in the external view is that for THU v1.1, two axial fans were used, which were placed on the façade, while the second version THU v1.2 used two tangential fans, which were fixed in the lower part of the external chamber. This difference improves aesthetics and heat dissipation in the thermoelectric system.

The thermoelectric system is fixed in the second layer and its function is to separate the two chambers and supply heat to the room. Finally, the third layer connects the internal chamber with the room. This is composed of a group of heat sinks and two tangential fans (fixed in the lower part of the internal chamber). They allow the passage of air into the inner chamber for supplying hot air in the room. In this model, an air exit grill on the top of the wall was placed for extracting the cold air of the room.

2.4. Mathematical model

The Peltier modules consist of two or more elements of n-type- and p-type-doped semiconductor material that are electrically connected in series and thermally connected in parallel. These thermoelectric elements and their electrical interconnects are typically mounted between two ceramic substrates. Applying a voltage to a thermoelectric module creates a temperature difference. This temperature difference can be used to transfer heat from a cold side to a hot side and vice versa. Therefore, Peltier modules can be used to control the climate in rooms: to heat in winter and to cool in summer. In this regard, it is necessary to obtain a better heat transfer between the Peltier cells and the room air for increasing the heat transfer area of the ceramic plates with heat sinks [39, 40]. In this section, a brief overview of the basic equations that influence the functioning of a THU system is presented. The equations that mainly govern the thermoelectric effect are the electric power and the heat flow. The electric power shows the difference between the heat dissipated on the hot side and the heat absorbed at the cold side of the Peltier modules, and this is given by

$$P_{elect} = q_{hot} - q_{cold} = V \cdot I \tag{1}$$

where I is the load current, V is the output voltage, q_h is the heat dissipated on the hot side (W) and q_c is the heat absorbed at the cold side of the Peltier modules (W). The heat conduction from the hot side to the cold side is given by

$$q_{e,com} = K(T - T_o) \tag{2}$$

The heat flow is given by

$$q_1 = \alpha I_g T - \frac{1}{2} I_g^2 R + K(T - T_o) \tag{3}$$

and

$$q_1 = \alpha I_g T + \frac{1}{2} I_g^2 R + K(T - T_o) \tag{4}$$

where α is the total Seebeck coefficient (V/K), $\alpha = m(\alpha_p - \alpha_n)$, the subscripts p and n stand for p-type and n-type semiconductors, m is the number of Peltier cells, R is the total electrical resistance (Ω), $R = m(\rho_p I_p/S_p + \rho_n I_n/S_n)$, ρ is the electrical resistivity, l is the length of the semiconductor arms, S is the cross-sectional area of semiconductor arms, S is the cross-sectional area of semiconductor arms, K is the total thermal conductance, $R = \kappa_p S_p/l_p + \kappa_n S_n/l_n$, κ is the thermal conductivity of the semiconductor materials, I_g is the operational electrical current of a multi-couple Peltier cell.

A key parameter used to measure the performance of any air-conditioning system is the COP, defined as the useful thermal power output per unit of heat power. Its mathematical expression can be given as follows [42]:

$$COP_{(thermal)} = \frac{Useful\ Power\ (kW)}{Input\ Power\ (kW)} \tag{5}$$

The air-conditioned systems can be used in heating and cooling modes. In this work, the heating cycle is only considered, so the COP in heating mode for conventional system is given by [43]

$$COP_{(heat)} = 1 + \frac{T_a' - \Delta T_{evap}'}{T_{room}' - T_a' \Delta T_{cond}' + T_{evap}'} \tag{6}$$

where T_a' is the ambient temperature outside the evaporator in the heating mode (°K), T_{room}' is the room air temperature outside the condenser in the heating mode (°K), T_{cond}' is the temperature difference between refrigerant in condenser and ambient temperature ($^\circ K$) and T'_{evap} is the temperature in the evaporator ($^\circ K$).

In the case of thermoelectric system, the ideal COP in the heating mode is given by [43]

$$COP_{(heat)} = \frac{T_h}{T_h - T_c}\left(1 - 2\frac{1 + Z\,T_{m-1}}{Z\,T_m}\right) \tag{7}$$

where T_h is the hot side temperature at ceramic plate location in a thermoelectric module ($^\circ K$), T_c is the cold side temperature at ceramic plate location in a thermoelectric module ($^\circ K$), Z is the figure of merit of thermocouple and T_m is the arithmetical average temperature of a thermocouple($^\circ K$) .

3. Techno-economic parameters

3.1. Economic indicators

The economic evaluation is based on investment costs, operational costs and maintenance costs. The investment costs consider the cost of each piece of the prototype, including the electrical equipment, structure, heating system and instrumentation equipment and electrical installation. For the determination of the investment costs, these costs were divided into three categories: engineering costs, supply/handing cost and auxiliary costs. The engineering costs combine design, manufacturing processes, modelling of the pieces, architectural plans and installations. The supply/handing costs involve the material supply. In this case, the prices are quoted for Pamplona, Spain. Finally, the auxiliary costs depend on the finishing touches of the project.

Operational costs refer to the costs for the proper operation of each prototype. These costs mainly depend on the electrical consumption of the prototype subsystems (cooling–heating system, ventilation and control system). The THU v1.2 prototype under investigation was designed with a power nominal consumption of 1 kW, while that the conventional air-conditioning system is of 1.04 kW.

Maintenance costs consider all types of activities related to the repair and replacement of damaged pieces in the prototype subsystems. These costs have been estimated based on the price of the prototype and the maintenance of each subsystem. In the case of the conventional v2.0 system (Split 1x1MSZ-HJ35VA Mitsubishi), these costs are related to the use of special chemicals, checking the pressure, voltage drop, amperage drop, cleaning and blowing the dirty parts. According to [40], the maintenance cost of this system varies from $737 to $2156 Euros each year, depending on the capacity of cooling/heating. It represents between 10 and 20% of the total investment cost of the Split cost. In the case of THU v1.2, the authors have estimated that the maintenance cost could be approximately 6–10% of the heating system cost. This estimation was based on 1.5 years of test with the prototype [36].

3.2. Lifetime of the prototypes

The lifetime of the prototypes reflects the useful life of each system or the prototypes during a determined time. It includes the operational, physical and technological lifetime. In this study, the operational lifetime of thermoelectric device reported by Marlow Industries. Inc. [41] is in the range of 20,000–350,000 h at normal conditions, and Mitsubishi Company guarantees 15 years for inverter air-conditioning [44]. It is estimated that the physical lifetime of the structure is 30–40 years because the structural design combines durability, resistance and anti-corrosive materials. Also, it is assumed that the technological lifetime of the THU system is as long as the lifespan of the building (30–40 years), since it has a digital display that allows controlling the Peltier system and a sophisticated PLC that can be reprogrammed to the user necessities.

3.3. Environmental benefits

In addition to an economic assessment, the THU systems have social benefits that play an important role in taking care of the environment. In other words, the benefits associated with the use of THU systems are mainly related to reducing carbon dioxide emission. THU systems do not emit CO_2 in the operational and maintenance phase as inverter air-conditioning systems, because they do not have a working fluid. Therefore, THU systems are a good option for avoiding greenhouse gas emissions. Their electronic components can also be recycled. Moreover, a photovoltaic system could be added into this system to generate electricity and could reduce the annual operational costs, according to [14, 15].

4. Results and discussion

The investment costs of the THU v1.2 prototype and conventional air-conditioning system are reported in **Table 3**. The results show that the overall cost of this protect was approximately 84,860 Euros. This cost is because the authors considered the architectural and engineering aspects of both prototypes. Also, it can be observed that the highest value was for the engineering costs at 69.27% of the total investment cost, so that it is suggested that the designer has to pay attention for proposing competitive and viable prototypes.

The improvements of THU v1.1 prototype reduced the total investment cost by 30%. This percentage is directed directly related to the design, manufacture process and size of the prototype. On the other hand, **Table 3** shows that the supply/handing cost represented no more than 18.89% of the investment cost and that the auxiliary cost contributed only 14.54%, as it was expected. The above data indicate that the design plays an important role in engineering aspects. This means that the designer should select appropriate construction materials, the number of Peltier cells and the distribution of each system considering their cost. Also, the results indicate that the conventional v2.0 system is more economically viable than THU v1.2 because the THU system is the first product built in a prefabricated module. This prototype would be more viable if a considerable number of THU systems were manufactured.

Concerning manufacturing process of heating system, it was noted that investment costs are directly influenced by the size and number of Peltier modules, that is, an increase of Peltier modules increases the number of finned heat sinks, so that the investment costs increase. Also, the use of heat pipe sinks increases the investment costs by 30%. Although the heat pipe sinks offer better performance in terms of heat dissipation, the manufacturing process of a finned heat sink is less complicated than that of a heat pipe sink, so that the finned heat sink

Description	Costs (€)
Engineering costs	**68.88%**
-Construction of sills, general electricity networks, water and fibre optic installation	18,115.38
-Gardening work	
-Manufacture of the heat exchange module based on the Peltier cells	38,829.71
-Design, installation and start-up of equipment for measurement and control	
Supply/handing costs	**15.22%**
-Supply of the materials for the manufacture of the outside coating façade and the finishes of the test modules	2523.90
-Supply of insulation: blankets and insulation plates allocated to cover façades, roofs and floors (inside and outside)	2381.40
-Supply of materials for the interior walls and flooring of the modules: substructures and plasterboard plate	1095.96
-Transfer of Rockwool materials	
-Supply of four motorised doors to control the ventilated camera	632.80
-Supply and assembly of structures and enclosures	5993.00
-Split 1x1MSZ-HJ35VA 3.15 W cool-3.5 W heat MITSUBISHI and miscellaneous accessories	1332.07
Auxiliary cost	**15.90%**
-Installing the insulation (inside and outside) and coating the walls and floors with plasterboards	1769.68
-Placing metallic elements on the façades	10,829.71
-Constructing and installing the stairs	
-Painting	513.60
-Installing the Split 1x1MSZ-HJ35VA	860.53
Total Cost	**84,860.10**

Table 3. Investment costs of the prototypes v2.0 and conventional air-conditioning system.

is more economic. Moreover, it was seen that an increase in insulation level is beneficial in reducing heating demand. In the supply cost can be see that represent no more that 16% of the investment costs. According to the authors' experiences, these costs can be increased or reduced depending on the location of the supplier. Also, **Table 3** shows that the conventional air-conditioning system is more economically viable than THU v1.2, due to the manufacturing cost.

In regard to the operational costs, two 24-h thermal performance tests in January, from 13:30 to 13:30 h, were carried out in both prototypes, see **Figures 5** and **6**. Firstly, it was noted that after 30 min, the internal temperature of the room in the THU v1.2 reached 21°C, while in conventional system it was 26°C. In both tests, it was observed that there was a difference of 5°C in the internal temperature of the room. This means that THU v1.2 prototype could not reach 26°C in the room. It is because the THU v1.2 prototype was designed with 1/4TR of heating tonnage

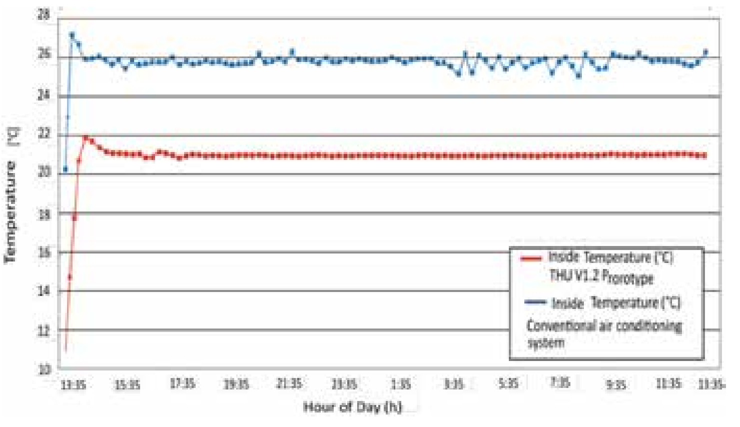

Figure 5. The inside temperature of the room in THU v1.2 and conventional v2.0 system, from January 12 (13:30 h) to 13 (13:30 h) in Pamplona, Spain.

and conventional v2.0 system is about 1TR of heating tonnage. To increase the temperature in the room, an increase of Peltier modules is needed. Therefore, it was deduced that the number of Peltier modules have an important impact on the thermal performance of the prototype.

The results showed that THU v1.2 had a more stable thermal behaviour than the conventional air-conditioning system, despite variation in the outside temperature, see **Figures 7** and **8**. It can be claimed that the active mechanism may be a key parameter in the efficiency.

The conducted tests showed that the nominal consumption of the Peltier equipment, with a set point of 22°C, is approximately 0.45 kW, while the conventional v2.0 system has a consumption of 0.15 kW, with a set point of 26°C. This affirms that the THU v1.2 design should improve the physical model of THU v1.2 prototype, and the annual maintenance cost is between 6 and 10% of the total investment cost of the system. Compared with the conventional air-conditioning system,

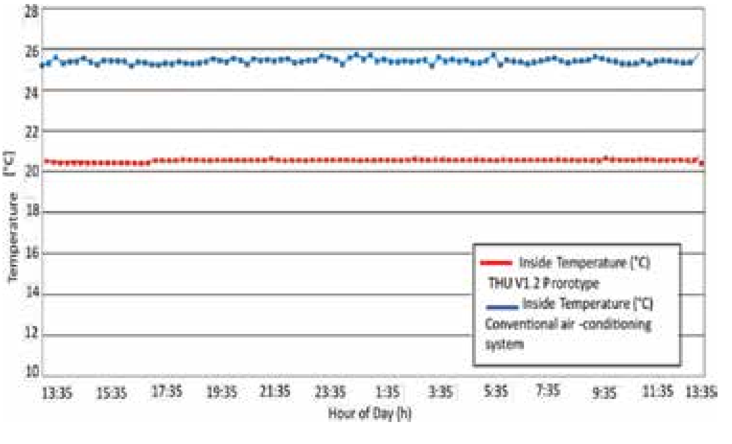

Figure 6. The inside temperature of the room in THU v1.2 and conventional v2.0 system, from January 13 (13:30 h) to 14 (13:30 h) in Pamplona, Spain.

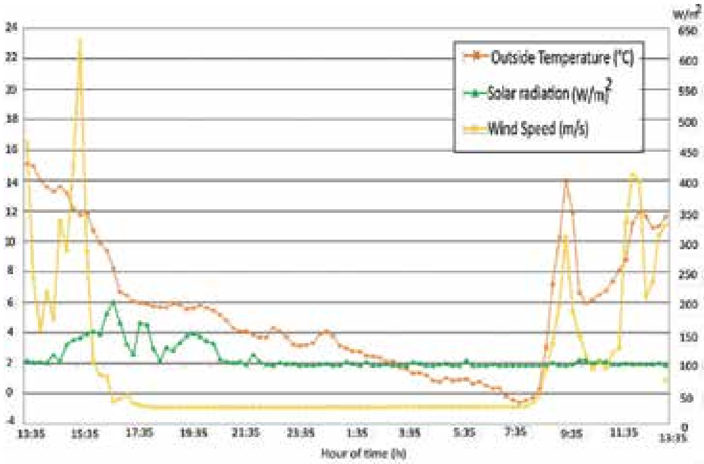

Figure 7. The variations of solar radiation, wind speed and outside temperature from January 12 (13:30 h) to 13 (13:30 h) in Pamplona, Spain.

THU v1.2 prototype is more economically viable in maintenance, so that the conventional air-conditioning system frequently needs maintenance and the replacement of parts.

The indicator associated with COP heat of the conventional air-conditioning system showed that it is in a range of 2.6–3, while the THU v1.2 prototype is between 0.46 and 1.07, as is illustrated in **Figure 9**. Considering the annual experimental data, the COP Carnot in a heating mode for THU v1.2 prototype is between 5 and 18%. Comparing the results of [43], it could be deduced that the conventional air-conditioning system has a COP of 30%. Thus, it can be noted that the conventional air-conditioning system is more efficient than the THU v1.2 prototype.

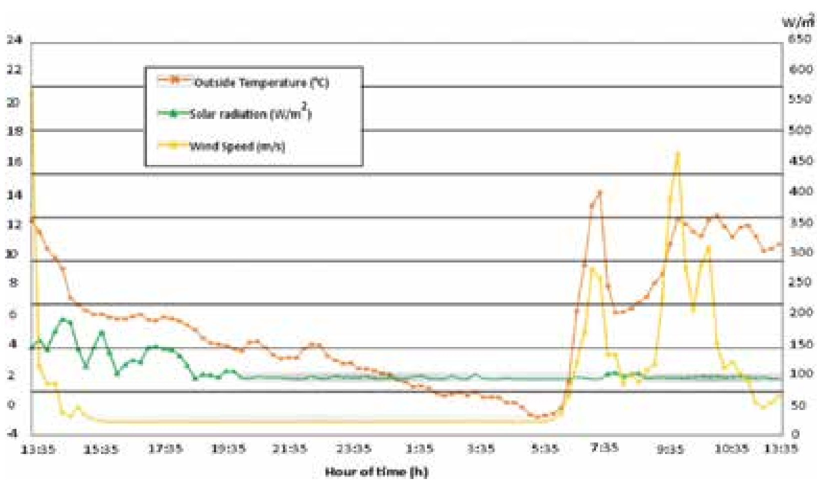

Figure 8. The variations of solar radiation, wind speed and outside temperature from January 13 (13:30 h) to 14 (13:30 h) in Pamplona, Spain.

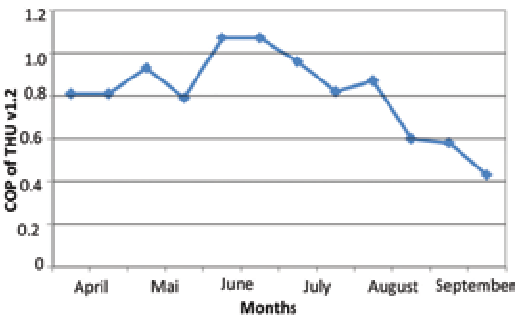

Figure 9. Experimental measurement COP of THU v1.2 prototype versus the months.

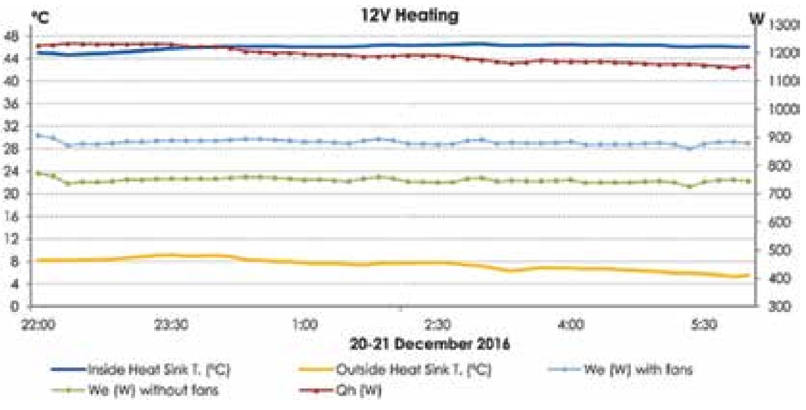

Figure 10. Graphic of the TCHU v1.1 with 12 V in heating.

Moreover, other tests have been published in [45, 46], where it is seen that the power consumption has higher values in Peltier systems, which is associated with the behaviour of Peltier in relation with the weather. As shown in **Figure 10**, the THU version 1.1 system consumes approximately 1.2 kW of power, while the THU version 1.2 system consumes approximately 1 kW. Therefore, the THU version 1.2 THU system has a great economic advantage on the THU version 1.1 prototype.

In summary, the techno-economic analysis gives rise to several interesting ideas for future research, such as the inclusion of photovoltaic panels and batteries in the prototypes, which will create an autonomous and efficient system.

5. Conclusions

The goal of this study was to describe the conceptual design and the operating mode of an innovative thermoelectric heating unit (THU) prototype and compare the thermal performance of a THU prototype with a conventional air-conditioning system. The analysis of investment costs, maintenance costs and operational costs was used as a reference point in the comparison. We found that the overall cost of this project was approximately 84,860 Euros.

By focusing on the investment costs of the THU system, the results reveal that THU v1.2 prototype design is 30% more economical than THU v1.1 design, due to a better design strategy in the manufacture process and the dissipation systems. By considering only dissipation systems, it was noted that the use of heat pipe sinks increase by 30% the investment costs. Although the heat pipe sinks offer better performance in terms of heat dissipation, the manufacturing process of a finned heat sink is less complicated than that of a heat pipe sink, so that the finned heat sink system is more economic.

From a comparative point of view, the results show that the conventional air-conditioning system is economically viable than a THU system; therefore, if THU was to enter the market, it is necessary to implement a strategy that reduces costs. Regarding the thermal performance, the results demonstrate that THU v1.2 had a more stable thermal behaviour than the conventional air-conditioning system. The maintenance costs indicated that THU v1.2 prototype is more economically viable in maintenance than the conventional air-conditioning system. Moreover, verifying the environmental benefits between the studied systems, it was found that the maintenance of a conventional air-conditioning system has a greater environmental impact than the THU v1.2 system. The authors recommended a life cycle analysis (LCA) of both prototypes, in order to know the pros and cons of the environment.

Acknowledgements

The authors acknowledge financial support from Conacyt (México), PRODEP, Universidad de Navarra Project no. 1804805, Ministerio de Ciencia e Innovación del Gobierno de España BIA2013-46463-R, Asociación de Amigos de la Universidad de Navarra, Aislamientos San Fermin, Berotza, Jacar, Rock wool, Teczone, Trox.

Conflict of interest

There is no conflict of interest.

Nomenclature

ABE	active building envelope
ASTRW	active solar thermoelectric radiant wall
CFM	cubic foot per minute
COP	coefficient of performance

HVAC	heating ventilating and air conditioning
I	load current (A)
K	total thermal conductance (W/K)
l	length of the semiconductors (m2)
m	number of Peltier cells
PLC	programmable logic controller
PV	photovoltaic
q	heat dissipated
R	resistance (Ω)
S	cross-sectional area of semiconductor arms (m)
TE-AD	thermoelectric air duct
TEM	thermoelectric modules
THU	thermoelectric heating unit
TR	refrigeration tons
V	voltage
V1.1	version 1.1
v1.2	version 1.2

Greek letters

α	total Seebeck coefficient
κ	thermal conductivity of the semiconductor materials
ρ	electrical resistivity

Subscripts

a	ambient
c	cold side
cond	conductivity
eva	evaporator
H	hot side
n	n-type semiconductors
p	p-type semiconductors

Author details

Lizbeth Salgado-Conrado[1], César Martín-Gómez[2]*, María Ibáñez Puy[2] and José Antonio Sacristán Fernández[2]

*Address all correspondence to: cmargom@unav.es

1 Facultad de Ingeniería Mecánica y Eléctrica, Universidad Autónoma de Coahuila, Torreón, Coahuila, Mexico

2 Construction, Building Services and Structures Department, Universidad de Navarra, Pamplona, Spain

References

[1] Astrain el D, Vian JG, Dominguez M. Increase of COP in the thermoelectric refrigeration by the optimization of heat dissipation. Applied Thermal Engineering. 2003;**23**(17): 2183-2200

[2] Yang J, Stabler FR. Automotive applications of thermoelectric materials. Journal of Electronic Materials. 2009;**38**(7):1245-1251

[3] Zhang HY, Mui YC, Tarin M. Analysis of thermoelectric cooler performance for high power electronic packages. Applied Thermal Engineering. 2010;**30**(6):561-568

[4] Martín-Gómez et al. Building services cabinets as teaching material in a degree in architecture. European Journal of Engineering Education. 2014;**39**:143-156

[5] Enescu D, Virjoghe EO. A review on thermoelectric cooling parameters and performance. Renewable and Sustainable Energy Reviews. 2014;**38**:903-916

[6] Cheng T-C et al. Development of an energy-saving module via combination of solar cells and thermoelectric coolers for green building applications. Energy. 2011;**36**(1):133-140

[7] Konz I et al. Design and evaluation of a new Peltier-cooled laser ablation cell with on-sample temperature control. Analytica Chimica Acta. 2014;**809**:88-96

[8] Orvatinia M, Heydarianasl M. A new method for detection of continuous infrared radiation by pyroelectric detectors. Sensors and Actuators A: Physical. 2012;**174**:52-57

[9] Muñoz-García MA et al. Water harvesting for young trees using Peltier modules powered by photovoltaic solar energy. Computers and Electronics in Agriculture. 2013;**93**:60-67

[10] Da S, Luciana W, Kaviany M. Micro-thermoelectric cooler: Interfacial effects on thermal and electrical transport. International Journal of Heat and Mass Transfer. 2004;**47**(10):2417-2435

[11] Tomc U et al. A new magnetocaloric refrigeration principle with solidstate thermoelectric thermal diodes. Applied Thermal Engineering. 2013;**58**:1-10

[12] Rodriguez A et al. Development and experimental validation of a computational model in order to simulate ice cube production in a thermoelectric ice-maker. Applied Thermal Engineering. 2009;**29**:2961-2969

[13] Khire RA et al. Design of thermoelectric heat pump unit for active building envelope systems. International Journal of Heat and Mass Transfer. 2005;**48**:4028-4040

[14] Xu X et al. Study of the performance of thermoelectric modules for use in active building envelopes. Building and Environment. 2007;**42**:1489-1502

[15] Liu Z et al. Experimental evaluation of an active solar thermoelectric radiant wall system. Energy Conversion and Management. 2015;**94**:253260

[16] V'azquez J, et al. An active thermal wall based on thermoelectricity. In: Sixth European Workshop on Thermoelectrics. Freiburg, Germany. 2001. http://www.iit.upcomillas.es/palacios/thermo/ets2001-window.pdf

[17] Irshad K et al. Thermal comfort study of a building equipped with thermoelectric air duct system for tropical climate. Applied Thermal Engineering. 2015;**91**:1141-1155

[18] Liu Z et al. Experimental evaluation of a solar thermoelectric cooled ceiling combined with displacement ventilation system. Energy Conversion and Management. 2014;**87**:559-565

[19] Xu X et al. Evaluation of a prototype active building envelope window-system. Energy and Buildings. 2008;**40**:168-174

[20] Sadineni SB et al. Passive building energy savings: A review of building envelope components. Renewable and Sustainable Energy Reviews. 2011;**15**:3617-3631

[21] Luo Y et al. Dynamical simulation of building integrated photovoltaic thermoelectric wall system: Balancing calculation speed and accuracy. Applied Energy. 2017;**204**:887-897

[22] Luo Y et al. Performance analysis of a self-adaptive building integrated photovoltaic thermoelectric wall system in hot summer and cold winter zone of China. Energy. 2017;**140**:584-600

[23] Luo Y et al. Numerical evaluation on energy saving potential of a solar photovoltaic thermoelectric radiant wall system in cooling dominant climates. Energy. 2018;**142**:384-399

[24] Wang C, Calderón C, Wang YD. An experimental study of a thermoelectric heat exchange module for domestic space heating. Energy and Buildings. 2017;**145**:1-21

[25] Perez-Lombard L et al. A review of HVAC systems requirements in building energy regulations. Energy and Buildings. 2011;**43**:2, 255-268

[26] Kumar V et al. Techno-economic performance evaluation of building cooling systems: A study of snow storage and conventional chiller systems. Cold Regions Science and Technology. 2016;**130**:8-20

[27] Kim H, Kim W. A way of achieving a low $/W and a decent power output from a thermoelectric device. Applied Energy. 2015;**139**:205211

[28] Dames C. Cost optimization of thermoelectric materials for power generation: The case for ZT at (almost) any cost. Scripta Materialia. 2015. DOI: 10.1016/j.scriptamat.2015.06.018

[29] LeBlanc S. Thermoelectric generators: Linking material properties and systems engineering for waste heat recovery applications. Sustainable Materials and Technologies. 2014;**12**:26-35. DOI: 10.1016/j.susmat.2014.11.002

[30] Mathews EH et al. HVAC control strategies to enhance comfort and minimise energy usage. Energy and Buildings. 2001;**33**(8):853-863

[31] Magraner T et al. Comparison between design and actual energy performance of a HVAC-ground coupled heat pump system in cooling and heating operation. Energy and Buildings. 2010;**42**(9):1394-1401

[32] Vakiloroaya V et al. A review of dierent strategies for HVAC energy saving. Energy Conversion and Management. 2014;**77**:738-754

[33] Ibáñez-Puy M et al. Theoretical design of a active fa¸cade system with peltier cells. Energy Procedia. 2014;**61**:700-703

[34] Martín-Gómez C et al. Construction of an Active Fa¸cade Envelope with Peltier Cells, 39th World Congress on Housing Science Changing Needs, Adaptive Buildings, Smart Cities 1; 2013. pp. 517-524. http://hdl.handle.net/10171/34136

[35] Martín-Gómez C et al. Prototype thermoelectric climate system for its use in residential buildings, XXXVII IAHS World Congress on Housing. October 2010. pp. 26-29. http://hdl.handle.net/10171/13927

[36] Martín-Gómez C et al. Thermoelectric cooling heating unit prototype, Building Services Engineering Research and Technology. 2015. pp. 1-19. DOI: 10.1177/0143624415615533

[37] Martín-Gómez C, Eguaras M, Mambrilla N. Construction and monitoring of a prototype thermoelectric climate control system applied to an inhabited space. In: Twenty-Ninth International Conference on Thermoelectric, Shanghai, China: International Thermoelectric Society; 2010. p. 232

[38] Martín Gómez C. Las instalaciones y la arquitectura. Tect'onica. 2006;**21**:4-27. ISSN 1136-0062

[39] Sahin AZ, Yilbas BS. Thermodynamic irreversibility and performance characteristics of thermoelectric power generator. Energy. 2013;**55**:899904

[40] Juan Carlos RG et al. Modelado de un sistema de climatizaci'on basado en células termol'ectricas mediante TRNSYS. VIII Congreso Nacional de Ingeniería Termodinámica, Burgos (España). Libro de Actas: Universidad de Burgos; 2013. pp. 485-492. ISBN 978-84-92681-62-4

[41] Agyenim F. The use of enhanced heat transfer phase change materials (PCM) to improve the coefficient of performance (COP) of solar powered LiBr/H_2O absorption cooling systems. Renewable Energy. 2016;**87**:229-239

[42] Available from: https://www.energystar.gov/index.cfm?c=mostefficient.me cac ashp

[43] Available from: http://www.marlow.com/thermoelectric-coolers.html

[44] Available from: http://www.mitsubishielectric.com/bu/air/technologies/inverter.html

[45] Ibañez-Puy M et al. Thermoelectric cooling heating unit performance under real conditions. Applied Energy. 2017;**200**:303-314

[46] Ibañez-Puy M et al. Ventilated active thermoelectric envelope (VATE): Analysis of its energy performance when integrated in a building. Energy and Buildings. 2018;**158**: 1586-1592

Chapter 9

Energy Storage in Concrete Bed

Adeyanju Anthony Ademola

Additional information is available at the end of the chapter

http://dx.doi.org/10.5772/intechopen.77205

Abstract

The energy storage ability and temperature arrangement of a concrete bed which was charged and discharged at the same time was examined mathematically in this research. This was carried out by modeling a single globe-shaped concrete which was utilized to simulate a series of points along the concrete bed axis. Charging and discharging mode of the system were compared for 0.0094, 0.013, and 0.019 m^3/s air flow rates. Higher change in temperature response was detected between the charging and fluid to solid heat transfer process at the inception of the concrete bed and the heat gain by the cool air flowing inside the copper tube was fairly high. The analysis of energy storage efficiency was also carried out and it was noticed that the globe-shaped concrete of 0.11 m diameter has the highest storage efficiency of 60.5% at 0.013 m^3/s airflow rate.

Keywords: energy storage, heat transfer model, globe-shaped concrete, charging and discharging

1. Introduction

Heat can be transferred in a concrete bed through the following means: (i) heat transfer by convection from the bed wall to the fluid flowing inside the bed; (ii) heat transfer by convection from the globe-shaped concretes to fluid flowing in the bed, and this is known as fluid to particle mode; (iii) heat transfer by conduction from the bed walls to the globe-shaped concretes; (iv) heat transfer by conduction from one globe-shaped concrete to another, and this is known as particle to particle mode; (v) heat transfer by radiation; and (vi) heat transfer through fluid mixture [1]. The modes are as shown in **Figure 1**.

The particle to particle conduction mode can be further analyzed in axial and radial directions. Heat transfer through radiation mode will actually be important at higher temperatures.

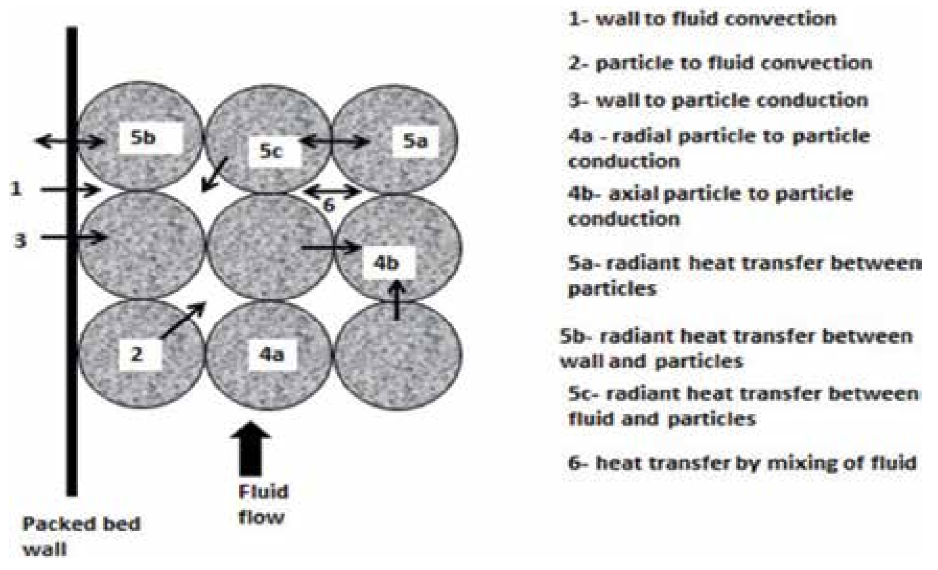

Figure 1. Schematic showing the modes of heat transfers in concrete bed.

Practically, it is found that two or three of the modes discussed earlier on can occur simultaneously. For example, the conduction between the particles may be affected by the convection between the particles and the fluid. This interaction among the different modes is one of the main reasons for the difficulty in correlating the total heat transfer and analyzing the experimental data in this field [2].

This research carried out numerically the temperature distribution in a concrete bed and also looked into the ability of a concrete bed to store energy simultaneously.

2. Review of literature

Anzelius [3] is the first author to publish a paper in heat transfer through packed beds but Schumann [4] is usually the first reference cited in most literature [1]. Both authors made some assumptions in order to find solution to equations that guide heat transfer for an incompressible fluids passing uniformly through a bed of solid particles with perfect conductivity. The following are the heat transfer equations derived for the system:

$$\frac{(T_s–T_{s,0})}{(T_s–T_{s,0})} = 1–e^{-Y-Z}\Sigma Y^n M^n(yz) = e^{-Y-Z}\Sigma Z^n M_n \tag{1}$$

$$\frac{\left(T_f–T_s\right)}{\left(T_{f,0}–T_{s,0}\right)} = 1–e^{-Y-Z}\Sigma[Y^n M^n(yz)] = e^{-Y-Z}\Sigma[Z^n M_n(yz)] \tag{2}$$

where T_s is the solid temperature, T_f is the temperature of fluid and Y and Z are dimensionless quantities. Eqs. (1) and (2) was solved simultaneously and the result were analyzed graphically to form Schumann curves. Knowing the outlet air and bed temperature, these curves can be used to determine the volumetric heat transfer coefficients and also the heat transfer coefficients of a packed bed undergoing heat exchange with a fluid provided the following conditions which were the simplifying assumptions made by Schumann were satisfied:

1. Due to the infinitesimal nature of the solid particles, resistance to heat transfer was so small.
2. Resistance to conduction heat transfer in the fluid was so small.
3. At any section of the bed, the heat transfer rate from fluid to solid or from solid to fluid was directly proportional to their average difference in temperature between the solid and fluid within the bed.
4. The transport properties of solid and fluid were not dependent on temperature, for example the density.

Furnas [5] utilized and expanded the Schumann curves to cover more range of temperatures and suggested an empirical relation for determination of heat transfer coefficient as shown in Eq. (3):

$$h_v = \frac{BG^{0.7}T^{0.3}10^{1.68\varepsilon-3.56\ \varepsilon 2}}{{d_p}^{0.9}} \tag{3}$$

where, h_v is the volumetric heat transfer coefficient. B is a constant dependent on the bed material, G is the mass velocity of the fluid, T is the average air temperature, d_p is the particle diameter and ε is the porosity.

Saunders and Ford [6] utilized dimensional analysis to derive correlations to calculate heat transfer coefficient. The research was for spherical shaped alone and the application is not suitable for other solid particle geometries.

Another correlation for the determination of heat transfer coefficient between gases and randomly packed solid spheres was postulated by Kays and London [7]. Using the Colburn j-factor, the relationship was written as:

$$j_h = \frac{0.23}{{Re_p}^{0.3}} \tag{4}$$

$$\text{where, } j_h = St.Pr^{2/3}$$

$$200 < Re_p < 50,000 \text{ and } 0.37 < \varepsilon < 0.39$$

Löf and Hawley [8] studied heat transfer between air and packed bed of granitic gravel. Unsteady state heat transfer coefficients were correlated with the air mass velocity and particle diameter to obtain the equation:

$$h = 0.652\ \left(G/d_p\right)^{0.7} \tag{5}$$

This was calculated for 8 mm < d_p < 33 mm; 50 < Rep 500 and temperature range of 311–394 K. The author reached a conclusion that the temperature of the entering air had no appreciable effect on the hat transfer coefficient.

Leva et al. [9] studied and analyzed heat transfer coefficient between smooth spheres of low thermal conductivities and fluids (air and carbon dioxide) in packed beds and tubes of 50.8 and 6.4 mm diameters, respectively. The ratio of particles to tube diameters was varied from 0.08 to 0.27; gas flow rate was of Reynolds number range 250 to 3000. Correlation of film coefficient was determined as:

$$h = 3.50\left(\frac{k}{D_t}\right) e^{-4.6\frac{Dp}{Dt}\left(\frac{DpG}{\mu}\right)0.7} \tag{6a}$$

which is approximately:

$$h = 0.40\,(k/D_t)\,\left(DpG/\mu\right)\,0.7 \tag{6b}$$

$$\text{Or, } N = 0.4\,Re^{0.7} \tag{6c}$$

Maximum film coefficient was predicted and verified at a value of Dp/Dt equal 0.153.

Riaz [10] and Jefferson [11] studied the dynamic behavior of beds undergoing heat exchange with air using single and two phased modes. By incorporating factors of axial bed conduction and intra-particle resistance, which Schumann ignored, the heat transfer coefficients were evaluated and found to be 1 + Bi/5 times smaller than those predicted using Schumann curves.

Ball [12], Norton [13], Meek [14], Bradshaw and Meyers [15], Harker and Martyn [16] and also, Bouguettaia and Harker [17] have all researched on various packed beds using air and other gases as fluids and have developed correlations involving the heat transfer coefficient.

3. Methodology

3.1. Heat transfer model for a globe-shaped concrete bed

The modeling of heat transfer in a concrete bed was carried out mathematically. It was done through a single globe-shaped concrete which was simulated mathematically to represent series of points along the concrete bed axis.

A one dimensional finite difference formulation was used in modeling the single globe-shaped concrete material, where heat conduction to neighboring globe-shaped concrete was ignored.

Using this assumption reduced the globe-shaped concrete model to that of an isolated sphere in cross flow, where the total surface area of the sphere was exposed to convection. Also, the thermal properties of the materials within the bed accounted for temperature dependence.

3.2. Finite difference formulation of a single spherical shaped concrete material

Since conduction to other globe-shaped concrete has been neglected, the geometry allows the concrete to be reduced to one dimension along its radius.

http://dx.doi.org/10.5772/intechopen.77205

A finite difference method was utilized to model this mathematically, [18]. For this approach, the globe-shaped concrete can be characterized by three different nodal equations:

i. a general, interior node

ii. the center node

iii. the surface node

All exposed to convection as shown in **Figure 2**.

For the general and interior node within the globe-shaped concrete model, the conduction equation for $T_{(r,t)}$ is:

$$\rho_c C_c \frac{\partial T}{\partial t} = \frac{1}{r^2} \frac{\partial}{\partial r} \left(K_c r^2 \frac{\partial T}{\partial r} \right) + \dot{q}_{(r,t)} \tag{7}$$

where C_c = specific heat of concrete.

$K_c =$ thermal conductivity of concrete.

$\dot{q} =$ heat generation.

And this equation was represented in finite difference form.

The specific heat, thermal conductivity, and the heat generation, are temperature dependent and varied with the temperature along the radial direction.

Because the thermal properties are functions of temperature, and consequently functions of the globe-shaped concrete radius, the finite difference equations are derived by the volume integration over a finite difference node.

Multiplying Eq. (7) by r^2 and integrating both sides of the equation from $r_n - \Delta r/2$ to $r_n + \Delta r/2$ resulted to:

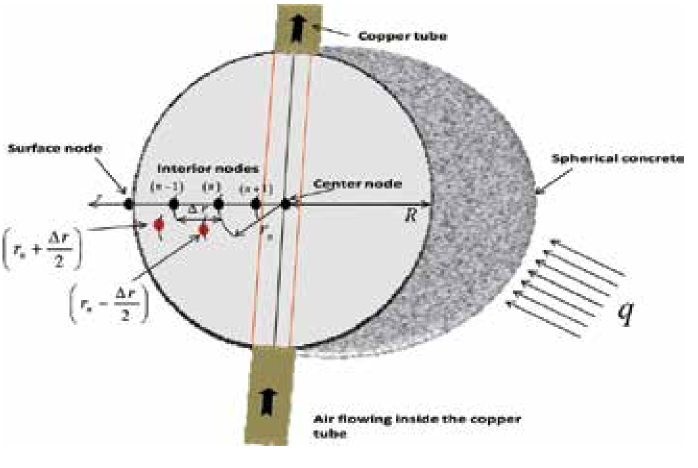

Figure 2. Schematic showing the cross-section of the globe-shaped concrete materials imbedded with copper tube.

$$\rho_c C_c \frac{\partial T}{\partial t} \int_{r_{n-\frac{\Delta r}{2}}}^{r_{n+\frac{\Delta r}{2}}} r^2 dr = \int_{r_{n-\frac{\Delta r}{2}}}^{r_{n+\frac{\Delta r}{2}}} \frac{\partial}{\partial r}\left(K_c r^2 \frac{\partial T}{\partial r}\right) dr + \int_{r_{n-\frac{\Delta r}{2}}}^{r_{n+\frac{\Delta r}{2}}} r^2 \dot{q}_{(r,t)} dr \tag{8}$$

The specific heat was assumed constant with respect to *r*, and therefore brought outside the integral.

By evaluating the integrals in Eq. (8) and representing the derivatives in finite difference form using the fully implicit method gives:

$$\rho_c C_c \left(\frac{T_n^{Z+1} - T_n^{Z}}{\Delta t}\right)\left(\frac{r_{n^+}^3 - r_{n^-}^3}{3}\right) = \int_{r_{n-\frac{\Delta r}{2}}}^{r_{n+\frac{\Delta r}{2}}} 2K_c r dT + \dot{q} \int_{r_{n-\frac{\Delta r}{2}}}^{r_{n+\frac{\Delta r}{2}}} r^2 dr \tag{9}$$

$$\rho_c C_c \left(\frac{T_n^{Z+1} - T_n^{Z}}{\Delta t}\right)\left(\frac{r_{n^+}^3 - r_{n^-}^3}{3}\right) = \left[\frac{2K_c r^2}{2}\frac{dT}{\Delta r}\right]_{r_{n-\frac{\Delta r}{2}}}^{r_{n+\frac{\Delta r}{2}}} + \dot{q}_n \left[\frac{r^3}{3}\right]_{r_{n-\frac{\Delta r}{2}}}^{r_{n+\frac{\Delta r}{2}}} \tag{10}$$

$$\begin{aligned} \rho_c C_c \left(\frac{T_n^{Z+1} - T_n^{Z}}{\Delta t}\right)\left(\frac{r_{n^+}^3 - r_{n^-}^3}{3}\right) &= K_{c(n^+)} r_{n^+}^2 \left(\frac{T_{n+1}^{Z+1} - T_n^{Z+1}}{\Delta r}\right) - \\ K_{c(n^-)} r_{n^-}^2 \left(\frac{T_n^{Z+1} - T_{n-1}^{Z+1}}{\Delta r}\right) + q_n \left[\frac{r_{n^+}^3 - r_{n^-}^3}{3}\right]_{r_{n-\frac{\Delta r}{2}}}^{r_{n+\frac{\Delta r}{2}}} \end{aligned} \tag{11}$$

where T_n^Z and T_n^{Z+1} indicate temperatures for an arbitrary node at times t^Z and t^{Z+1} respectively.

Also,

$$\mathrm{W}_n = \mathrm{W}\,\mathrm{at}\, T_n^{Z+1} \tag{12}$$

and,

$$K_{n^+} = \frac{K\left[T_{n+1}^{Z+1} + K\right]}{2}, \mathrm{at}\, T_n^{Z+1} \tag{13}$$

also,

$$r_{n^+} = r_n + \frac{\Delta r}{2} \tag{14}$$

$$r_{n^-} = r_n - \frac{\Delta r}{2} \tag{15}$$

Eq. (11) can be rearranged and solved for T_n^Z plus a known quantity which resulted to:

$$\rho_c C_c \left(\frac{T_n^{Z+1} - T_n^Z}{\Delta t}\right) = \frac{3K_{c(n^+)} r_{n^+}^2}{r_{n^+}^3 - r_{n^-}^3} \left(\frac{T_{n+1}^{Z+1} - T_n^{Z+1}}{\Delta r}\right) - \frac{3K_{c(n^-)} r_{n^-}^2}{r_{n^+}^3 - r_{n^-}^3} \left(\frac{T_n^{Z+1} - T_{n-1}^{Z+1}}{\Delta r}\right) + \dot{q}_n \left[\frac{3r_{n^+}^3 - r_{n^-}^3}{3r_{n^+}^3 - r_{n^-}^3}\right] \tag{16}$$

$$\rho_c C_c \frac{T_n^{Z+1}}{\Delta t} - \rho_c C_c \frac{T_n^Z}{\Delta t} = \frac{3K_{c(n^+)} r_{n^+}^2}{r_{n^+}^3 - r_{n^-}^3} \left(\frac{T_{n+1}^{Z+1} - T_n^{Z+1}}{\Delta r}\right) - \frac{3K_{c(n^-)} r_{n^-}^2}{r_{n^+}^3 - r_{n^-}^3} \left(\frac{T_n^{Z+1} - T_{n-1}^{Z+1}}{\Delta r}\right) + \dot{q}_n \tag{17}$$

Multiply Eq. (17) by Δt and divide by $\rho_c C_c$ resulted to:

$$T_n^{Z+1} - T_n^Z = \frac{3K_{c(n^+)} r_{n^+}^2 \Delta t}{\rho_{c(m)} C_{c(m)} \Delta r \left(r_{n^+}^3 - r_{n^-}^3\right)} \left[T_{n+1}^{Z+1} - T_n^{Z+1}\right] - \frac{3K_{c(n^-)} r_{n^-}^2 \Delta t}{\rho_{c(m)} C_{c(m)} \Delta r \left(r_{n^+}^3 - r_{n^-}^3\right)} \left[T_n^{Z+1} - T_{n-1}^{Z+1}\right] + \frac{3\Delta t \dot{q}_n}{\rho_{c(m)} C_{c(m)}} \tag{18}$$

$$\therefore T_n^Z + \frac{3\Delta t \dot{q}_n}{\rho_{c(m)} C_{c(m)}} = T_n^{Z+1} - \left[\frac{3K_{c(n^+)} r_{n^+}^2 \Delta t}{\rho_{c(m)} C_{c(m)} \Delta r \left(r_{n^+}^3 - r_{n^-}^3\right)}\right] \left[T_{n+1}^{Z+1}\right] + \left[\frac{3K_{c(n^+)} r_{n^+}^2 \Delta t}{\rho_{c(m)} C_{c(m)} \Delta r \left(r_{n^+}^3 - r_{n^-}^3\right)}\right] \left[T_n^{Z+1}\right] + \left[\frac{3K_{c(n^-)} r_{n^-}^2 \Delta t}{\rho_{c(m)} C_{c(m)} \Delta r \left(r_{n^+}^3 - r_{n^-}^3\right)}\right] \left[T_n^{Z+1}\right] + \left[\frac{3K_{c(n^-)} r_{n^-}^2 \Delta t}{\rho_{c(m)} C_{c(m)} \Delta r \left(r_{n^+}^3 - r_{n^-}^3\right)}\right] \left[T_{n-1}^{Z+1}\right] \tag{19}$$

Collecting the like terms from Eq. (19) yielded:

$$\therefore T_n^Z + \frac{3\Delta t \dot{q}_n}{\rho_{c(m)} C_{c(m)}} = \left[\left(\frac{3\Delta t}{\rho_{c(m)} C_{c(m)} \Delta r}\right) \frac{K_{c(n^-)} r_{n^-}^2}{\left(r_{n^+}^3 - r_{n^-}^3\right)}\right] \left[T_{n-1}^{Z+1}\right] + \left[1 + \left\{\left(\frac{3\Delta t}{\rho_{c(m)} C_{c(m)} \Delta r}\right) \frac{\left(K_{c(n^-)} r_{n^-}^2 + K_{c(n^+)} r_{n^+}^2\right)}{\left(r_{n^+}^3 - r_{n^-}^3\right)}\right\}\right] \left[T_n^{Z+1}\right] - \left[\left(\frac{3\Delta t}{\rho_{c(m)} C_{c(m)} \Delta r}\right) \frac{K_{c(n^+)} r_{n^+}^2}{\left(r_{n^+}^3 - r_{n^-}^3\right)}\right] \left[T_{n+1}^{Z+1}\right] \tag{20}$$

This resulting equation is valid for any general, interior node within the globe-shaped concrete $0 < r_n < R$.

At the center node, where $r_n = 0$ the temperature profile is axisymmetric, and $\frac{\partial T}{\partial r} = 0$, when $r = 0$ thus, the temperature on either side of the node is equal.

$$T_{n-1}^{Z+1} = T_{n+1}^{Z+1}$$

$$likewise, K_{c(n^-)} = K_{c(n^+)}$$

$\therefore$Eq. (20) simplified to:

$$\therefore T_n^Z + \frac{\Delta t \dot{q}_n}{\rho_{c(m)} C_{c(m)}} = T_n^{Z+1} - \left(\frac{6\Delta t}{\rho_{c(m)} C_{c(m)} \Delta r^2} K_{c(n^+)} \right) T_{n+1}^{Z+1} \tag{21}$$

This occur at $r_n = 0$.

This simplified form of Eq. (20) was used to represent the center node.

The conduction through the surface of the globe-shaped concrete is equal to the convection at the surface.

$$\therefore -K \frac{\partial T}{\partial r}_{at,\, r=R} = -U_C (T_{r=R} - T_\infty) \tag{22}$$

However, this boundary condition cannot be directly represented in finite difference form, since such formulation requires a volume element and Eq. (22) applies at a point.

Instead a first law energy balance was utilized to obtain the nodal equation for the surface of the globe-shaped concrete. This energy balance can be written as:

$$\dot{E}_{in} - \dot{E}_{out} + \dot{E}_{gen} = \dot{E}_{st} \tag{23}$$

where,

$$\dot{E}_{in} = -KA \frac{\partial T}{\partial r} \tag{24}$$

$$\dot{E}_{out} = U_C A \left(T - T_g \right) \tag{25}$$

$$\dot{E}_{gen} = \dot{q} V \tag{26}$$

$$\dot{E}_{st} = \rho C V \frac{\partial T}{\partial t} \tag{27}$$

Representing Eq. (23) in a finite difference form consistent with Eq. (20) and (21) resulted to:

$$-KA \frac{\partial T}{\partial r} - U_C A \left(T - T_g \right) + \dot{q} V = \rho C V \frac{\partial T}{\partial t} \tag{28}$$

This can be written in finite difference form to give:

$$\begin{aligned} &-4\pi r_{n^-}^2 K_{n^-} \frac{T_n^{Z+1} - T_{n-1}^{Z+1}}{\Delta r} - 4\pi r_n^2 U_C \left(T_n^{Z+1} - T_\infty \right) + \frac{4}{3} \pi \left(r_n^3 - r_{n^-}^3 \right) \dot{q}_n = \\ &\frac{4}{3} \pi \rho C_n \left(r_n^3 - r_{n^-}^3 \right) \frac{T_n^{Z+1} - T_n^Z}{\Delta t} \end{aligned} \tag{29}$$

where, U_c = convection coefficient.

Solving for T_n^Z plus known quantities involving $\dot{q}$ and U_c, in a similar manner to Eq. (20) and (24) resulted to:

$$\begin{aligned}&\frac{-4\pi r_{n^-}^2 K_{n^-} T_n^{Z+1}}{\Delta r} + \frac{-4\pi r_{n^-}^2 K_{n^-} T_{n-1}^{Z+1}}{\Delta r} - 4\pi r_n^2 U_C T_n^{Z+1} - 4\pi r_n^2 U_C T_\infty + \\ &\frac{4}{3}\pi\left(r_n^3 - r_{n^-}^3\right)\dot{q}_n = \frac{4}{3}\pi\rho C_n \frac{\left(r_n^3 - r_{n^-}^3\right)}{\Delta t} T_n^{Z+1} - \frac{4}{3}\pi\rho C_n \frac{\left(r_n^3 - r_{n^-}^3\right)}{\Delta t} T_n^Z\end{aligned} \tag{30}$$

Multiply Eq. (30) by Δt and divide by $\frac{4}{3}\pi\rho\left(r_n^3 - r_{n^-}^3\right)$ resulted to:

$$\begin{aligned}&T_n^Z - T_n^{Z+1} = \frac{3\Delta t}{\Delta r \rho C_n}\left(\frac{r_{n^-}^2 K_{n^-}}{r_n^3 - r_{n^-}^3}\right) T_n^{Z+1} - \frac{3\Delta t}{\Delta r \rho C_n}\left(\frac{r_{n^-}^2}{r_n^3 - r_{n^-}^3}\right) T_{n-1}^{Z+1} + \\ &\frac{3\Delta t U_C}{\rho C_n}\left(\frac{r_{n^-}^2}{r_n^3 - r_{n^-}^3}\right) T_n^{Z+1} + \frac{3\Delta t U_C}{\rho C_n}\left(\frac{r_n^2}{r_n^3 - r_{n^-}^3}\right) T_\infty - \frac{\dot{q}_n \Delta t}{\rho C_n}\end{aligned} \tag{31}$$

$$\begin{aligned}&T_n^Z + \frac{\Delta t}{\rho C_n}\dot{q}_n + \frac{3\Delta t U_C}{\rho C_n}\left(\frac{r_{n^-}^2}{r_n^3 - r_{n^-}^3}\right) = -\left(\frac{3\Delta t}{\Delta r \rho C_n}\frac{r_{n^-}^2 K_{n^-}}{r_n^3 - r_{n^-}^3}\right) T_{n-1}^{Z+1} + \\ &\left[1 + \frac{3\Delta t}{\rho C_n \Delta r}\left(\frac{r_{n^-}^2 K_{n^-}}{r_n^3 - r_{n^-}^3}\right) + \frac{3\Delta t U_C}{\rho C_n}\left(\frac{r_n^2}{r_n^3 - r_{n^-}^3}\right)\right] T_n^{Z+1}\end{aligned} \tag{32}$$

$$\begin{aligned}&T_n^Z = -\left(\frac{3\Delta t}{\Delta r \rho C_n}\frac{r_{n^-}^2 K_{n^-}}{r_n^3 - r_{n^-}^3}\right) T_{n-1}^{Z+1} + \\ &\left[1 + \frac{3\Delta t}{\rho C_n \Delta r}\left(\frac{r_{n^-}^2 K_{n^-}}{r_n^3 - r_{n^-}^3}\right) + \frac{3\Delta t U_C}{\rho C_n}\left(\frac{r_n^2}{r_n^3 - r_{n^-}^3}\right)\right] T_n^{Z+1} - \frac{\Delta t}{\rho C_n}\dot{q}_n - \frac{3\Delta t U_C}{\rho C_n}\left(\frac{r_{n^-}^2}{r_n^3 - r_{n^-}^3}\right)\end{aligned} \tag{33}$$

Eqs. (20), (21) (32) and (33) constitute a system of algebraic equations for heat transfer modeling in globe-shaped concrete.

4. Result and discussion

The values of Eq. (33) are obtained from the values in **Table 1**. Since the thermal properties are constant, average temperatures could therefore be used to determine thermal properties of bed materials.

The following data were obtained from the theoretical/mathematical modeling carried out on thermal performance of packed bed energy storage system as shown in **Figure 3**.

The following are the definitions of the symbols:

Time = the interval time of measurements, in minutes.

$\mathbf{T_{s\text{-}in}}$ = the inlet air temperature to the packed bed storage tank in °C.

$\mathbf{T_{s\text{-}out}}$ = the outlet air temperature from the packed bed storage tank in °C.

Parameters	Values
Airflow rate	0.01316 m^3/s (28 cfm)
Air—density	1.07154 Kg/m^3
Air—specific heat capacity	1008 J/Kg K
Concrete—density	2400 Kg/m^3
Concrete—specific heat capacity	1130 J/Kg K
Copper tube—density	8900 Kg/m^3
Copper tube—specific heat capacity	384 J/Kg K
Area of globe-shaped concrete	0.013 m^2
Area of copper tube + header	0.664 m^2
Volumetric heat transfer coefficient	106.5 W/m^3 K

Table 1. Modeling parameters.

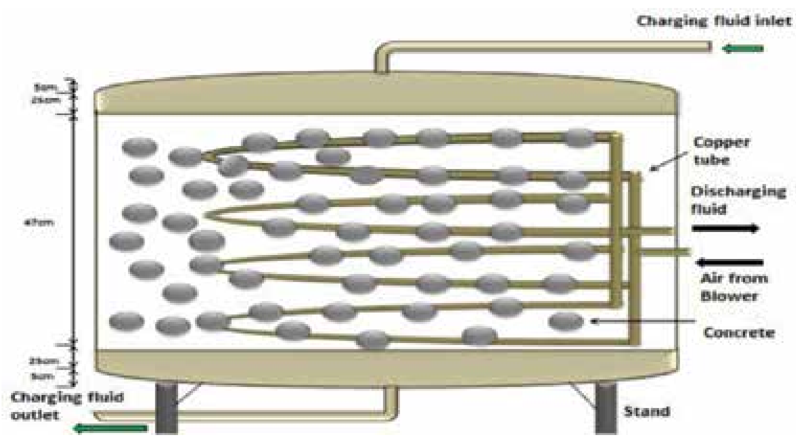

Figure 3. Schematic of the storage tank systems.

$\mathbf{T_{t\text{-}in}}$ = the inlet air temperature to the copper tube in °C.

$\mathbf{T_{t\text{-}out}}$ = the outlet air temperature from the copper tube in °C.

$\mathbf{T_{A1}}$, $\mathbf{T_{A2}}$, $\mathbf{T_{A3}}$, **and** $\mathbf{T_{A4}}$ = the air stream temperatures (°C) through the bed at different heights of the storage tank 117.5, 235, 352.5, and 470 cm, respectively.

$\mathbf{T_{ci1}}$, $\mathbf{T_{ci2}}$, $\mathbf{T_{ci3}}$, **and** $\mathbf{T_{ci4}}$ = the core temperatures of the globe-shaped concrete (°C) through the bed at different heights of the storage tank 117.5, 235, 352.5, and 470 cm, respectively.

$\mathbf{T_{ti1}}$, $\mathbf{T_{ti2}}$, $\mathbf{T_{ti3}}$, **and** $\mathbf{T_{ti4}}$ = the temperatures of air flowing inside the copper tube (°C) through the bed at different heights of the storage tank 117.5, 235, 352.5, and 470 cm, respectively.

T_{ct1}, T_{ct2}, T_{ct3}, and T_{ct4} = the temperatures of the contact made between globe-shaped concrete and imbedded copper tube (°C) through the bed at different heights of the storage tank 117.5, 235, 352.5, and 470 cm, respectively.

T_{t1}, T_{t2}, T_{t3}, and T_{t4} = the surface temperatures of the copper tube (°C) through the bed at different heights of the storage tank 117.5, 235, 352.5, and 470 cm, respectively.

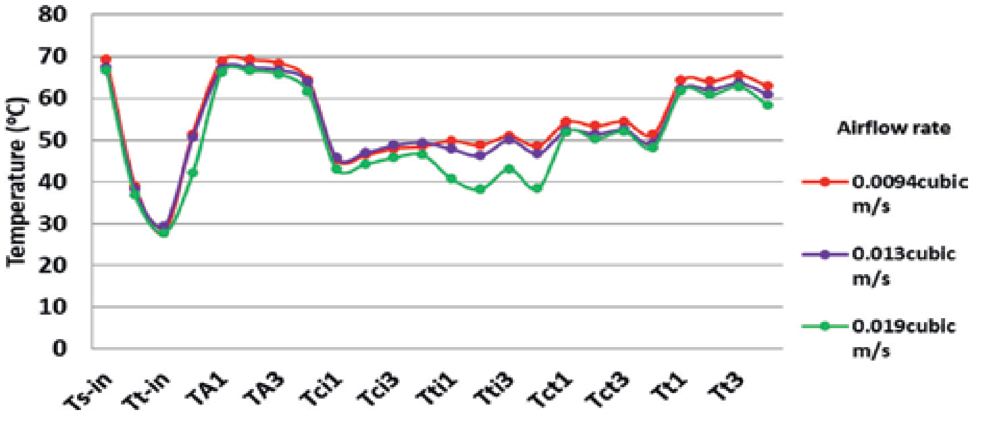

Figure 4. Average temperature measurement of charging packed bed storage system for globe-shaped concrete of size 0.11 m diameter and flow rate of 0.0094, 0.013, and 0.019 m^3/s.

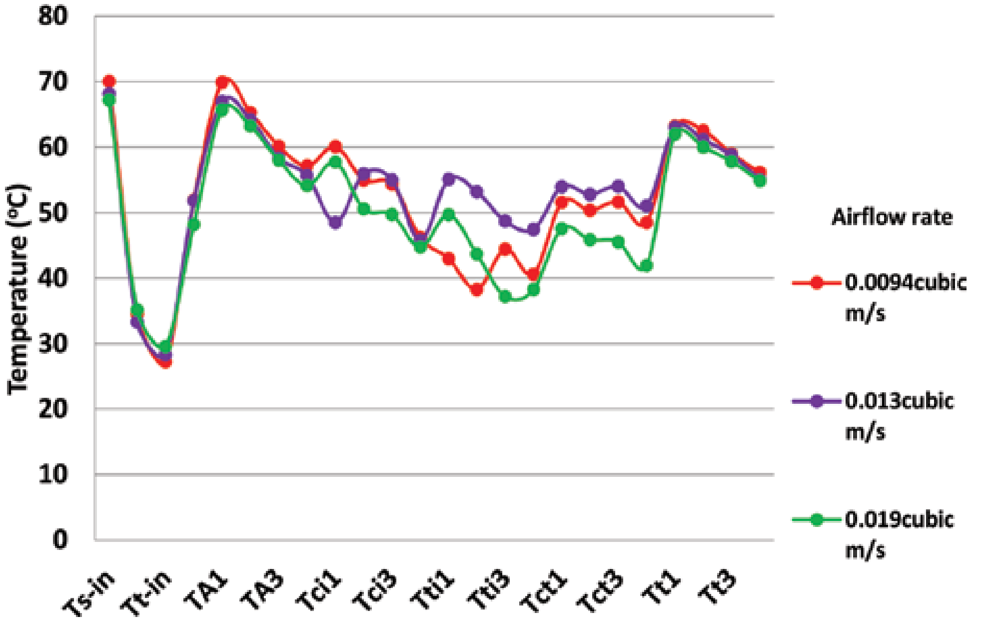

Figure 5. Average temperature measurement of charging packed bed storage system for globe-shaped concrete of size 0.08 m diameter and flow rate of 0.0094, 0.013, and 0.019 m^3/s.

The results of the experimentation were shown in **Figures 4–6** for globe-shaped concrete of size 0.11; 0.08 and 0.065 m diameter respectively while the discharging only temperature measurements were shown in **Figures 7–9** respectively for air flow rate of 0.0094, 0.013, and 0.019 m^3/s.

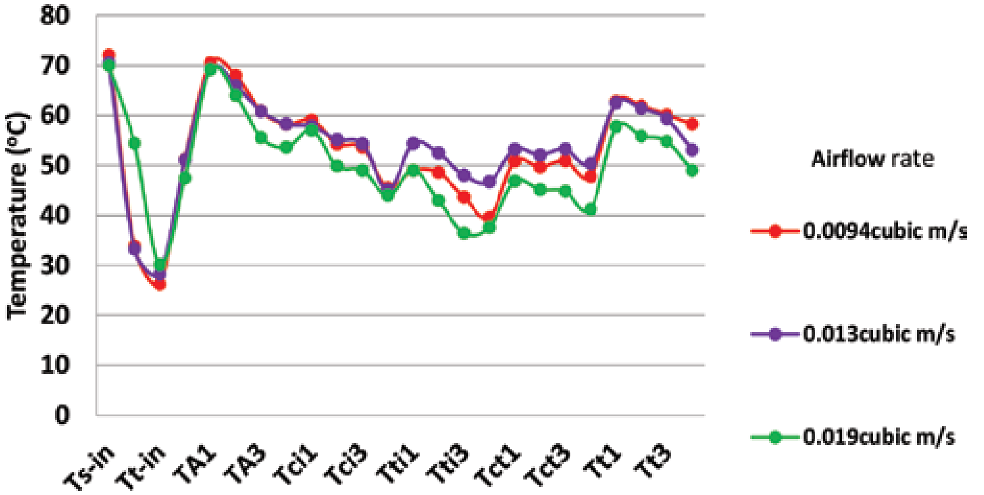

Figure 6. Average temperature measurement of charging packed bed storage system for globe-shaped concrete of size 0.065 m diameter and flow rate of 0.0094, 0.013, and 0.019 m^3/s.

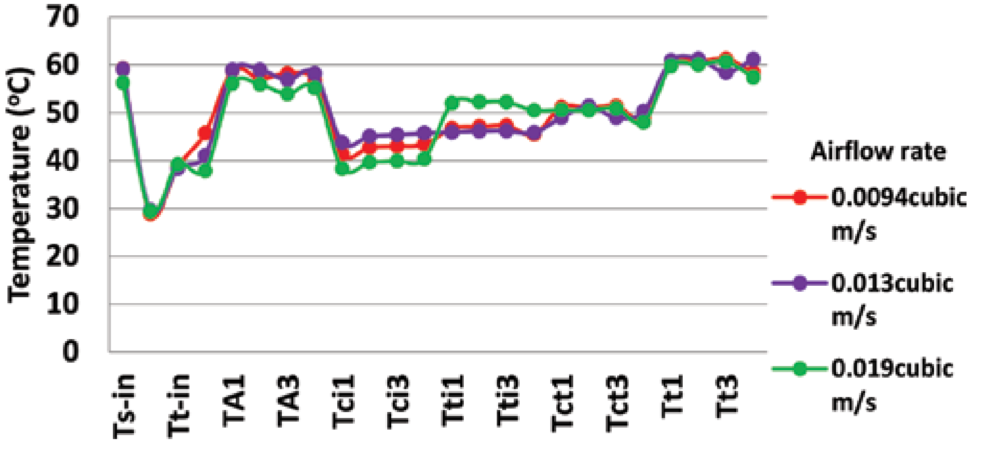

Figure 7. Average temperature measurement of discharging packed bed storage system for globe-shaped concrete of size 0.11 m diameter and flow rate of 0.0094, 0.013, and 0.019 m^3/s.

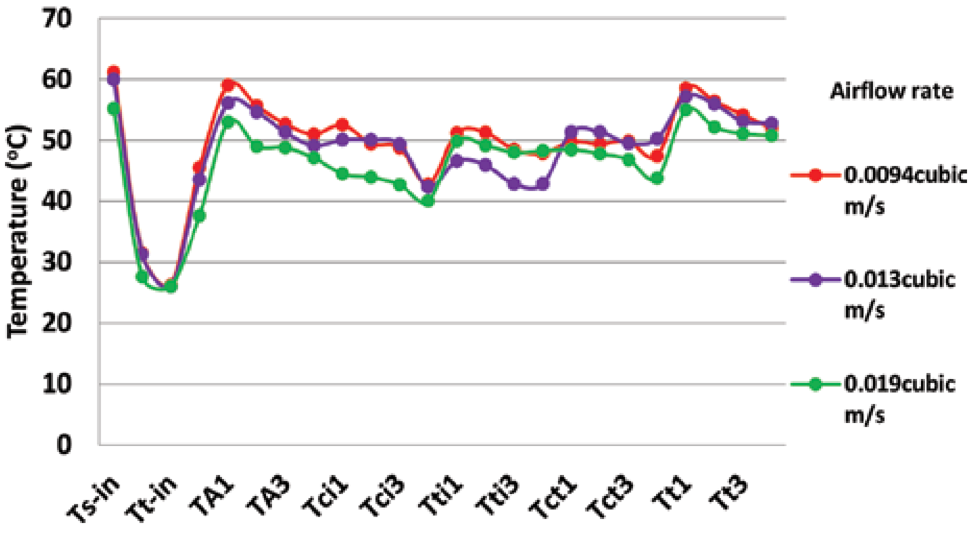

Figure 8. Average temperature measurement of discharging packed bed storage system for globe-shaped concrete of size 0.08 m diameter and flow rate of 0.0094, 0.013, and 0.019 m^3/s.

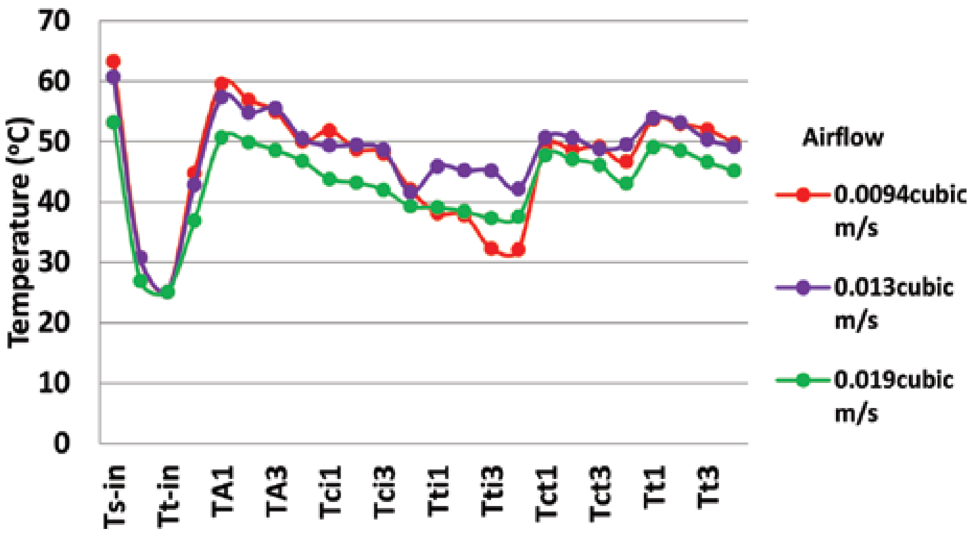

Figure 9. Average temperature measurement of discharging packed bed storage system for globe-shaped concrete of size 0.065 m diameter and flow rate of 0.0094, 0.013, and 0.019 m^3/s.

Figure 10 presents the comparison of the temperature variations with time at Ts-in, $T_{s\text{-}out}$, $T_{t\text{-}in}$, $T_{t\text{-}out}$, T_{A1}, T_{A2}, T_{A3}, T_{A4}, T_{ci1}, T_{ci2}, T_{ci3}, T_{ci4}, T_{ti1}, T_{ti2}, T_{ti3}, T_{ti4}, T_{ct1}, T_{ct2}, T_{ct3}, T_{ct4}, T_{t1}, T_{t2}, T_{t3}, and T_{t4} during the simultaneous charging and discharging while **Figure 11** presents for discharging only. The comparisons were presented for air flow rates of 0.0094, 0.013, and 0.019 m^3/s.

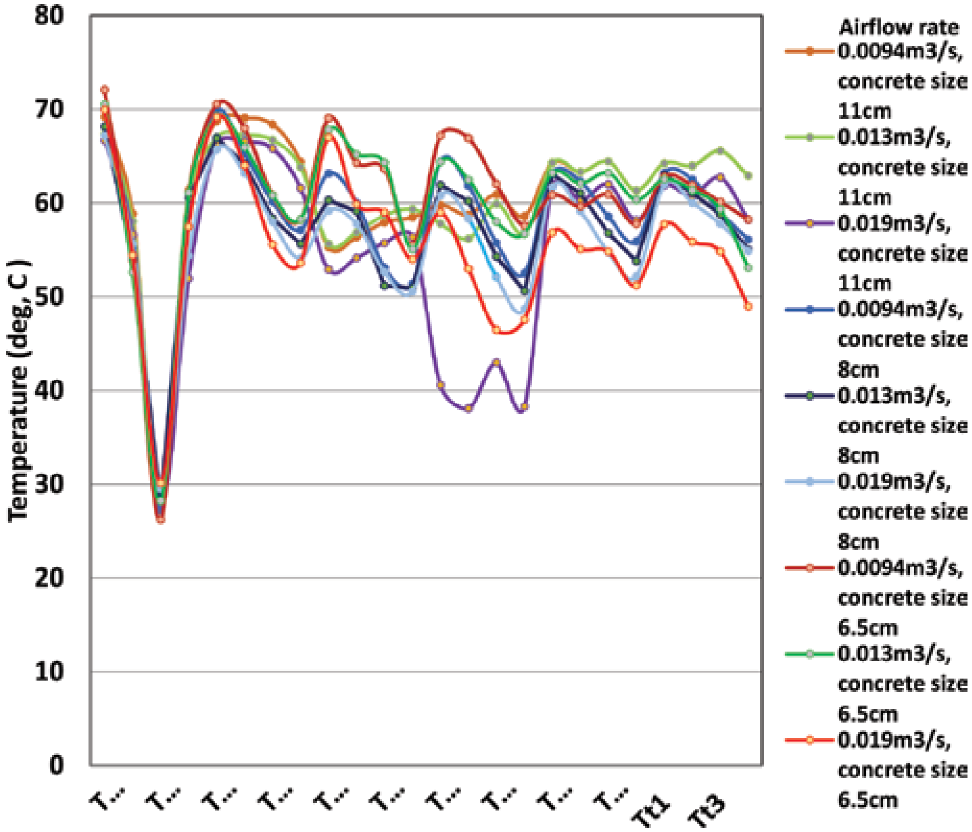

Figure 10. Comparison of average temperature measurement of charging packed bed storage system for globe-shaped concrete of size 0.065, 0.08, 0.11 m in diameter and flow rate of 0.0094, 0.013, and 0.019 m^3/s.

These figures show that the difference of the temperature response between the charging and fluid to solid heat transfer process at the initial period (<30 min) of the packed bed was large (large inlet–outlet temperature difference means large heat supply), and the heat recovered by the cool air (approximately 27°C) flowing inside the copper tube was fairly high (larger inlet–outlet temperature difference compared with the later period indicates larger heat recovery).

Therefore, a relatively large part of the heat supplied by the simulated air heater was used to heat the air flowing inside the copper tube through conduction and convection and also stores the rest for continuous usage.

The following are the storage efficiency for globe-shaped concrete of size 0.11 m, 0.08 m and 0.065 m diameter at airflow rate of 0.0094, 0.013 and 0.019 m^3/s (**Figure 12**):

For 0.11 m diameter globe-shaped concrete:

http://dx.doi.org/10.5772/intechopen.77205

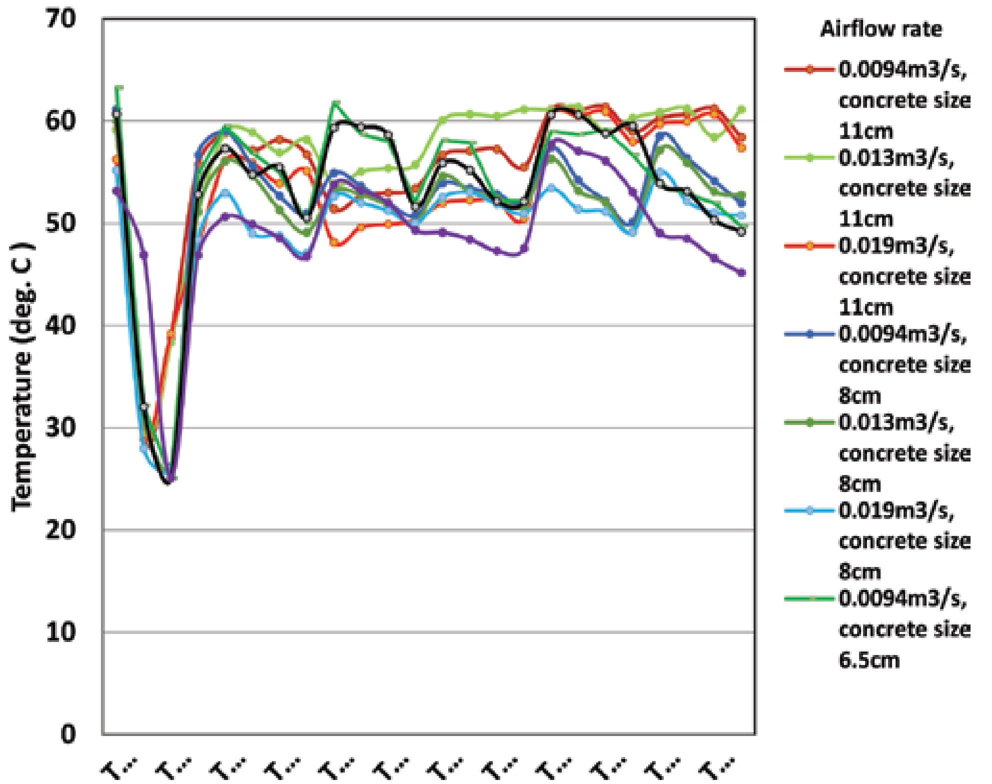

Figure 11. Comparison of average temperature measurement of discharging packed bed storage system for globe-shaped concrete of size 0.065, 0.08, 0.11 m in diameter and flow rate of 0.0094, 0.013, and 0.019 m^3/s.

i. Storage efficiency at air flow rates of 0.0094 m^3/s = 40.7%

ii. Storage efficiency at air flow rates of 0.013 m^3/s = 60.5%

iii. Storage efficiency at air flow rates of 0.019 m^3/s = 57.5%

For 0.08 m diameter globe-shaped concrete:

i. Storage efficiency at air flow rates of 0.0094 m^3/s = 23.5%

ii. Storage efficiency at air flow rates of 0.013 m^3/s = 51.3%

iii. Storage efficiency at air flow rates of 0.019 m^3/s = 50.2%

For 0.065 m diameter globe-shaped concrete:

i. Storage efficiency at air flow rates of 0.0094 m^3/s = 14.8%

ii. Storage efficiency at air flow rates of 0.013 m^3/s = 35.06%

iii. Storage efficiency at air flow rates of 0.019 m^3/s = 40.3%

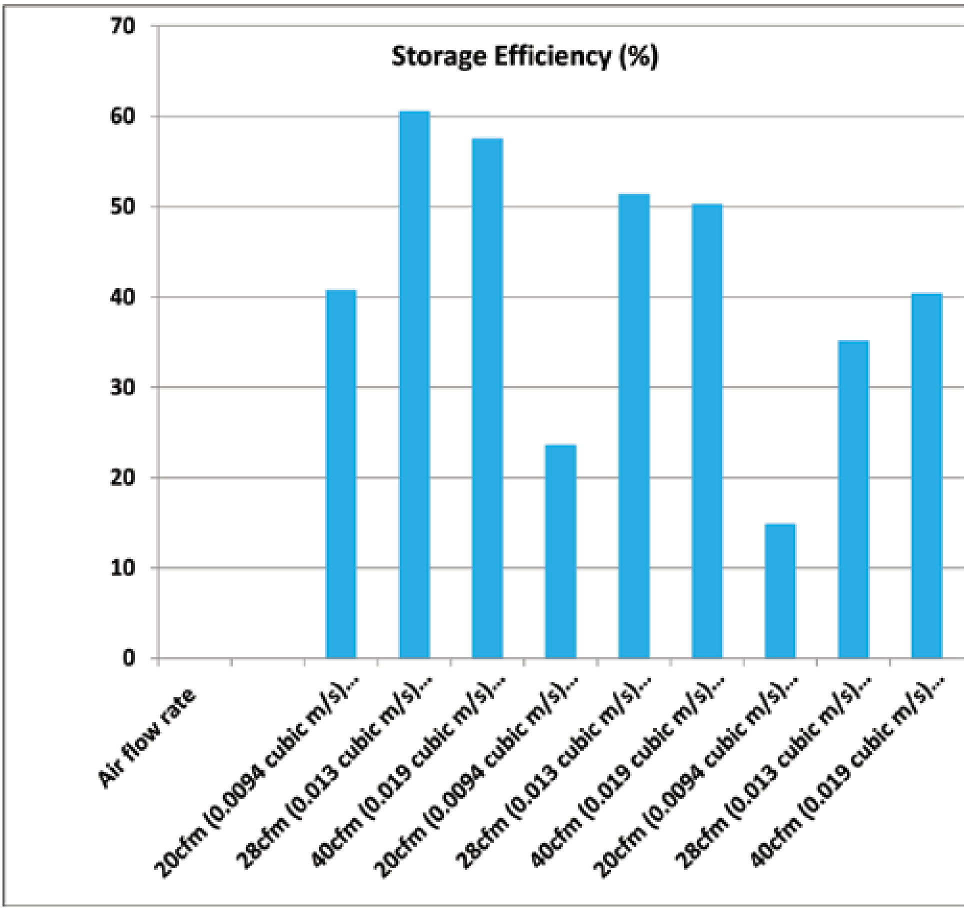

Figure 12. Storage efficiency of simultaneous charging and discharging packed bed storage system for globe-shaped concrete of diameter 0.065, 0.08, 0.11 m and air flow rate 0.0094, 0.013, and 0.019 m^3/s.

5. Conclusion

The study led to the following findings and conclusions:

1. The mathematical model developed can accurately predict the temperature within the concrete bed for energy storage purpose.
2. The steady intermittent input temperature variation actually led to continuous discharge temperature at the copper tube outlet.
3. The mathematical model may be extended to specify the packed bed storage system dimensions.
4. Globe-shaped concrete of 0.11 m diameter has the highest storage efficiency of 60.5% at 0.013 m^3/s airflow rate.

http://dx.doi.org/10.5772/intechopen.77205

Author details

Adeyanju Anthony Ademola

Address all correspondence to: anthony.adeyanju@sta.uwi.edu

Mechanical and Manufacturing Engineering Department, University of the West Indies, St. Augustine, Trinidad and Tobago

References

[1] Adeyanju AA, Manohar K. Theoretical and experimental investigation of heat transfer in packed beds. Research Journal of Applied Sciences. 2009;**4**(5):166-177

[2] Balakrishnan AR, Pei DCT. Heat transfer in fixed bed. In: Industrial and Engineering Chemical Process Design Development. Vol. 13. Washington DC, USA: ACS Publication; 1974. pp. 441-446

[3] Anzelius A. 1926. Heating by means of percolating media. Journal of Mechanical and Agriculture, ASAE, 41st ed 6:291-296. AE 1996

[4] Schumann TEW. Heat transfer: A liquid flowing through a porous prism. Journal of Heat Transfer. 1929;**5**:208-212

[5] Furnas CC. Heat transfer from a gas stream to a bed of broken solids. Journal of Chemical Engineering. 1930;**22**:26-721

[6] Saunders OA, Ford. Heat transfer in the flow of gas through a bed of solid particles. Journal of Iron and Steel. 1940;**141**:291-296

[7] Kays WM, London AC. Compact Heat Exchangers. New York: McGrawHILL; 1964

[8] Löf GOG, Hawley RW. Unsteady state heat transfer between air and loose solids. Journal of Industrial Engineering. 1948;**40**(6):1061-1070

[9] Leva M, Grummer M. Concentration and temperature profiles in a tubular reactor. Industrial and chemical engineering fundamental. ACS Publication. 1948;**40**:747-753

[10] Riaz M. Analytical solution for single and two phase models of packed bed thermal storage systems. Journal of Heat Transfer. 1977;**99**:489-492

[11] Jefferson CP. Prediction of break through curves in packed beds: Applicability of single parameter models. AlChE Journal. 1972;**18**(2):409-416

[12] Ball WE. Heat transfer properties of a packed bed: Determination by a frequency response technique [Dissertation Abstract], Vol. **19**; 1958. p. 494

[13] Norton CL. Pebble heater: New heat transfer unit for industry. Journal of the American Ceramic Society. 1946;**29**:187-193

[14] Meek RMG. The measurement of heat transfer coefficients in packed beds by the cyclic method. In: International Heat Transfer Development. New York, USA: ASME; 1961

[15] Bradshaw RC, Myers JE. Heat and mass transfer in fixed and fluidized beds of large particles. AIChE Journal. 1963;**9**:590-599

[16] Harker JH, Martyn EJ. Energy storage in gravel beds. Journal of the Institute of Energy. 1985;**58**:94-99

[17] Bouguettaia H, Harker JH. Energy storage in packed beds of spheres containing palm oil. Journal of the Institute of Energy. 1991;**64**:89-94

[18] Lanz JE. A numerical model of thermal effects in a microwave irradiated catalyst bed [M.Sc. thesis]; Virginia, USA: Virginia Polytechnic Institute and State University; 1998

Edited by Mohsen Sheikholeslami Kandelousi

In this book, various aspects of heating, ventilation, and air-conditioning (HVAC) systems are investigated. HVAC systems are milestones of building mechanical systems that provide thermal comfort for occupants accompanied with indoor air quality. HVAC systems can be classified into central and local systems according to multiple zones, location, and distribution. Primary HVAC equipment includes heating equipment, ventilation equipment, and cooling or air-conditioning equipment. Central HVAC systems are located away from buildings in a central equipment room and deliver the conditioned air by a delivery ductwork system. Central HVAC systems contain all-air, air-water, or all-water systems. Two systems should be considered as central such as heating and cooling panels and water-source heat pumps.

Published in London, UK

IntechOpen

ISBN 978-1-83881-719-0